



National Library
of Canada

Acquisitions and
Bibliographic Services Branch

395 Wellington Street
Ottawa, Ontario
K1A 0N4

Bibliothèque nationale
du Canada

Direction des acquisitions et
des services bibliographiques

395, rue Wellington
Ottawa (Ontario)
K1A 0N4

Your file - Votre référence

Our file - Notre référence

NOTICE

The quality of this microform is heavily dependent upon the quality of the original thesis submitted for microfilming. Every effort has been made to ensure the highest quality of reproduction possible.

If pages are missing, contact the university which granted the degree.

Some pages may have indistinct print especially if the original pages were typed with a poor typewriter ribbon or if the university sent us an inferior photocopy.

Reproduction in full or in part of this microform is governed by the Canadian Copyright Act, R.S.C. 1970, c. C-30, and subsequent amendments.

AVIS

La qualité de cette microforme dépend grandement de la qualité de la thèse soumise au microfilmage. Nous avons tout fait pour assurer une qualité supérieure de reproduction.

S'il manque des pages, veuillez communiquer avec l'université qui a conféré le grade.

La qualité d'impression de certaines pages peut laisser à désirer, surtout si les pages originales ont été dactylographiées à l'aide d'un ruban usé ou si l'université nous a fait parvenir une photocopie de qualité inférieure.

La reproduction, même partielle, de cette microforme est soumise à la Loi canadienne sur le droit d'auteur, SRC 1970, c. C-30, et ses amendements subséquents.

Canada

University of Alberta

Dimetallic Trifluoropropyne Bridged Complexes of Ruthenium and Osmium

by

Kenneth Charles Hoffman ©

A Thesis

submitted to the Faculty of Graduate Studies and Research in partial fulfillment of the
requirements of the degree of Master of Science

Department of Chemistry

Edmonton, Alberta

Fall, 1994



National Library
of Canada

Acquisitions and
Bibliographic Services Branch

395 Wellington Street
Ottawa, Ontario
K1A 0N4

Bibliothèque nationale
du Canada

Direction des acquisitions et
des services bibliographiques

395, rue Wellington
Ottawa (Ontario)
K1A 0N4

Your file - Votre référence

Our file - Notre référence

The author has granted an irrevocable non-exclusive licence allowing the National Library of Canada to reproduce, loan, distribute or sell copies of his/her thesis by any means and in any form or format, making this thesis available to interested persons.

L'auteur a accordé une licence irrévocable et non exclusive permettant à la Bibliothèque nationale du Canada de reproduire, prêter, distribuer ou vendre des copies de sa thèse de quelque manière et sous quelque forme que ce soit pour mettre des exemplaires de cette thèse à la disposition des personnes intéressées.

The author retains ownership of the copyright in his/her thesis. Neither the thesis nor substantial extracts from it may be printed or otherwise reproduced without his/her permission.

L'auteur conserve la propriété du droit d'auteur qui protège sa thèse. Ni la thèse ni des extraits substantiels de celle-ci ne doivent être imprimés ou autrement reproduits sans son autorisation.

ISBN 0-315-95048-X

Canada

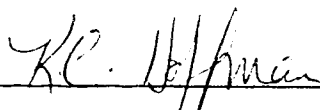
University of Alberta

Release Form

Name of Author: Kenneth Charles Hoffman
Title of Thesis: Dimetallic Trifluoropropyne Bridged Complexes of
Ruthenium and Osmium
Degree: Master of Science
Year this Degree Granted: 1994

Permission is hereby granted to the University of Alberta to reproduce single copies of this thesis and to lend or sell such copies for private, scholarly, or scientific research purposes only.

The author reserves all other publication rights, and neither the thesis nor extensive extracts from it may be printed or otherwise reproduced without the author's written permission.



K. C. Hoffman

10806-71 Avenue
Edmonton, Alberta
Canada, T6E 0X7

August 24, 1994

University of Alberta

Faculty of Graduate Study and Research

The undersigned certify that they have read, and recommend to the Faculty of Graduate Studies and Research for acceptance, a thesis entitled **Dimetallic Trifluoropropyne Bridged Complexes of Ruthenium and Osmium** submitted by Kenneth Charles Hoffman in partial fulfillment of the requirements for the degree of Master of Science.

J. Takats

M. Cowie

M. Klobukowski

E. E. Knaus

August 24, 1994

Abstract

The preparation and reactions of $\text{Ru}(\text{CO})_4(\eta^2\text{-HC}_2\text{CF}_3)$ and $\text{Os}(\text{CO})_4(\eta^2\text{-HC}_2\text{CF}_3)$ were investigated.

$\text{Ru}(\text{CO})_4(\eta^2\text{-HC}_2\text{CF}_3)$ (**1a**) reacts with $\text{Ru}(\text{CO})_5$ and $\text{Ru}(\text{CO})_4(\text{PMe}_3)$ (**2**) to yield the dimetallacyclobutene products $\text{Ru}_2(\text{CO})_8(\mu\text{-}\eta^1, \eta^1\text{-HC}_2\text{CF}_3)$ (**3**) and $\text{Ru}_2(\text{CO})_7(\text{PMe}_3)(\mu\text{-}\eta^1, \eta^1\text{-HC}_2\text{CF}_3)$ (**6**). $\text{Os}(\text{CO})_4(\eta^2\text{-HC}_2\text{CF}_3)$ (**1b**) reacts with $\text{Ru}(\text{CO})_5$, $\text{Os}(\text{CO})_5$, and $\text{Ru}(\text{CO})_4(\text{PMe}_3)$ to generate the dimetallacyclobutene complexes $\text{OsRu}(\text{CO})_8(\mu\text{-}\eta^1, \eta^1\text{-HC}_2\text{CF}_3)$ (**4**), $\text{Os}_2(\text{CO})_8(\mu\text{-}\eta^1, \eta^1\text{-HC}_2\text{CF}_3)$ (**5**), and $\text{OsRu}(\text{CO})_7(\text{PMe}_3)(\mu\text{-}\eta^1, \eta^1\text{-HC}_2\text{CF}_3)$ (**7**). In each case a single regioisomer was observed.

The reactions of PMe_3 with $\text{Ru}_2(\text{CO})_8(\mu\text{-}\eta^1, \eta^1\text{-HC}_2\text{CF}_3)$ (**3**) and $\text{OsRu}(\text{CO})_8(\mu\text{-}\eta^1, \eta^1\text{-HC}_2\text{CF}_3)$ (**4**) promotes carbonyl insertion and formation of the dimetallacyclopentenone products $\text{Ru}_2(\text{CO})_7(\text{PMe}_3)(\mu\text{-}\eta^1, \eta^1\text{-C}(\text{O})\text{HC}_2\text{CF}_3)$ (**8**) and $\text{OsRu}(\text{CO})_7(\text{PMe}_3)(\mu\text{-}\eta^1, \eta^1\text{-C}(\text{O})\text{HC}_2\text{CF}_3)$ (**9**). These two transformations represent the first documented examples of simple carbonyl insertion into a dimetallacyclobutene ring. Both reactions proceed in a regioselective fashion, the carbonyl inserting into the weaker Ru-C(H) bond.

The reaction of $\text{Ru}(\text{CO})_4(\eta^2\text{-HC}_2\text{CF}_3)$ (**1a**) with $\text{Cp}'\text{Rh}(\text{CO})_2$ and $\text{Cp}^*\text{Ir}(\text{CO})_2$ resulted in the formation of the dimetallacyclobutene complexes $\text{Cp}'\text{RhRu}(\text{CO})_5(\mu\text{-}\eta^1, \eta^1\text{-HC}_2\text{CF}_3)$ ($\text{Cp}' = \text{Cp}$ (**10**), Cp^* (**11**)) and $\text{Cp}^*\text{IrRu}(\text{CO})_5(\mu\text{-}\eta^1, \eta^1\text{-HC}_2\text{CF}_3)$ (**12**). From the preparation of **11** a trinuclear complex $\text{Cp}^*_2\text{CpRh}_2\text{Ru}(\text{CO})_5(\mu\text{-HC}_2\text{CF}_3)$ (**11a**) was also isolated. Again, a single regioisomer was observed for each of the dimetallacyclobutene complexes.

A number of the complexes exhibit carbonyl ligand fluxionality and low-temperature NMR experiments were conducted to determine the nature and energetics of the processes.

Table of Contents

Chapter One Introduction

1.1	A Brief History of Binary, Mononuclear Metal Carbonyls	1
1.2	The Mononuclear, Binary Carbonyls of Group 8	2
1.3	A Survey of $M(\text{CO})_4\text{L}$ Complexes	5
1.4	A Survey of Alkyne Bridged Dimetallic Complexes	9
1.5	Scope of Present Research	12
1.6	References	14

Chapter Two Synthesis and Characterization of $\text{Ru}(\text{CO})_4(\eta^2\text{-HC}_2\text{CF}_3)$ and $\text{Ru}(\text{CO})_4(\text{PMe}_3)$

2.1	Introduction	17
2.2	Synthesis and Characterization of $\text{Ru}(\text{CO})_4(\eta^2\text{-HC}_2\text{CF}_3)$, 1a	18
2.3	Reactivity of $\text{Ru}(\text{CO})_4(\eta^2\text{-HC}_2\text{CF}_3)$	25
2.4	An Alternative Synthesis of $\text{Ru}(\text{CO})_4(\text{PMe}_3)$, 2	26
2.5	Conclusion	28
2.6	Experimental Section	31
2.7	References	38

Chapter Three **$MM'(CO)_7(L)(\mu-\eta^1,\eta^1-HC_2CF_3)$ Complexes (M,M' = Ru, Os; L = CO, PMe₃)**

3.1	Introduction	41
3.2	Synthesis and Characterization of $MM'(CO)_7(L)(\mu-\eta^1,\eta^1-HC_2CF_3)$	42
3.3	NMR Spectra and Product Regiochemistry	44
3.4	Solid-State Structure of $OsRu(CO)_7(PMe_3)(\mu-\eta^1,\eta^1-HC_2CF_3)$, 7	51
3.5	Fluxional Behaviour	54
3.6	Conclusion	57
3.7	Experimental	60
3.8	References	70

Chapter Four **Reactivity of $MRu(CO)_8(\mu-\eta^1,\eta^1-HC_2CF_3)$**

4.1	Introduction	73
4.2	Reaction of $MRu(CO)_8(\mu-\eta^1,\eta^1-HC_2CF_3)$ with PMe ₃	74
4.3	NMR Spectra	75
4.4	Solid-State Structure of $OsRu(CO)_7(PMe_3)(\mu-\eta^1,\eta^1-C\{O\}HC_2CF_3)$, 9	81
4.5	Further Attempts at Ligand Substitution	84
4.6	Conclusion	87
4.7	Experimental	92
4.8	References	99

Chapter Five **Synthesis and Characterization of Cp'MRu(CO)₅(μ-η¹,η¹-HC₂CF₃) Complexes (M = Rh, Ir; Cp' = Cp, Cp^{*})**

5.1	Introduction	102
5.2	Synthesis and Characterization of Cp'MRu(CO) ₅ (μ-η ¹ ,η ¹ -HC ₂ CF ₃)	103
5.3	NMR Spectra and Fluxional Behaviour	106
5.4	Thermal Disproportionation of Cp [*] RhRu(CO) ₅ (μ-η ¹ ,η ¹ -HC ₂ CF ₃), 11	110
5.5	Conclusion	115
5.6	Experimental	116
5.7	References	119

Chapter Six **Conclusions**

6.1	Conclusions	121
6.2	References	123

List of Tables

Chapter One

Table 1.1	Listing of $M(\text{CO})_5$ and $M(\text{CO})_4\text{L}$ Carbonyl Stretching Frequencies	6
------------------	--	---

Chapter Two

Table 2.1	Comparison of Infrared Stretching Frequencies (in cm^{-1}) for $\text{Ru}(\text{CO})_4(\eta^2\text{-RC}_2\text{R}')$ Complexes	21
Table 2.2	Solvents and Drying Agents	31

Chapter Three

Table 3.1	Reaction Conditions and Product Yields	43
Table 3.2	Summary of Alkyne $^{13}\text{C}\{^1\text{H}\}$ NMR Data	49
Table 3.3	Crystallographic Data for $\text{OsRu}(\text{CO})_7(\text{PMe}_3)(\mu\text{-}\eta^1,\eta^1\text{-HC}_2\text{CF}_3)$, 7	67
Table 3.4	Bond Distances (\AA) for $\text{OsRu}(\text{CO})_7(\text{PMe}_3)(\mu\text{-}\eta^1,\eta^1\text{-HC}_2\text{CF}_3)$, 7	68

Table 3.5	Bond Angles (deg) for OsRu(CO) ₇ (PMe ₃) (μ-η ¹ ,η ¹ -HC ₂ CF ₃), 7	69
------------------	---	----

Chapter Four

Table 4.1	Summary of Dimetallacycle Ring-carbon ¹³ C{ ¹ H} NMR Resonances	80
Table 4.2	Crystallographic Data for OsRu(CO) ₇ (PMe ₃) (μ-η ¹ ,η ¹ -C(O)HC ₂ CF ₃), 9	95
Table 4.3	Bond Distances (Å) for OsRu(CO) ₇ (PMe ₃) (μ-η ¹ ,η ¹ -C(O)HC ₂ CF ₃), 9	96
Table 4.4	Bond Angles (deg) for OsRu(CO) ₇ (PMe ₃) (μ-η ¹ ,η ¹ -C(O)HC ₂ CF ₃), 9	97

Chapter Five

Table 5.1	Reaction and Product Data	104
------------------	---------------------------	-----

List of Figures

Chapter Two

- Figure 2.1** Low-temperature $^{13}\text{C}\{^1\text{H}\}$ NMR Spectrum of $\text{Ru}(\text{CO})_4(\eta^2\text{-HC}_2\text{CF}_3)$, **1a** 24
- Figure 2.2** Photolysis Apparatus for Internal Photolysis, **A**, and External Photolysis, **B** 34

Chapter Three

- Figure 3.1** Solution IR Spectra of (a) $\text{OsRu}(\text{CO})_8(\mu\text{-}\eta^1, \eta^1\text{-HC}_2\text{CF}_3)$, **4**, and (b) $\text{OsRu}(\text{CO})_7(\text{PMe}_3)(\mu\text{-}\eta^1, \eta^1\text{-HC}_2\text{CF}_3)$, **7** 45
- Figure 3.2** Solid-State Structure of $\text{OsRu}(\text{CO})_7(\text{PMe}_3)(\mu\text{-}\eta^1, \eta^1\text{-HC}_2\text{CF}_3)$, **7** 53
- Figure 3.3** Variable Temperature $^{13}\text{C}\{^1\text{H}\}$ NMR Spectra of $\text{Ru}_2(\text{CO})_8(\mu\text{-}\eta^1, \eta^1\text{-HC}_2\text{CF}_3)$, **3** 55
- Figure 3.4** Low-temperature Limiting $^{13}\text{C}\{^1\text{H}\}$ NMR Spectra of Carbonyl Region for $\text{MM}'(\text{CO})_8(\mu\text{-}\eta^1, \eta^1\text{-HC}_2\text{CF}_3)$ 58
- Figure 3.5** $^{13}\text{C}\{^1\text{H}\}$ NMR Spectra of Carbonyl Region for $\text{MM}'(\text{CO})_7(\text{PMe}_3)(\mu\text{-}\eta^1, \eta^1\text{-HC}_2\text{CF}_3)$ 59

Chapter Four

- Figure 4.1** Solution IR Spectra of (a) OsRu(CO)₇(PMe₃) (μ-η¹,η¹-HC₂CF₃), **7**, and (b) OsRu(CO)₇(PMe₃) (μ-η¹,η¹-C(O)HC₂CF₃), **9** 76
- Figure 4.2** ¹³C{¹H} NMR Spectra of (a) Ru₂(CO)₇(PMe₃) (μ-η¹,η¹-C(O)HC₂CF₃), **8**, and (b) OsRu(CO)₇(PMe₃) (μ-η¹,η¹-C(O)HC₂CF₃), **9** 78
- Figure 4.3** Solid-State Structure of OsRu(CO)₇(PMe₃) (μ-η¹,η¹-C(O)HC₂CF₃), **9** 83
- Figure 4.4** View Along The Os-Ru bond: OsRu(CO)₇(PMe₃) (μ-η¹,η¹-C(O)HC₂CF₃), **9** 85

Chapter Five

- Figure 5.1** Solution IR Spectrum of CpRhRu(CO)₅ (μ-η¹,η¹-HC₂CF₃), **10** 105
- Figure 5.2** (a) Room Temperature ¹³C{¹H} NMR Spectrum of CpRhRu(CO)₅(μ-η¹,η¹-HC₂CF₃), **10**, and (b) -40°C Spectrum of Cp*IrRu(CO)₅ (μ-η¹,η¹-HC₂CF₃), **12** 108
- Figure 5.3** IR Spectrum of Cp*₂Rh₂Ru(CO)₅(HC₂CF₃), **11a** 112

List of Schemes

Chapter One

Scheme 1.1	Preparations of $M(\text{CO})_5$ ($M = \text{Ru}, \text{Os}$)	2
Scheme 1.2	Comparison of the $M(\text{CO})_5$ Complexes	3
Scheme 1.3	M-CO Bonding	4
Scheme 1.4	The Two Canonical Forms of Metal Carbonyl Bonding	6
Scheme 1.5	The σ - and π -Components of Metal-Alkyne Bonding	7
Scheme 1.6	The Two Valence Bond Extremes of Metal-Alkyne Bonding	8
Scheme 1.7	Six Types of Dimetallacyclic Structure	9
Scheme 1.8	Synthesis of $\text{Ru}_2(\text{CO})_4(\mu\text{-dmpm})_2(\mu\text{-}\eta^1, \eta^1\text{-PhC}_2\text{Ph})$	10
Scheme 1.9	Synthesis of $\text{Cp}_2\text{M}_2(\text{CO})_2(\mu\text{-CO})(\mu\text{-}\eta^1, \eta^1\text{-C}_2\{\text{CO}_2\text{Me}\}_2)$	11
Scheme 1.10	Synthesis of $\text{Ru}_2(\text{CO})_8(\mu\text{-}\eta^1, \eta^1\text{-F}_3\text{CC}_2\text{CF}_3)$	12

Chapter Two

Scheme 2.1	Preparation of Dimetallacycles Using $M(\text{CO})_4(\eta^2\text{-alkyne})$ Complexes	18
Scheme 2.2	Preparation of $\text{Ru}(\text{CO})_4(\eta^2\text{-HC}_2\text{CF}_3)$, 1a	19
Scheme 2.3	The Two Valence Bond Extremes of Metal-Alkyne Bonding	21
Scheme 2.4	Preparation of $\text{Ru}(\text{CO})_4(\text{PR}_3)$, 2	27
Scheme 2.5	The Two Canonical Forms of Metal Carbonyl Bonding	29

Chapter Three

Scheme 3.1	Three Types of Dimetallacyclic Structure	41
Scheme 3.2	Preparation of $MM'(CO)_7(L)(\mu-\eta^1, \eta^1-HC_2CF_3)$ Complexes	43
Scheme 3.3	The Two Possible Regioisomers of $OsRu(CO)_8$ $(\mu-\eta^1, \eta^1-HC_2CF_3)$, 4	46
Scheme 3.4	Alkyne-carbon Labelling System	48
Scheme 3.5	Possible Sites of PMe_3 Coordination: <i>trans</i> to C_1 (a), M (b), or CO (c)	51
Scheme 3.6	"Merry-go-round" Exchange Mechanism of $MM'(CO)_8$ $(\mu-\eta^1, \eta^1-HC_2CF_3)$	56

Chapter Four

Scheme 4.1	Three Types of Dimetallacyclic Structure	73
Scheme 4.2	Preparation of $MRu(CO)_7(PMe_3)(\mu-\eta^1, \eta^1-C(O)HC_2CF_3)$	74
Scheme 4.3	Dimetallacycle Regiochemistry and Carbon Atom Numbering Scheme	80
Scheme 4.4	The Two Resonance Forms of an α, β -Unsaturated Ketone	81
Scheme 4.5	Dimetallacyclopentenone Regiochemistry: $M = Ru$ or Os	88
Scheme 4.6	Carbonyl Insertion Mechanism for $RMn(CO)_5$	88
Scheme 4.7	A Proposed Mechanism for Carbonyl Insertion into Dimetallacycles	90

Chapter Five

Scheme 5.1	Three Types of Dimetallacyclic Structure	102
Scheme 5.2	Preparation of $\text{Cp}'\text{M}'\text{Ru}(\text{CO})_5(\mu\text{-}\eta^1, \eta^1\text{-HC}_2\text{CF}_3)$ Complexes	104
Scheme 5.3	Proposed Fluxional Exchange Process for $\text{Cp}'\text{M}'\text{Ru}(\text{CO})_5(\mu\text{-}\eta^1, \eta^1\text{-HC}_2\text{CF}_3)$	109
Scheme 5.4	Possible Structures for $\text{Cp}^*\text{Rh}_2\text{Ru}(\text{CO})_5(\text{HC}_2\text{CF}_3)$, 11a	113
Scheme 5.5	Structure of $\text{Cp}_2\text{Cp}^*\text{Rh}_3(\text{CO})_3(\text{F}_3\text{CC}_2\text{CF}_3)$	114

List of Abbreviations and Symbols

a	axial
A	Absorbance
Å	Angström(s); 10^{-10}m
atm	atmosphere(s)
b	path length
br	broad
c	concentration
ca.	<i>circa</i> (approximately)
calc	calculated
Cp	cyclopentadienyl, C_5H_5
Cp*	pentamethylcyclopentadienyl, $\text{C}_5(\text{CH}_3)_5$
δ	chemical shift
Δ	difference; change
d	doublet
dd	doublet of doublets
deg	degree(s)
DMAD	dimethyl acetylenedicarboxylate, $\text{C}_2\{\text{C}(\text{O})\text{OCH}_3\}$
dmpm	bis(dimethylphosphino)methane, $(\text{H}_3\text{C})_2\text{PCH}_2\text{P}(\text{CH}_3)_2$
dq	doublet of quartets
e	equatorial
ϵ	molar absorbtivity
eV	electron volt(s)
FAB	fast atom bombardment
FT-IR	Fourier Transform Infrared

GWV	Glaswerk Wertheim
h	hour(s)
HFB	hexafluoro-2-butyne, F₃CC₂CF₃
hν	light; electromagnetic radiation
Hz	Hertz; s⁻¹
IR	infrared
J	coupling constant
K	Kelvin
λ	wavelength
m	multiplet (NMR reference); medium (IR reference)
M⁺	parent ion
Me	methyl, H₃C-
mg	milligrams
MHz	megahertz
mL	millilitres
mmol	millimoles
MS	mass spectrometry
nm	nanometres; 10⁻⁹m
NMR	nuclear magnetic resonance
NOE	nuclear Overhauser effect
ν	stretching frequency
Ph	phenyl, C₆H₅-
ppm	parts per million
q	quartet
s	second(s) (time reference); singlet (NMR reference); strong (IR reference)
sh	shoulder

^tBu	<i>tertiary-butyl</i>, (H₃C)₃C-
TFP	trifluoropropyne, HC₂CF₃
u	unique
v	very
w	weak

Chapter One

Introduction

1.1 A Brief History of the Binary, Mononuclear Metal Carbonyls

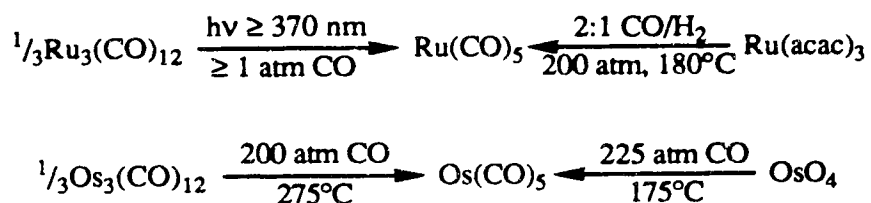
Among the innumerable complexes that comprise modern organo-transition metal chemistry, the binary transition metal carbonyls have perhaps the greatest historical legacy; Ludwig Mond's fortuitous discovery of the first binary metal carbonyl, $\text{Ni}(\text{CO})_4$, was reported in 1890¹ and was followed shortly after by the discovery of $\text{Fe}(\text{CO})_5$ in 1891². By 1910, the recently deceased Mond had catalogued an impressive array of binary metal carbonyls, including those of nickel, cobalt, iron, molybdenum, and an ill-defined ruthenium specimen³. That the late Ludwig Mond had left an impressive legacy is evidenced by the extensive development of metal carbonyl chemistry. That his impressive legacy lead to his lateness remains for forensic science to speculate.

While Mond had succeeded in establishing the empirical nature of the mononuclear binary metal carbonyls, it was the enterprise of Linus Pauling to establish their molecular nature. In the pre-Sidgwick era of Mond the ruthenium carbonyls were described and accepted as ' $\text{Ru}(\text{CO})$ ' and ' $\text{Ru}(\text{CO})_2$ '³. In what must be the first legitimate formulation of organometallic chemistry dogma, Pauling proposed, based on his electron-pair bonding theory that a transition metal should strive to use its nine *eigenfunctions*, filling the $(n-1)d$, ns , and np valence orbitals with nine electron pairs⁴. Based on their observed diamagnetism the known binary, mononuclear carbonyls were formulated as $\text{Ni}(\text{CO})_4$, $\text{Fe}(\text{CO})_5$, $\text{Cr}(\text{CO})_6$, and $\text{Mo}(\text{CO})_6$. Going yet further, in a flash of Mendeleevian foresight, Pauling predicted the existence of the mononuclear carbonyls $\text{Ru}(\text{CO})_5$ and $\text{Os}(\text{CO})_5$.

1.2 The Mononuclear, Binary Carbonyls of Group 8

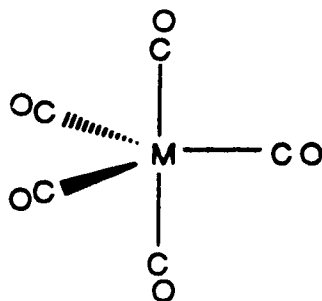
Apart from the Group 6 binary carbonyls⁵, the only other complete series of neutral, mononuclear, binary transition metal carbonyl complexes are the Group 8 carbonyls⁵. By representing a complete group of transition metals, the Group 8 carbonyls provide for a rich comparative chemistry precisely because any deviation in their properties can be ascribed to the metals themselves. Owing to their homology, the $M(\text{CO})_5$ complexes present a vast array of experimental and theoretical investigation into their comparative structure and reactivity.

The binary, mononuclear carbonyls of Group 8 are typically musty smelling and highly toxic complexes that are volatile liquids at ambient temperature. Matters are complicated by the instability of the complexes, making their characterization and purification problematic⁵. Both iron and ruthenium carbonyls can be prepared by the action of carbon monoxide on the finely divided metal; $\text{Fe}(\text{CO})_5$ can often be found inside gas cylinders of carbon monoxide. However, in practice $\text{Fe}(\text{CO})_5$ can be purchased commercially and $\text{Ru}(\text{CO})_5$ prepared by photolysis of $\text{Ru}_3(\text{CO})_{12}$ ^{6a} or reductive carbonylation of Ru(III) in an autoclave^{6b}. The preparation of $\text{Os}(\text{CO})_5$ requires a slightly more perilous approach involving OsO_4 or $\text{Os}_3(\text{CO})_{12}$ heated in an autoclave under high pressures of carbon monoxide^{6b,c} (scheme 1.1).



Scheme 1.1 Preparations of $M(\text{CO})_5$ ($M = \text{Ru}, \text{Os}$)

While the formulas of the $M(\text{CO})_5$ complexes have been well established for the better part of the past century, it was not until the early nineteen sixties that diffraction studies revealed the trigonal-bipyramidal structure of $\text{Fe}(\text{CO})_5$. Furthermore the determination of precise bond lengths and angles for $\text{Fe}(\text{CO})_5$ has only just recently appeared in the literature⁷. In the latter half of the nineteen sixties infrared studies undertaken by Calderazzo and L'Eplattenier verified that ruthenium and osmium pentacarbonyls possessed D_{3h} symmetry^{6b} and were isostructural with their iron congener (scheme 1.2). The three



M	Fe	Ru	Os
Infrared (cm^{-1})	2022 m, 2000 s	2036 m, 2002 s	2035 m, 1993 s
^{13}C NMR (ppm)	210.6	200.4	182.6

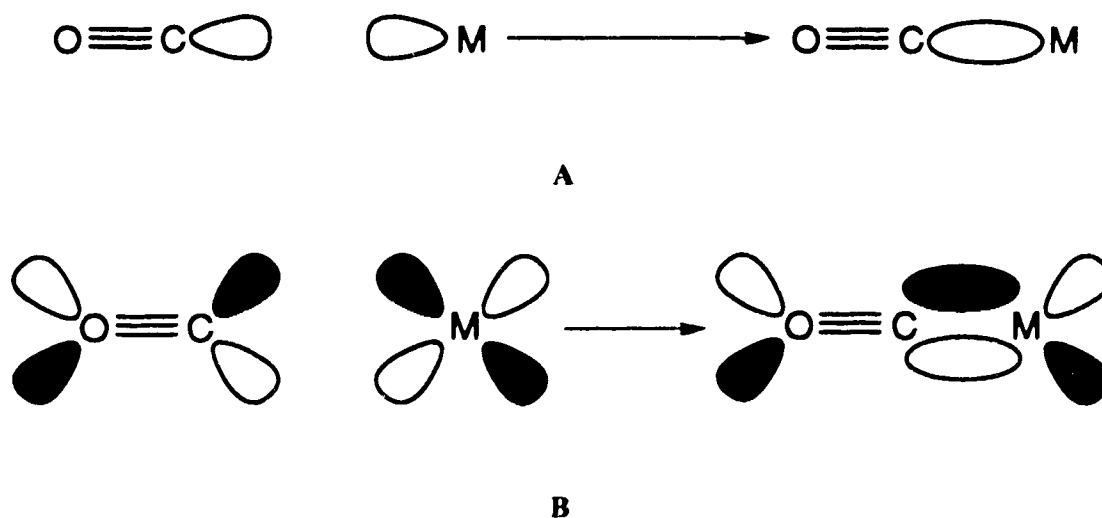
Scheme 1.2 Comparison of the $M(\text{CO})_5$ Complexes

complexes are fluxional in solution, readily exchanging axial and equatorial carbonyls; the energy barrier to carbonyl exchange for $\text{Fe}(\text{CO})_5$ is less than 8 kJ/mol⁸.

As mentioned earlier, any deviation in the properties of the mononuclear, binary carbonyls of group 8 can be traced to the metals themselves. From an experimental

standpoint it is well accepted that, within a specific group, the chemical properties of the second and third row transition metals share greater similarities with one another than either does with its first row congener⁵. An illuminating example of the aforementioned similarities is the trend in the covalent radii of iron (1.165 Å), ruthenium (1.24 Å), and osmium (1.26 Å)⁹. Theoretical studies have revealed further group trends. The mean M-CO bond energies for Ru(CO)₅ and Os(CO)₅ are quite similar (162.8 and 176.7 kJ mol⁻¹) and significantly less than that for Fe(CO)₅ (216.8 kJ mol⁻¹)¹⁰.

The typical interactions involved in metal-carbonyl bonding are outlined in scheme 1.3. Interaction A involves electron donation from a filled σ_{CO} -orbital to an empty σ_{M} -orbital



Scheme 1.3 M-CO Bonding: A, σ -interaction and B, π -interaction

and interaction B involves electron donation from a filled metal d_{π} -orbital to an empty π^*_{CO} -orbital. Theoretical calculations have shown that the energetics of metal-carbonyl bonding for all three metals are most dependent on π -bonding, with σ -bonding contributing

slightly more for ruthenium and osmium than for iron¹⁰. With this in mind, the observed energetic differences in M-CO bonding are attributed to two causes, the first being greater destabilization of M-CO σ -donation in $\text{Ru}(\text{CO})_5$ and $\text{Os}(\text{CO})_5$ due to repulsive interactions between filled metal-based orbitals and filled σ -bonding orbitals and the second being the stabilization of M-CO back-donation in $\text{Fe}(\text{CO})_5$ due to more favourable overlap of filled metal d_{π} -orbitals with empty carbonyl π^* -orbitals. Such calculations do have a basis in reality as experimental observations reveal that $\text{Fe}(\text{CO})_5$ is the most thermally stable of the $\text{M}(\text{CO})_5$ complexes, followed by $\text{Os}(\text{CO})_5$, and then $\text{Ru}(\text{CO})_5$.

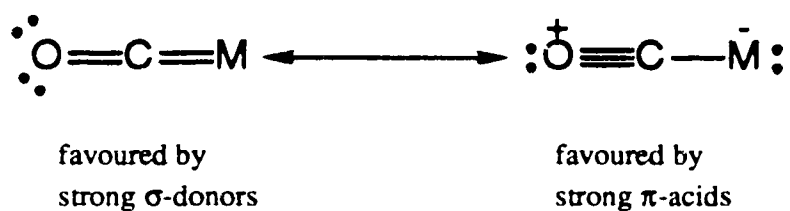
1.3 A Survey of $\text{M}(\text{CO})_4\text{L}$ Complexes

Of the three Group 8 mononuclear, binary carbonyl complexes the chemistry of iron is most well established, including oxidative addition, ligand substitution, and photochemical reactivity¹¹. In contrast, the chemistry of ruthenium and osmium pentacarbonyls are less well known, no doubt due to the difficulties in procuring the $\text{M}(\text{CO})_5$ complexes from both a synthetic and logistical standpoint. While iron is the most abundant of the transition metals, ruthenium and osmium are among the least prevalent of the naturally occurring elements, on the order of 10^7 - 10^8 times less abundant in the earth's crust than iron⁹.

Complexes of the type $\text{M}(\text{CO})_4\text{L}$, where L is a neutral, two electron donating ligand, are well established for iron and numerous reports have been devoted to such systems¹¹. Not unexpectedly, ruthenium¹² and osmium^{12a,d,13} both form complexes analogous to the phosphine, alkene, and alkyne complexes of iron.

The substitution of a phosphine for a carbonyl on an $\text{M}(\text{CO})_5$ complex can greatly alter the physical and chemical properties of the parent carbonyl complex. For instance, all three $\text{M}(\text{CO})_5$ complexes are liquids at room temperature⁵, while the $\text{M}(\text{CO})_4(\text{PMe}_3)$ complexes are solids^{12a}.

The bonding of phosphines to transition metals parallels that of carbon monoxide, as synergy between σ - and π -bonding interactions are extant in both instances. While it is accepted that phosphines are poorer π -acceptors than carbon monoxide, they are superior σ -donors, effectively rendering the metal center more electron rich⁵. Greater electron density on the metal allows for stronger metal-carbonyl interactions through greater back-donation from the metal (scheme 1.4), which in many cases can render an $M(CO)_4L$



Scheme 1.4 The Two Canonical Forms of Metal Carbonyl Bonding

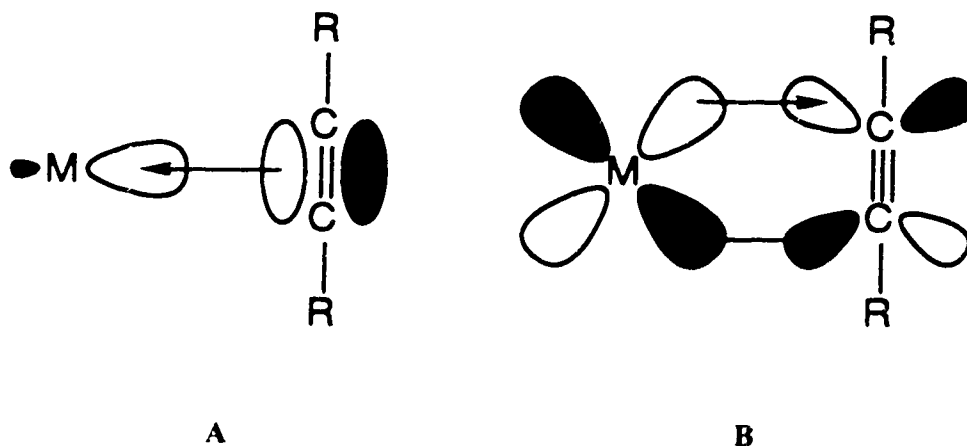
complex less labile than the parent pentacarbonyl. The stronger metal-carbonyl back-bonding results in a reduction of the C-O bond order and lowering of the average carbonyl stretching frequencies (table 1.1).

complex	ν_{CO} (in cm^{-1})	complex	ν_{CO} (in cm^{-1})
$Fe(CO)_5$	2022, 2000	$Fe(CO)_4(PMe_3)$	2051, 1978, 1937
$Ru(CO)_5$	2036, 2002	$Ru(CO)_4(PMe_3)$	2061, 1985, 1947
$Os(CO)_5$	2035, 1993	$Os(CO)_4(PMe_3)$	2061, 1983, 1946

Table 1.1 Listing of $M(CO)_5$ and $M(CO)_4L$ Carbonyl Stretching Frequencies

In contrast to the linear carbon monoxide ligand, phosphines are considerably more sterically demanding. Thus, the steric impact of the phosphine is an important consideration in any complex, and this has been the subject of exhaustive review¹⁴.

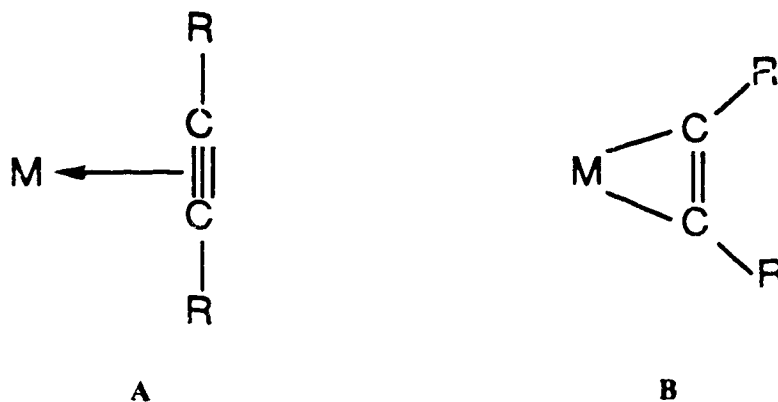
The bonding of alkenes and alkynes to transition metals also involves synergic interactions. The Dewar-Chat-Duncanson bonding description satisfactorily accounts for the bonding observed in both metal-alkene and -alkyne complexes¹⁵ (scheme 1.5). The



Scheme 1.5 The σ - and π -Components of Metal-Alkyne Bonding

unsaturated ligand acts as a σ -donor by donating its π -bonding electrons into the empty σ_M -orbital (scheme 1.5, A). The π -component of bonding arises from donation from the filled metal d_π -orbital into the empty π^*_{C-C} orbital on the alkyne (scheme 1.5, B). The synergy of these two bonding interactions dictate the nature of the metal alkyne interaction. If the σ -component dominates, the C-C bond distance will reflect a triple bond and the alkyne should be approximately linear (scheme 1.6, A). Conversely, when π -bonding dominates, the C-C bond distance approaches that of a double bond and the substituents on the alkyne are bent away from the metal (scheme 1.6, B). Thus, when R is an electron

donating group, such as CH_3 , structure **A** is favoured, while structure **B** is favoured by electron withdrawing groups, such as CF_3 .



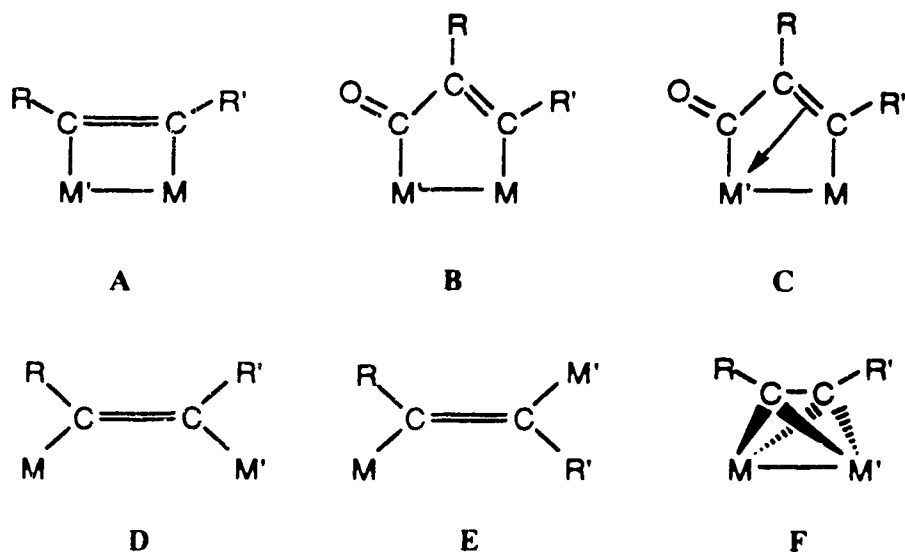
Scheme 1.6 The Two Valence Bond Extremes of Metal-Alkyne Bonding

In contrast to the axial coordination observed for simple phosphines^{12a}, both alkenes and alkynes occupy an equatorial site^{6a,11,12b,17d}. The equatorial preference of these unsaturated organic ligands is predicated on the basis of their competing less with the equatorial carbonyls for π -electron density¹⁶.

As well as the observed ligand dependence of the $\text{M}(\text{CO})_4\text{L}$ complexes, there is also a significant metal dependence. When L is acetylene, the osmium complex can be readily prepared *via* low-temperature photolysis^{17d}. This complex is stable up to 0°C , which contrasts markedly with the ruthenium analogue, prepared in the same fashion, which decomposes above -40°C ^{17d}. The iron complex has not been reported. The ethylene complexes provide a similar comparison. $\text{Os}(\text{CO})_4(\eta^2\text{-C}_2\text{H}_4)$ proves to be rather inert towards ligand substitution¹³, while the ruthenium complex is a versatile source of the ' $\text{Ru}(\text{CO})_4$ ' fragment, following loss of ethylene^{6a}. It is clear that properties of the $\text{M}(\text{CO})_4\text{L}$ complexes are intimately related to the nature of both the metal and the ligand.

1.4 Survey of Alkyne Bridged Dimetallic Complexes

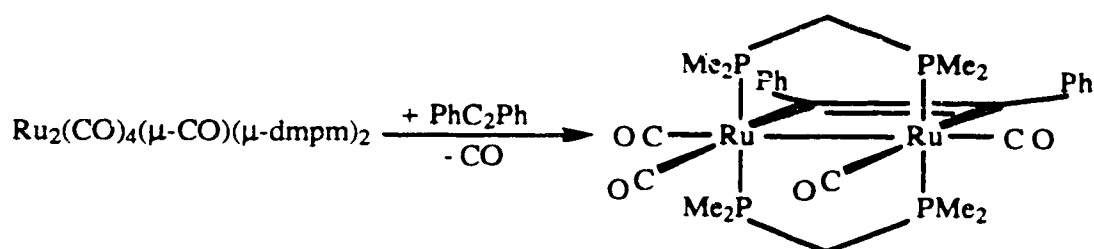
The metal-metal bonded dimetallic complexes that have been prepared with alkyne bridges fall into several categories: η^1, η^1 -dimetallacyclobutenes^{17a-p}, **A**, η^1, η^1 -dimetallacyclopentenones^{17b,d,n}, **B**, and η^1, η^3 -dimetallacyclopentenones^{17d,i,l,18a-d}, **C**, *cis* and *trans*-dimetallated alkenes¹⁹, **D** and **E**, and η^2, η^2 -dimetallacyclobutenes²⁰, **F** (scheme 1.7). The present discussion will focus on types **A**, **B**, and **C**.



Scheme 1.7 Six Types of Dimetallacyclic Structure

Since the first dimetallacyclobutene complex, $\text{Fe}_2(\text{CO})_8(\mu\text{-C}_6\text{F}_4)$, was reported in 1970²¹ numerous other examples have surfaced and have been reviewed in Hoffmann's seminal work on dimetallic alkyne complexes²⁰. For reasons of brevity the reader is referred to Hoffmann's treatise on dimetallacyclobutene and -pentenone complexes for a thorough review of these compounds prior to 1982.

Dimetallacyclic complexes can be prepared by a number of methods. For instance, alkynes will react with existing dimetallic complexes *via* ligand displacement. Very often the two metals are bridged by bidentate diphosphine ligands, as is the case with the complex $\text{Ru}_2(\text{CO})_4(\mu\text{-dmpm})_2(\mu\text{-CO})$ ($\text{dmpm} = \text{Me}_2\text{PCH}_2\text{PMe}_2$), reported by Gladfelter^{17e}. When this complex is treated with diphenyl acetylene, the alkyne displaces the bridging carbonyl to yield an η^1, η^1 -dimetallacyclobutene (scheme 1.8). When the



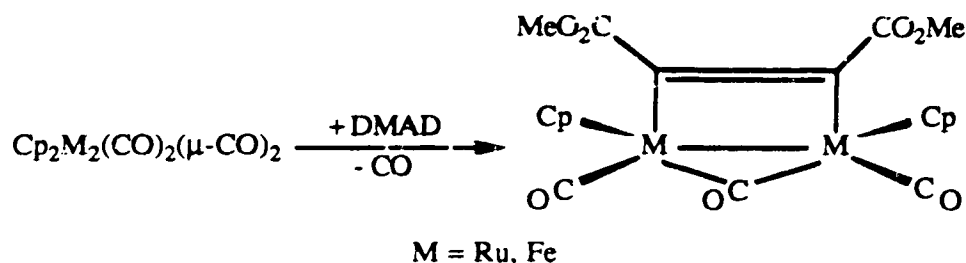
Scheme 1.8 Synthesis of $\text{Ru}(\text{CO})_4(\mu\text{-dmpm})_2(\mu\text{-}\eta^1, \eta^1\text{-PhC}_2\text{Ph})$

reaction is repeated with the strongly π -acidic alkyne DMAD ($\text{MeO}_2\text{CC}_2\text{CO}_2\text{Me}$) a dimetallacyclopentenone product, $\text{Ru}_2(\text{CO})_4(\mu\text{-dmpm})_2(\mu\text{-}\eta^1, \eta^1\text{-C}(\text{O})\text{C}_2(\text{CO}_2\text{Me})_2)$ ^{17b}, results *via* alkyne insertion into a bridging carbonyl-metal bond. Only three complexes having structure **B** have been reported^{17b,d,n}, and the majority of dimetallacyclopentenone complexes adopt structure **C**^{17d,i,l,18a-d}.

Much of the pioneering work on η^1, η^3 -dimetallacyclopentenones has been the domain of Knox, who has prepared numerous examples of these complexes *via* combined insertion and ligand displacement^{17i,l,18c,d}.

Knox has also prepared dimetallacyclobutenes by ligand displacement. When treated with DMAD, $\text{Cp}_2\text{M}_2(\text{CO})_2(\mu\text{-CO})_2$ ($\text{M} = \text{Fe}, \text{Ru}$) loses carbon monoxide to yield structure type **A**^{17l} (scheme 1.9). It is noteworthy that the majority of **A** structures are prepared from diphosphine bridged complexes.

Dimetallacycles have also been prepared from the reaction of alkynes with monomeric metal complexes. For example, Dixon has reported the preparation of a dimetallacyclobutene complex from heating $\text{CpRh}(\text{CO})_2$ in the presence of excess hexafluorobutyne (HFB)²².

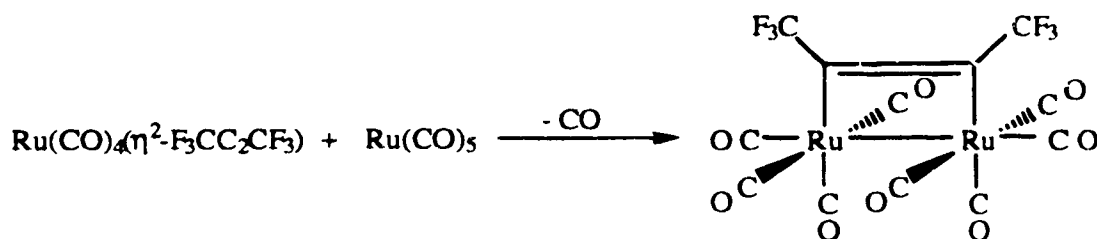


Scheme 1.9 Synthesis of $\text{Cp}_2\text{M}_2(\text{CO})_2(\mu\text{-CO})(\mu\text{-}\eta^1,\eta^1\text{-C}_2\{\text{CO}_2\text{Me}\}_2)$

The final method of preparation was first pioneered by Stone²³ and exploited more fully by this research group^{17d,f}. This method involves the combination, or condensation, of two monomeric metal complexes to yield an alkyne bridged dimetallic complex. It was discovered by this research group that such a reaction was occurring during the preparation of $\text{Ru}(\text{CO})_4(\eta^2\text{-HFB})$. The alkyne complex scavenged unreacted $\text{Ru}(\text{CO})_5$ and readily formed a dimetallacyclobutene complex, with concomitant loss of carbon monoxide (scheme 1.10). Even more remarkable was the condensation of $\text{Os}(\text{CO})_4(\eta^2\text{-HC}_2\text{H})$ and $\text{Ru}(\text{CO})_5$, both 18-electron complexes, which generated a dimetallacyclopentenone complex without ligand loss^{17d}.

The great advantage of the condensation method is that, in addition to π -acidic alkynes such as DMAD, diphenyl acetylene, and hexafluorobutyne, more σ -basic alkynes such as 2-butyne, propyne, and acetylene may also be employed²⁴, a distinction seldom enjoyed by the other methods outlined.

At this point it is worth commenting on the relation between dimetallacyclobutenes and dimetallacyclopentenones. In principle the two structures are related by simple carbonyl insertion and de-insertion reactions. While examples of de-insertion do exist¹⁷ⁿ, to this date there has been no reported example of carbonyl insertion into a preformed dimetallacyclobutene.



Scheme 1.10 Synthesis of $\text{Ru}_2(\text{CO})_8(\mu\text{-}\eta^1, \eta^1\text{-F}_3\text{CC}_2\text{CF}_3)$

1.5 Scope of Present Research

Transition metal alkyne complexes have proven to be intriguing chemical species both as mono- and dimetallic complexes. For example, Gladfelter has recently reported that $\text{Ru(CO)}_4(\eta^2\text{-HFB})$, a complex first prepared by the Takats research group^{17f}, is a useful source of metallic ruthenium in chemical vapour deposition²⁵. Also, the Knox research group has developed an extensive array of organic transformations employing dimetallacyclic alkyne complexes²⁶.

As outlined in the preceding survey most alkyne bridged dimetallic complexes are prepared from preformed dimetallic frameworks and tend to be homobimetallic in character. Research conducted in our laboratories have demonstrated that $\text{M(CO)}_4(\eta^2\text{-alkyne})$ complexes are convenient and versatile synthons in the preparation of dimetallic complexes,

affording the use of numerous electron rich alkynes that are not tenable with the other methods.

The present work was carried out on the premise of furthering the possibilities of metal and alkyne combinations. Specifically, it was of interest to investigate the regiochemistry of condensation reactions involving asymmetric alkynes and whether the gulf between dimetallacyclobutenes and dimetallacyclopentenones could be bridged.

1.6 References

- (1) Mond, L.; Langer, C.; Quincke, F. *J. Chem. Soc.* **1890**, 749.
- (2) Mond, L.; Langer, C. *J. Chem. Soc.* **1891**, 1090.
- (3) Mond, L.; Hirtz, H.; Cowap, M.P. *J. Chem. Soc.* **1910**, 798.
- (4) Pauling, L. *J. Am. Chem. Soc.* **1931**, 53, 1367.
- (5) Cotton, F. A.; Wilkinson, G. *Advanced Inorganic Chemistry*, 5th ed.; John Wiley & Sons: Toronto, 1988.
- (6) (a) Johnson, B. F. G.; Lewis, J.; Twigg, M. V. *J. Organomet. Chem.* **1974**, 67, C75. (b) Calderazzo, F.; L'Eplattenier, F. *Inorg. Chem.* **1967**, 6, 1220. (c) Rushman, P.; van Buuren, G. N.; Shiralian, M.; Pomeroy, R. K. *Organometallics* **1983**, 2, 693.
- (7) Braga, D.; Grepioni, F.; Orpen, A. G. *Organometallics* **1993**, 12, 1481.
- (8) Adams, R. D.; Cotton, F. A. In *Dynamic Nuclear Magnetic Resonance Spectroscopy*; Cotton, F. A.; Jackman, L. M. Eds.; Academic: New York, 1975.
- (9) Emsley, J. *The Elements*, 2nd ed.; Oxford: New York, 1991.
- (10) Ziegler, T.; Tschinke, V.; Ursenbach, C. *J. Am. Chem. Soc.* **1987**, 109, 4825.
- (11) Adams, R. D.; Shriver, D. F.; Whitmire, K. H.; Johnson, M. D.; Deeming, A. J. In *Comprehensive Organometallic Chemistry*; Wilkinson, G.; Stone, F. G. A.; Abel, E. W. Eds.; 1982; Vol. 5.
- (12) (a) Einstein, F. W. B.; Martin, L. R.; Pomeroy, R. K. *Inorg. Chem.* **1985**, 24, 2777, and references therein. (b) Takats, J.; Grevels, F.-W.; Reuvers, J. G. A. In *Inorganic Syntheses*, Shreeve, J. M. Ed.; 1986; Vol. 24. (c) Johnson, B. F. G.; Lewis, J.; Twigg, M. V. *J. Organomet. Chem.* **1974**, 67, C75. (d) Burn, M. J.; Kiel, G.-Y.; Seils, F.; Takats, J.; Washington, J. *J. Am. Chem. Soc.* **1989**, 111, 6850.

- (13) (a) Burke, M. R.; Takats, J.; Grevels, F.-W.; Reuvers, J. G. A. *J. Am. Chem. Soc.* **1983**, *105*, 4092. (b) Takats, J. *Polyhedron* **1988**, *7*, 931. (c) Bender, B. R.; Norton, J. R.; Miller, M. M.; Anderson, O. P.; Rappé, A.K. *Organometallics* **1992**, *11*, 3427.
- (14) Rahman, M. M.; Liu, H.-Y.; Eriks, K.; Prock, A.; Giering, W. P. *Organometallics* **1989**, *8*, 1.
- (15) (a) Dewar, M. J. S.; *Bull. Soc. Chim. Fr.* **1951**, *18*, C79. (b) Chatt, J.; Duncanson, L. A. *J. Chem. Soc.* **1953**, 2939.
- (16) Rossi, A. R.; Hoffmann, R. *Inorg. Chem.* **1975**, *14*, 365.
- (17) (a) Jenkins, J. A.; Cowie, M. *Organometallics* **1992**, *11*, 2767. (b) Johnson, K. A.; Gladfelter, W. L. *Organometallics* **1992**, *11*, 2534. (c) Mague, J. T. *Polyhedron* **1990**, *9*, 2635. (d) Burn, M. J.; Kiel, G.-Y.; Seils, F.; Takats, J.; Washington, J. *J. Am. Chem. Soc.* **1989**, *111*, 6850. (e) Johnson, K. A.; Gladfelter, W. L. *Organometallics* **1989**, *8*, 2866. (f) Gagné, M. R.; Takats, J. *Organometallics* **1988**, *7*, 561. (g) Burke, M. R.; Takats, J. *J. Organomet. Chem.* **1986**, *302*, C25. (h) Mague, J. T. *Organometallics* **1986**, *5*, 918. (i) Gracey, B. P.; Knox, S. A. R.; Macpherson, K. A.; Orpen, A. G.; Stobart, S. R. *J. Chem. Soc., Dalton Trans.* **1985**, 1935. (j) Cowie, M.; Dickson, R. S.; Hames, B. W. *Organometallics* **1984**, *3*, 1879. (k) Cowie, M.; Sutherland, B. R. *Organometallics* **1984**, *3*, 1869. (l) Dyke, A. F.; Knox, S. A. R.; Naish, P. J.; Taylor, G. E. *J. Chem. Soc., Dalton Trans.* **1982**, 1297. (m) Cowie, M.; Southern, T. G. *Inorg. Chem.* **1982**, *21*, 246. (n) Dickson, R. S.; Gatehouse, B. M.; Nesbit, M. C.; Pain, G. N. *J. Organomet. Chem.* **1981**, *215*, 97. (o) Cowie, M.; Dickson, R. S. *Inorg. Chem.* **1981**, *20*, 2682. (p) Koie, Y.; Sinoda, S.; Saito, Y.; Fitzgerald, B. J.; Pierpont, C. G. *Inorg. Chem.* **1980**, *19*, 770.
- (18) (a) Kiel, G.-Y.; Takats, J. *Organometallics* **1989**, *8*, 839. (b) Fontaine, X. L. R.; Jacobsen, G. B.; Shaw, B. L.; Thornton-Pett, M. *J. Chem. Soc., Dalton Trans.*

- 1988, 741. (c) Hogarth, G.; Kayser, F.; Knox, S. A. R.; Morton, D. A. V.; Orpen, A. G.; Turner, M. L. *J. Chem. Soc., Chem. Commun.* **1988**, 358. (d) Dyke, A. F.; Knox, S. A. R.; Naish, P. J.; Taylor, G. E. *J. Chem. Soc., Chem. Commun.* **1980**, 409.
- (19) Adams, R. D.; Chen, L.; Wu, W. *Organometallics* **1993**, *12*, 1257, and references therein.
- (20) Hoffman, D. M.; Hoffmann, R.; Fisel, C. R. *J. Am. Chem. Soc.* **1982**, *104*, 3858 and references therein.
- (21) (a) Roe, D. M.; Massey, A. G. *J. Organomet. Chem.* **1970**, *23*, 547. (b) Bennett, M. J.; Graham, W. A. G.; Stewart, R. P.; Tuggle, R. M. *Inorg. Chem* **1973**, *12*, 2944.
- (22) (a) Dickson, R. S.; Mok, C.; Pain, G. *J. Organomet. Chem.* **1979**, *166*, 385. (b) Dickson, R. S.; Kirsch, H. D.; Lloyd, D.J. *J. Organomet. Chem.* **1975**, *101*, 97.
- (23) Boag, N.M.; Green, M.; Stone, F. G. A.; Wadepohl, H. *J. Chem. Soc., Dalton Trans.* **1981**, 862.
- (24) Washington, J. Ph. D. Thesis, University of Alberta, 1994.
- (25) Gladfelter, W. L.; McCormick, F. B.; Senzaki, Y. *Materials*, **1992**, *4*, 747.
- (26) Knox, S. A. R. *J. Organomet. Chem.* **1990**, *400*, 255.

Chapter Two

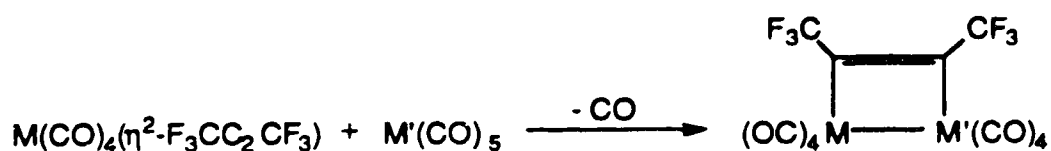
Synthesis and Characterization of $\text{Ru}(\text{CO})_4(\eta^2\text{-HC}_2\text{CF}_3)$ and $\text{Ru}(\text{CO})_4(\text{PMe}_3)$

2.1 Introduction

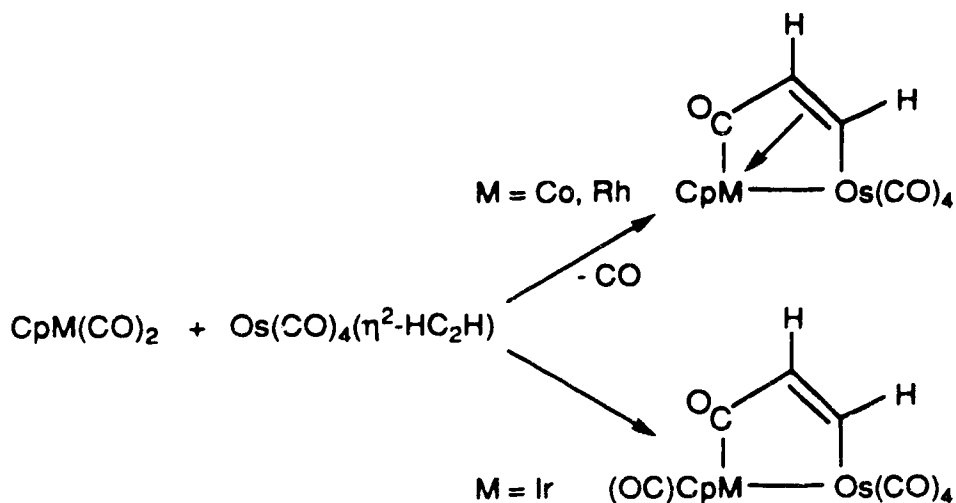
Previous research from this group has involved preparation of ruthenium and osmium tetracarbonyl-alkyne complexes from the photoreaction of $\text{M}(\text{CO})_5$ ($\text{M} = \text{Ru}, \text{Os}$) in the presence of an appropriate alkyne ligand. To this end, several $\text{M}(\text{CO})_4(\eta^2\text{-RC}_2\text{R}')$ ($\text{M} = \text{Ru}, \text{Os}$) complexes have been prepared^{1a-d}. The ruthenium tetracarbonyl-alkyne complexes are much less thermally robust than the analogous osmium complexes, with the exception of the π -acidic alkyne, hexafluorobutyne. For example, while $\text{Os}(\text{CO})_4(\eta^2\text{-HC}_2\text{H})$ subsists in solution above 0°C ^{1c}, $\text{Ru}(\text{CO})_4(\eta^2\text{-HC}_2\text{H})$ decomposes above -40°C ^{1b}, rendering it an unviable participant in the preparation of dimetallacycles. In stark contrast, $\text{Ru}(\text{CO})_4(\eta^2\text{-F}_3\text{CC}_2\text{CF}_3)$ is thermally stable at room temperature^{1d}, and with this in mind it was hoped that introducing a single perfluoromethyl group onto the alkyne would impart similar thermodynamic stability to $\text{Ru}(\text{CO})_4(\eta^2\text{-HC}_2\text{CF}_3)$.

The complexes $\text{Os}(\text{CO})_4(\eta^2\text{-HC}_2\text{H})$ ^{1a,c} and $\text{M}(\text{CO})_4(\eta^2\text{-F}_3\text{CC}_2\text{CF}_3)$ ^{1d} ($\text{M} = \text{Ru}, \text{Os}$) have been shown to undergo condensation reactions with $\text{M}'(\text{CO})_5$ ($\text{M}' = \text{Ru}, \text{Os}$) and $\text{Cp}'\text{M}'(\text{CO})_2$ ($\text{M}' = \text{Co}, \text{Rh}, \text{Ir}$; $\text{Cp}' = \text{Cp}, \text{Cp}^*$) to give dimetallacyclic products (scheme 2.1). The impetus behind preparing $\text{Ru}(\text{CO})_4(\eta^2\text{-HC}_2\text{CF}_3)$ was, in part, to extend the dimetallacyclic chemistry to include asymmetric alkynes; however, of paramount interest was the development of a reliable synthetic method leading to $\text{Ru}(\text{CO})_4(\eta^2\text{-HC}_2\text{CF}_3)$ and its subsequent characterization.

As opposed to the liquid binary carbonyls $\text{Ru}(\text{CO})_5$ and $\text{Os}(\text{CO})_5^2$, complexes of the type $\text{M}(\text{CO})_4\text{PR}_3$ ($\text{M} = \text{Ru}, \text{Os}$; $\text{R} = \text{alkyl, alkoxy}$)³ are sublimable, moderately air-stable solids, allowing for easier handling and quantification in comparison to the parent carbonyls. Owing to their desirable properties, $\text{Ru}(\text{CO})_4(\text{PR}_3)$ complexes are prime



$\text{M}, \text{M}' = \text{Ru}, \text{Os}$



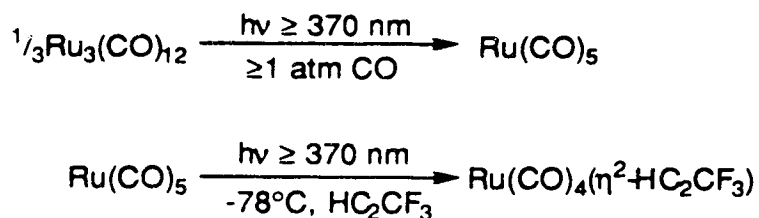
Scheme 2.1 Preparation of Dimetallacycles Using $\text{M}(\text{CO})_4(\eta^2\text{-alkyne})$ Complexes

candidates for the preparation of dimetallacycles, not only from a synthetic standpoint, but also from a spectroscopic standpoint; ^{31}P is a spin one-half nucleus and could provide valuable coupling information useful in elucidating the regiochemistry of the condensation

reactions. A further goal in exploiting the $\text{Ru}(\text{CO})_4(\text{PR}_3)$ complexes as useful precursors in dimetallacycle preparation was the development of an improved synthetic procedure which would give a single, mono-substituted phosphine complex in high yield, a heretofore elusive accomplishment.

2.2 Synthesis and Characterization of $\text{Ru}(\text{CO})_4(\eta^2\text{-HC}_2\text{CF}_3)$, **1a**

The title compound was prepared using essentially the same procedure employed to prepare the other $\text{M}(\text{CO})_4(\eta^2\text{-RC}_2\text{R}')$ ^{1a-d} complexes (scheme 2.2), the exception being that the reaction temperature was reduced from -20°C to -70°C to accommodate the change in alkyne ligands (trifluoropropyne vapourizes at -48°C ⁴, hexafluorobutyne at -25°C ⁴). While the hexafluorobutyne complex could be isolated in *ca.* 80% yield, the trifluoropropyne complex could only be obtained in 54% yield. In the case of the hexafluorobutyne complex, the yield was determined by weighing the product; however, weighing is not possible with the trifluoropropyne complex as it decomposes to an orange, rancid smelling liquid above -20°C . Therefore, it was necessary to determine the yield of the trifluoropropyne complex indirectly *via* infrared spectroscopy, the details of which will be outlined in section 2.6.



Scheme 2.2 Preparation of $\text{Ru}(\text{CO})_4(\eta^2\text{-HC}_2\text{CF}_3)$, **1a**

Both the trifluoropropyne and hexafluorobutyne complexes are white, sublimable, air stable solids. It is noteworthy that the thermal stability of the complexes is extremely alkyne dependent: the hexafluorobutyne complex is stable at room temperature^{1d}, the trifluoropropyne complex decomposes above -20°C, and the acetylene complex decomposes above -40°C^{1b}.

The infrared spectrum of the pure trifluoropropyne complex exhibits three carbonyl stretching frequencies at 2131, 2056, and 2025 cm⁻¹. The coordinated alkyne stretching frequency occurs at 1771 cm⁻¹. However, invariably the spectrum is contaminated by numerous bands in the terminal carbonyl region, many of which are coincident with those observed for the condensation product Ru₂(CO)₈(μ-η¹,η¹-HC₂CF₃), **3** (*vide infra*). When a freshly prepared sample of Ru(CO)₄(η²-HC₂CF₃) was allowed to warm to room temperature from -50°C in an infrared cell, the original bands disappeared, while new bands increased in intensity at 2130, 2114, 2089, 2050, 2036, and 2021 cm⁻¹. Apart from the band at 2114 cm⁻¹, all of the observed carbonyl stretching frequencies correspond to Ru₂(CO)₈(μ-η¹,η¹-HC₂CF₃) in wavenumber and relative intensity. Finally, the infrared bands for Ru(CO)₄(η²-HC₂CF₃) were confirmed by correlation with the frequencies and relative intensities observed for Ru(CO)₄(η²-HC₂H)^{1c} and Ru(CO)₄(η²-F₃CC₂CF₃)^{1d}. The infrared data for these three complexes are summarized in table 2.1.

The most notable feature of the data in table 2.1 is that the carbonyl stretching frequencies shift to progressively higher energy as the hydrogens are replaced with perfluoromethyl groups. The high energy shift can be explained by the increasing π-acid strength⁸ of the alkyne, due to the strongly electron withdrawing nature of the perfluoromethyl groups. The increased π-acidity of the alkyne gives rise to greater competition for metal π-electron density with the carbonyls and, as a result, the observed increase in carbon-oxygen bond strength, as reflected by the higher carbonyl stretching frequencies.

The alkyne bond stretching frequencies of the free ligands reflect the intrinsic strength of each carbon-carbon triple-bond; it requires more energy to stretch the triple bond in

hexafluorobutyne than in acetylene. Sigma bonding of the alkyne to the $\text{Ru}(\text{CO})_4$ fragment would result in weakening of the alkyne triple bond as electron density is donated from the alkyne bonding orbitals to the empty metal σ -orbitals. As a result, the coordinated triple

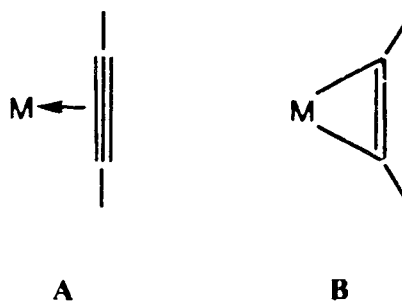
	R = R' = H	R = CF₃; R' = H	R = R' = CF₃
ν_{CO}	2115 w 2036 s 2028 m 2002 s	2131 vw 2056 s 2025 m	2143 w 2072 vs 2042 vs
ν_{CC} (coord)	1670 m	1771 vw	1856 w, 1818 vw
ν_{CC} (free)	1973 ⁵	2165 ⁶	2300 ⁷
Δ (free - coord)	273	394	444, 482

Table 2.1 Comparison of Infrared Stretching Frequencies (in cm^{-1}) for $\text{Ru}(\text{CO})_4(\eta^2\text{-RC}_2\text{R}')$ Complexes

bond stretching frequency should decrease in a way that reflects the nature of the donor. Hexafluorobutyne is the weakest σ -donor of the three alkynes, due to the strongly electron withdrawing perfluoromethyl groups, and its triple bond should undergo the smallest weakening, as reflected by Δ , the change in frequency upon coordination. However, experiment reveals that Δ becomes increasingly large as R and R' become more electron withdrawing, suggesting a commensurate reduction in the carbon-carbon bond order

inconsistent with σ -donation. Such a reduction in bond order is consistent with π -backbonding to the alkyne ligand from the $\text{Ru}(\text{CO})_4$ fragment. As the alkyne becomes more π -acidic, back-donation dominates in the bonding interaction. The observed shifts in triple bond stretching frequencies are consistent with experimental precedence⁹.

In short, when $\text{R} = \text{R}' = \text{H}$ the complex can be best regarded as approaching the valence bond limit of a σ -bound alkyne, **A**⁸, while when $\text{R} = \text{R}' = \text{CF}_3$ the complex approaches the valence bond limit of a metallacyclopropene, **B**⁸ (scheme 2.3).



**Scheme 2.3 The Two Valence Bond Extremes of Metal-Alkyne Bonding:
 σ -donation dominant, A; π -back donation dominant, B.**

The ^1H NMR spectrum of $\text{Ru}(\text{CO})_4(\eta^2\text{-HC}_2\text{CF}_3)$ consists of a quartet at δ 6.73, there being a four-bond coupling to fluorine of 2.9 Hz. In contrast, the chemical shift of the alkyne proton of free trifluoropropyne was determined to be δ 3.10^{1b}. The chemical shifts of protons attached to multiply bonded carbon atoms are influenced by the effects of diamagnetic anisotropy¹⁰, which dictate that magnetic fields induced by the multiple bonds result in the deshielding of alkene protons and shielding of alkyne protons. Thus, the downfield shift of the alkyne proton is consistent with the complex having metallacyclopropene character (scheme 2.3). Low-field shifts of the alkyne proton

resonances have been well established within this research group for a series of $M(\text{CO})_4(\eta^2\text{-RC}_2\text{R}')$ complexes^{1a-c}.

The $^{19}\text{F}\{^1\text{H}\}$ NMR shift of $\text{Ru}(\text{CO})_4(\eta^2\text{-HC}_2\text{CF}_3)$, δ -55.28, is comparable to that of the analogous hexafluorobutyne complex of δ -57.58^{1d} and rather unremarkable.

A sample of ^{13}C enriched $\text{Ru}(\text{CO})_4(\eta^2\text{-HC}_2\text{CF}_3)$ was prepared, in an analogous fashion to the non-enriched material, using ^{13}C enriched $\text{Ru}(\text{CO})_5$. The $^{13}\text{C}\{^1\text{H}\}$ NMR spectrum was determined at -35°C and consisted of three signals at δ 196.20, 194.84, and 189.04, in a 1:1:2 ratio (fig. 2.1). The molecule is non-fluxional at -35°C , adopting an idealized trigonal-bipyramidal geometry with the π -acceptor alkyne ligand occupying an in-plane, equatorial coordination site, as is observed for $\text{Ru}(\text{CO})_4(\eta^2\text{-F}_3\text{CC}_2\text{CF}_3)$ ¹¹. The high-field resonance corresponds to the two equivalent axial carbonyls, while the two lower field resonances correspond to the two inequivalent equatorial carbonyls, CO_{eq} at δ 194.84 and CO_{eq} at δ 196.20. The assignment of the two low-field resonances is based upon the presumed greater inductively withdrawing effect of the perfluoromethyl group on the carbonyl trans to it, CO_{eq} .

While $\text{Ru}(\text{CO})_4(\eta^2\text{-F}_3\text{CC}_2\text{CF}_3)$ is also non-fluxional^{1d}, $\text{Ru}(\text{CO})_4(\eta^2\text{-HC}_2\text{H})$ undergoes axial-equatorial carbonyl exchange down to a temperature of -108°C , at which point the fluxional exchange ceases^{1c}. Clearly, the perfluoromethyl group has a strong influence on the solution-rigidity of the trifluoropropyne and hexafluorobutyne complexes and, taken in concert with crystallographic data, leads further to the conclusion that these complexes are approaching metallacyclopropenes **B** (scheme 2.3).

The carbon atoms of the bound trifluoropropyne ligand were detected as three quartets at δ 122.52, 89.46, and 81.49, having carbon-fluorine coupling of 264.2, 7.2, and 46.7 Hz, respectively. The signal at δ 89.46 exhibits a disparately large intensity relative to the other alkyne carbons, as well as the smallest fluorine coupling, and is assigned as the *sp*-carbon with an attached proton. The observed intensity gain is attributable to the Nuclear Overhauser Effect (NOE)¹². The lowest field carbon signal has a typical one-bond,

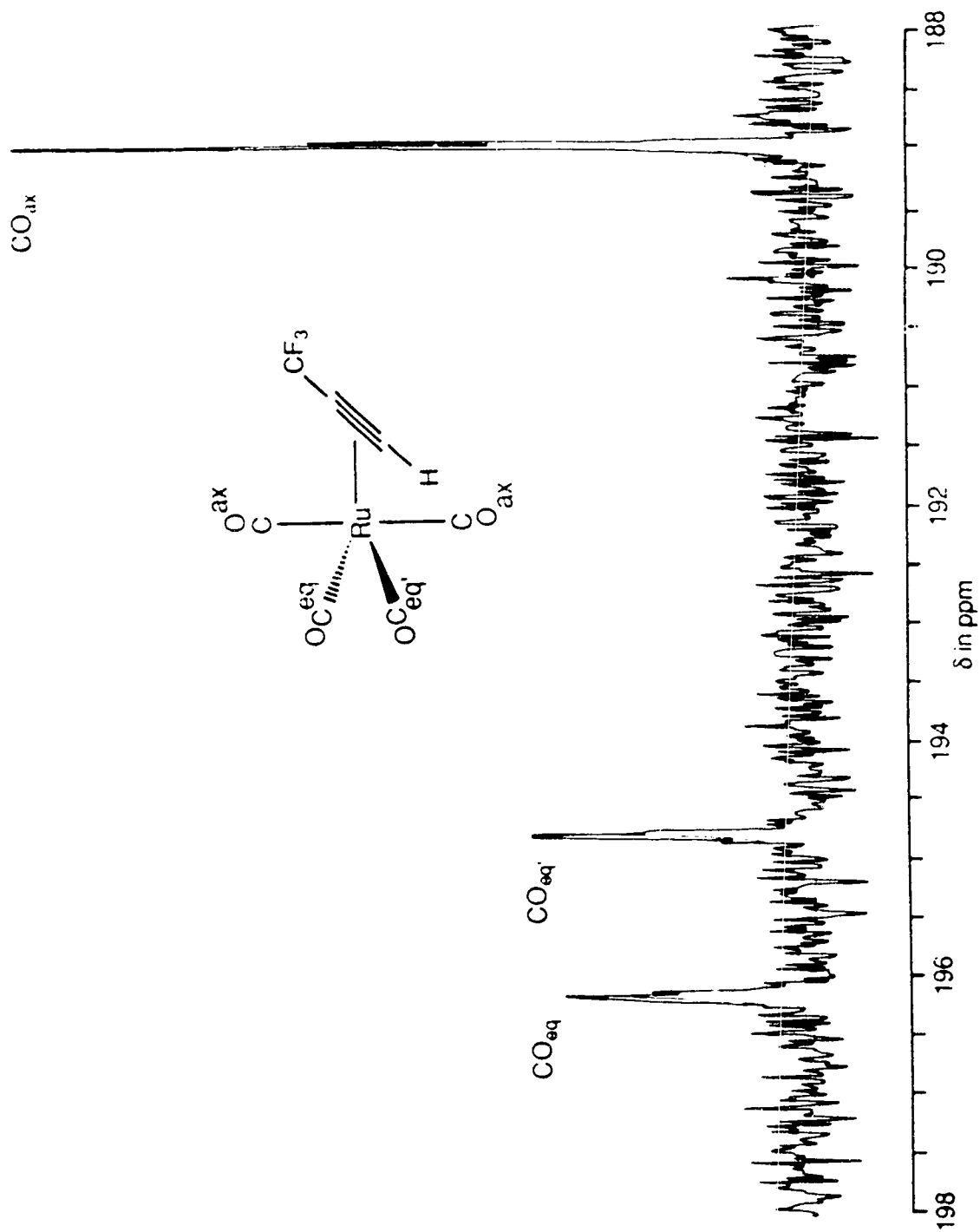


Figure 2.1 Low-temperature $^{13}\text{C}\{^1\text{H}\}$ NMR Spectrum of $\text{Ru}(\text{CO})_4(\eta^2\text{-HC}_2\text{CF}_3)$, **1a**

carbon-fluorine coupling¹³ and is assigned to the sp^3 , perfluoromethyl carbon. It remains that the highest field signal is the perfluoromethyl-bearing sp -carbon. The sp -carbon resonances of the free trifluoropropyne ligand occur at δ 75.9, for the proton-bearing carbon, and δ 69.2 for the perfluoromethyl-bearing carbon^{1b}. The low-field shift of the coordinated carbon resonances is, again, indicative of the complex having increased metallacyclopropene character.

2.3 Reactivity of $\text{Ru}(\text{CO})_4(\eta^2\text{-HC}_2\text{CF}_3)$, 1a

An interesting observation made by this research group was that $\text{Ru}(\text{CO})_4(\eta^2\text{-F}_3\text{CC}_2\text{CF}_3)$ and most $\text{Os}(\text{CO})_4(\eta^2\text{-RC}_2\text{R}')$ complexes could be enriched with ^{13}C by stirring a solution of the complex under an atmosphere of ^{13}C ; however, $\text{Ru}(\text{CO})_4(\eta^2\text{-HC}_2\text{CF}_3)$ cannot be enriched in this way. Stirring the trifluoropropyne complex under *ca.* 1 atmosphere ^{13}C and slowly warming the solution to 0°C results in decomposition of the complex with no enrichment, as judged by infrared spectroscopy. However, under a carbon monoxide atmosphere the complex does subsist above its normally observed decomposition temperature of *ca.* -20°C to almost -10°C . In comparison, the osmium analogue, $\text{Os}(\text{CO})_4(\eta^2\text{-HC}_2\text{CF}_3)$, readily undergoes ^{13}C substitution under the aforementioned conditions without apparent decomposition^{1a}.

However, much like other $\text{M}(\text{CO})_4(\eta^2\text{-RC}_2\text{R}')$ complexes^{1b,14}, $\text{Ru}(\text{CO})_4(\eta^2\text{-HC}_2\text{CF}_3)$ undergoes ligand substitution reactions with phosphines. It was hoped that by substituting a carbonyl with a phosphine ligand greater thermal stability would be imparted to the complex, due to the increased π -back donation from the metal to the carbonyl and trifluoropropyne ligands. As a result of this increased donation, decomposition *via* carbonyl and/or alkyne dissociation would be less favourable.

When two equivalents of trimethylphosphine were added to a stirred hydrocarbon solution of $\text{Ru}(\text{CO})_4(\eta^2\text{-HC}_2\text{CF}_3)$, cooled to -35°C , substitution appeared to occur immediately as noted by the appearance of new, lower energy carbonyl bands in the infrared spectrum at 1990 and 1928 cm^{-1} and an alkyne band at 1702 cm^{-1} . Similarly, when one equivalent of triphenylphosphine was employed the bands shifted to 1990 , 1927 , and 1700 cm^{-1} . However, neither pure substitution product could be isolated from either reaction.

2.4 An Alternative Synthesis of $\text{Ru}(\text{CO})_4(\text{PMe}_3)$, 2

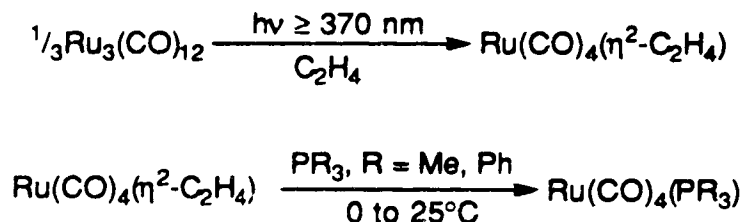
Complexes of the type $\text{Ru}(\text{CO})_4(\text{PR}_3)$ ($\text{R} = \text{alkyl, alkoxy}$) are well established in the organometallic literature³, being first prepared in the late nineteen sixties. To this end, Calderazzo and L'Eplattenier reported in 1968 the preparation of $\text{Ru}(\text{CO})_4(\text{PPh}_3)$ by the photoreaction of $\text{Ru}(\text{CO})_5$ and one equivalent of triphenylphosphine in tetrahydrofuran at room temperature¹⁵. In 1985, Pomeroy *et al.* reported the preparation of $\text{Ru}(\text{CO})_4(\text{PMe}_3)$ by the autoclave reaction of $\text{Ru}_3(\text{CO})_{12}$ and PMe_3 ³, while Cardaci reported the preparation of the same compound by the thermal reaction of $\text{Ru}_3(\text{CO})_{12}$ and PMe_3 in diethyl ether at room temperature¹⁶. Pomeroy has also reported the preparation of $\text{Ru}(\text{CO})_4(\text{PPh}_3)$ and $\text{Ru}(\text{CO})_4(\text{P}(\text{OCH}_2)_3\text{CCH}_3)$ by the thermal substitution of $\text{Ru}(\text{CO})_5$ ³.

In the aforementioned preparations yields of less than 50% have been reported, when reported at all. Furthermore, the preparations have been fraught with the formation of by-products such as $\text{Ru}(\text{CO})_3(\text{PR}_3)_2$ and phosphine-substituted triruthenium carbonyl complexes.

Transfer reagents of the " $\text{Ru}(\text{CO})_4$ " fragment, such as $\text{Ru}(\text{CO})_5$ ¹⁷, $\text{Ru}(\text{CO})_4(\eta^2\text{-H}_2\text{CCH}_2)$ ¹⁷, and $\text{Ru}(\text{CO})_4(\eta^2\text{-H}_2\text{CCHCH}_3)$ ¹⁸, have been employed by this research group in the preparation of $\text{Ru}(\text{CO})_4(\eta^1\text{-Ph}_2\text{PCH}_2\text{PPh}_2)$ ¹⁸ and $\text{Ru}(\text{CO})_4$

(η^1 -Me₂PCH₂PMe₂)¹⁹. The olefin transfer reagents have proved indispensable in such preparations, owing to the lability of the olefinic ligands towards phosphine substitution and their relative inertness towards decomposition under an olefin atmosphere.

In a typical preparation of Ru(CO)₄(PMe₃), Ru(CO)₄(η^2 -C₂H₄) was prepared in an analogous fashion to Ru(CO)₅, simply substituting ethylene for carbon monoxide atmosphere. Following photolysis the solution was frozen in liquid nitrogen and the ethylene atmosphere evacuated. The solution was then allowed to thaw under an inert atmosphere and 1.1 equivalents of trimethylphosphine were added to the stirred, cooled solution. Following sublimation, the trimethylphosphine substituted product was isolated in 83.7% yield and the triphenylphosphine substituted product in 50.4% yield (scheme 2.4). This method is analogous to that first proposed by Lewis in 1974¹⁷. Unlike the



Scheme 2.4 Preparation of Ru(CO)₄(PR₃), 2

other methods outlined, no disubstitution or phosphine substituted triruthenium by-products were observed by either infrared or ¹H NMR spectroscopies. It should be noted that this method, as outlined in the experimental section, allows for preparation of Ru(CO)₄(PMe₃) in 50 to 250 mg quantities. Preparations in gram quantities using this method is impractical, as the preparation of Ru(CO)₄(η^2 -C₂H₄) is restricted by the limited solubility of ethylene in hydrocarbon solvent.

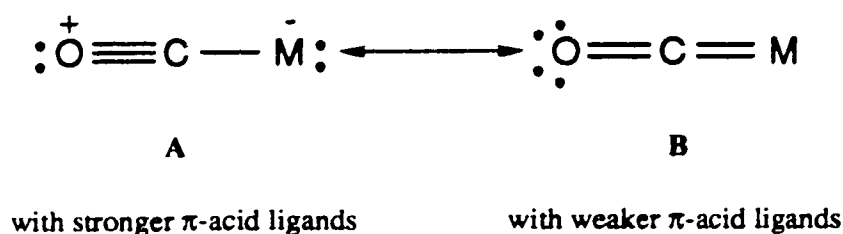
The ^{13}C enriched material was prepared by the trimethylphosphine substitution of ^{13}C enriched $\text{Ru}(\text{CO})_5$ (*ca.* 20% enrichment). A variable temperature $^{13}\text{C}\{^1\text{H}\}$ NMR experiment was conducted in an attempt to determine the low-temperature, limiting spectrum of the compound, but the carbonyl scrambling process remained rapid down to -100°C , no signal broadening being observed. Such behaviour is not surprising and may well be expected given the propensity of $\text{M}(\text{CO})_5$ and $\text{M}(\text{CO})_4\text{L}$ complexes towards stereochemical fluxionality^{20,21}.

2.5 Conclusion

The photolytic synthesis of $\text{Ru}(\text{CO})_4(\eta^2\text{-HC}_2\text{CF}_3)$ has proven to be problematic, plagued by side reactions and thermal instability of the product, the latter being the greatest pitfall in the preparation. In contrast to the analogous acetylene complex, the strongly π -accepting trifluoropropyne ligand attenuates the fluxionality of the complex, rendering it non-fluxional. However, the single perfluoromethyl group is insufficient to impart stability to the complex, as it decomposes above -20°C . It would appear that, as with any good valence bond model, the trifluoropropyne complex can be described by a compromise of extremes **A** and **B** (scheme 2.3), existing somewhere in the continuum that lies between the two; the complex has sufficient metallacyclopropene character to render it non-fluxional, yet sufficient σ -alkyne character to render it thermally unstable.

As was alluded to in section 2.3, it was previously proposed that decomposition of $\text{Os}(\text{CO})_4(\eta^2\text{-HC}_2\text{H})$ was initiated by CO loss, as decomposition could be delayed under a CO atmosphere. Ultimately, it would appear that the lability of the $\text{M}(\text{CO})_4(\eta^2\text{-alkyne})$ complexes depends on the nature of the alkyne, all other factors, particularly the metal center, being the same. Clearly, a more π -acidic alkyne such as hexafluorobutyne will increase carbon-oxygen bond orders, as in canonical form **A** (scheme 2.5), but

commensurate with this change should be a decrease in metal-carbon bond order. For a poorer π -acid like acetylene canonical form **B** should be dominant, as there is less competition between the alkyne ligand and the carbonyls for metal d_{π} -electron density. As was discussed in section 2.2, the more π -acidic the alkyne ligand becomes, the closer the metal-alkyne bonding approaches the metallacyclopropene limit. At some point a compromise must be struck between the metal and its ligands; metallacyclopropene character will be gained at the expense of greater CO lability, while stronger metal-carbonyl interactions will be gained at the expense of alkyne lability.



Scheme 2.5 The Two Canonical Forms of Metal-Carbonyl Bonding

The observed stability ordering of $\text{Ru}(\text{CO})_4(\eta^2\text{-F}_3\text{CC}_2\text{CF}_3) \gg \text{Ru}(\text{CO})_4(\eta^2\text{-HC}_2\text{CF}_3) > \text{Ru}(\text{CO})_4(\eta^2\text{-HC}_2\text{H})$ appears to reflect also the relative reactivity of these complexes. In the absence of any metal-dependence it would appear that the limiting factor in determining both how stable and how reactive an $\text{M}(\text{CO})_4(\eta^2\text{-alkyne})$ complex will be is the π -acidity of the alkyne. A strongly π -acidic alkyne will give the complex sufficient metallacyclopropene character so as to mitigate against alkyne dissociation, while rendering the carbonyls sufficiently labile for dissociation: the complex will react as an ' $\text{M}(\text{CO})_3(\eta^2\text{-alkyne})$ ' fragment. On the other hand, a less π -acidic alkyne will render the complex more susceptible to alkyne dissociation, while rendering the carbonyls inert with respect to dissociation: the complex will now react as an ' $\text{M}(\text{CO})_4$ ' fragment.

The outlined preparation of $\text{Ru}(\text{CO})_4(\text{PR}_3)$ is an improved route to such phosphine adducts. Whereas previously published preparations have been plagued by side-products, the outlined method affords a single product in moderately-high yield.

The utility of both $\text{Ru}(\text{CO})_4(\eta^2\text{-HC}_2\text{CF}_3)$, **1a**, and $\text{Ru}(\text{CO})_4(\text{PR}_3)$, **2**, in the preparation of bimetallic complexes is the topic of the following chapter.

2.6 Experimental Section

General Techniques and Solvents

All reactions, unless otherwise noted, were carried out under purified nitrogen or argon atmospheres, using standard Schlenk techniques²². Purification of the inert gases was accomplished by passing them through a heated column (100°C) containing BASF catalyst (Cu-based, R3-11) to remove any oxygen and through a column of Malinkrodt Aquasorb (P₂O₅ on an inert support) to remove water. According to published methods²³, solvents were dried by refluxing and distilling them from an appropriate drying agent (table 2.2). When necessary, degassing of solvents was accomplished by a cycle of freezing,

Table 2.2 Solvents and Drying Agents

<u>Solvent</u>	<u>Drying Agent</u>
dichloromethane	phosphorus pentoxide
hexane	potassium metal
pentane	calcium hydride
toluene	sodium metal

evacuation, and thawing. Prior to reflux or distillation, pentane and hexane solvents were preconditioned by first washing with concentrated H₂SO₄, followed by aqueous NaHCO₃, water, and finally drying over Na₂SO₄. Deuterated solvents were dried over molecular

sieves and stored under a dry nitrogen or argon atmosphere. All glassware was cleaned by treatment in a 95% KOH-ethanol solution, followed by a dilute HCl solution, and finally oven-dried at 200°C.

Physical Measurements

Infrared spectra were collected over a range from 2200 to 1600 cm^{-1} using either a Bomem MB-100 or a Nicolet MX-1 Fourier Transform Interferometer. The spectra were obtained in KCl-solution cells (path length 0.1 mm). Mass spectra were determined on an A.E.I. MS-12 spectrometer, operated at either 16 or 70 eV. ^{31}P and ^{19}F NMR spectra were determined on a Bruker WH-200 spectrometer, ^1H and variable temperature $^{13}\text{C}\{^1\text{H}\}$ NMR spectra on a Bruker WM-360 spectrometer, and overnight $^{13}\text{C}\{^1\text{H}\}$ NMR on a Bruker AM-300. ^1H and ^{13}C chemical shifts are reported as δ (in p.p.m.), relative to the residual solvent resonances (*versus* TMS). ^{19}F and ^{31}P chemical shifts are reported as δ (in p.p.m.), relative to CFCl_3 for the ^{19}F spectra (upfield being negative) and relative to an 85% H_3PO_4 external standard for the ^{31}P spectra.

Starting Materials and Reagents

Following a published method²⁴, dodecacarbonyltriruthenium was prepared from ruthenium trichloride hydrate (Johnson Matthey Inc.). Trimethylphosphine was purchased from Aldrich Chemical Company and triphenylphosphine from BDH Chemicals Ltd.. $\text{CpCo}(\text{CO})_2$ and *t*-butyl isocyanide were purchased from Strem Chemicals Inc.. Trifluoropropyne was purchased from PCR Inc.. ^{13}C -enriched carbon monoxide (99.1%) and unenriched carbon monoxide were purchased from Isotec (Matheson) Inc. and

Matheson, respectively. All reagents were used as received from the supplier. The complexes $\text{CpM}(\text{CO})_2$ ($M = \text{Rh}^{25}$, and Ir^{26}) and $\text{Cp}^*\text{M}(\text{CO})_2$ ($M = \text{Co}^{27}$, Rh^{28} , and Ir^{29}) were prepared according to published literature methods.

Photochemical Techniques

All photochemical experiments were conducted using either of the two assemblies illustrated in figure 2.2. The apparatus **A** was employed when the reaction solution required cooling (internal photolysis). Cooling of the reaction solution and the apparatus was achieved using a methanol solution circulated through a Lauda SK-65 cooling bath. The apparatus **B** was employed when the solution could be kept at room temperature (external photolysis). Cooling of the apparatus was achieved using cold tap water. Both methods employed as the radiation source a Philips HPK 125 Watt mercury vapour lamp, filtered through GWV (Glass Wertheim) glass ($\lambda_{\text{max}} \geq 370 \text{ nm}$).

Synthesis of $\text{Ru}(\text{CO})_4(\eta^2\text{-HC}_2\text{CF}_3)$, **1a**

$\text{Ru}_3(\text{CO})_{12}$ (255 mg, 0.398 mmol), 125 mL pentane, and a stir bar were transferred into a Schlenk tube. The slurry was degassed by first freezing, using liquid nitrogen, and then evacuating the Schlenk tube. The slurry was allowed to thaw and the procedure was then repeated. Under static vacuum, the Schlenk tube was pressurized with carbon monoxide (>1 atm). The slurry was stirred and irradiated with a Philips HPK 125 W, high-pressure mercury lamp, filtered through a GWV-glass cutoff filter ($h\nu \geq 370 \text{ nm}$), at room temperature. The conversion to $\text{Ru}(\text{CO})_5$ was complete when all the $\text{Ru}_3(\text{CO})_{12}$ had dissolved and the resulting solution became colourless. The $\text{Ru}(\text{CO})_5$ solution was then

transferred into apparatus A, precooled to -70°C . Trifluoropropyne was condensed into the solution over a two minute interval, until a positive pressure was achieved in the immersion well. The stirred solution was photolyzed for 4 h, until all the $\text{Ru}(\text{CO})_5$ had

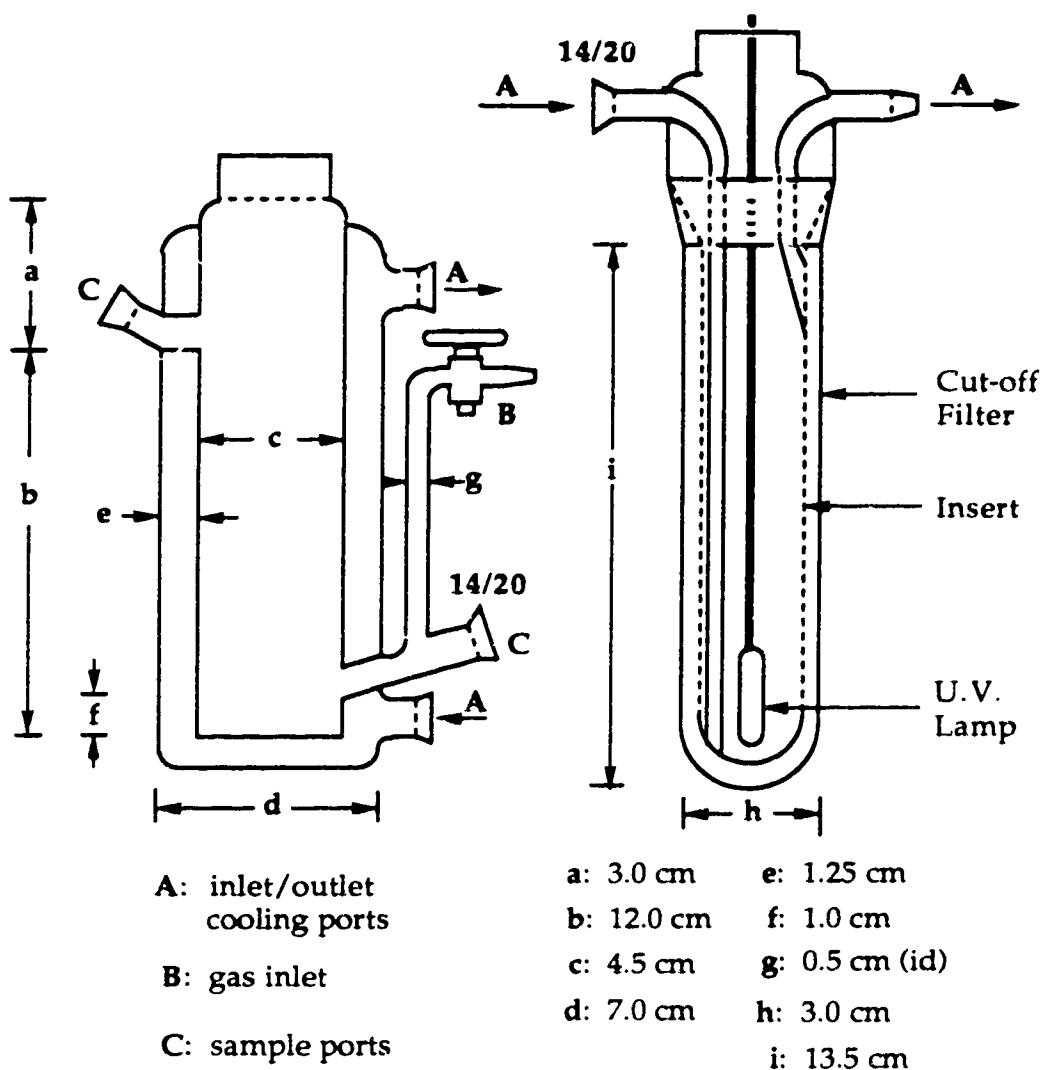


Figure 2.2 Photolysis Apparatus for (A) internal photolysis (left) and (B) external photolysis (right) (figure courtesy of Dr. J. S. Washington)

been consumed (as monitored by IR). The radiation source used was that outlined above. The solution was then transferred by cannula into a single-neck flask, precooled in dry ice, and the solvent was removed *in vacuo* at -50°C . The solid residue was then sublimed, under static vacuum, onto a dry-ice cooled probe, as the flask was allowed to warm from -50°C to room temperature. The white, air-stable solid was washed into a single-neck flask with 50 mL of cooled hexane (-35°C). The product decomposes in hydrocarbon solution above -20°C . $\text{Os}(\text{CO})_4(\eta^2\text{-HC}_2\text{CF}_3)$, **1b**, was prepared in an analogous fashion starting with $\text{Os}(\text{CO})_5$. The reader is referred to reference 1a for further details.

IR(pentane, $<-20^{\circ}\text{C}$): ν_{CO} 2131 vw, 2056 s, 2025 m cm^{-1} ; ν_{CC} 1771 vw cm^{-1}

^1H NMR (CD_2Cl_2 , 360 MHz, 238 K): δ 6.73 (q, $^4J_{\text{HF}} = 2.9$ Hz)

^{19}F NMR (CD_2Cl_2 , 376.5 MHz, 238 K): δ -55.28 (d, HCCCF_3)

$^{13}\text{C}\{^1\text{H}\}$ NMR (CD_2Cl_2 , 90 MHz, 238 K): δ 189.04 (2CO_{ax}), 194.84 (1CO_{eq}), 196.20 (1CO_{eq}), 122.52 (q, HCCCF_3 , $^1J_{\text{CF}} = 264.2$ Hz), 89.46 (q, HCCCF_3 , $^3J_{\text{CF}} = 7.2$ Hz), 81.49 (q, HCCCF_3 , $^2J_{\text{CF}} = 46.7$ Hz)

Determination of $\text{Ru}(\text{CO})_4(\eta^2\text{-HC}_2\text{CF}_3)$ Yield

Recent publication of the molar absorptivity constants of $\text{Ru}(\text{CO})_5$ in hexane solution³⁰ has allowed for the reliable determination of solution concentrations.

A Schlenk tube was charged with 212 mg (0.332 mmol) $\text{Ru}_3(\text{CO})_{12}$, 70 mL hexane, and a stir bar. The mixture was degassed twice and then pressurized with ≥ 1 atmosphere carbon monoxide. The slurry was photolyzed, following the procedure outlined above, for 1 hour to yield a colourless solution. Infrared data and Beer's Law calculations revealed that conversion to $\text{Ru}(\text{CO})_5$ was greater than 99% (0.995 mmol). The solution was

cannulated into a cooled 50 mL hexane solution of $\text{Ru}(\text{CO})_4(\eta^2\text{-HC}_2\text{CF}_3)$ (prepared from 1.194 mmol $\text{Ru}(\text{CO})_5$). The solution was stirred and allowed to warm to room temperature over 2 h, at which point the infrared spectrum of the reaction solution was determined. The absorbance of the carbonyl band of $\text{Ru}(\text{CO})_5$ at 2002 cm^{-1} was determined to be 0.233 (the carbonyl band at 2037 cm^{-1} was obscured by reaction products). Using Beer's Law ($\epsilon = 8100^{30}$; $b = 0.010\text{ cm}$) the amount of remaining ruthenium pentacarbonyl corresponded to 0.346 mmol. Assuming that no $\text{Ru}(\text{CO})_5$ had decomposed, 0.649 mmol of ruthenium pentacarbonyl had been consumed in reaction. Assuming formation of a single product, and a 1:1 product relation between $\text{Ru}(\text{CO})_5$: $\text{Ru}(\text{CO})_4(\eta^2\text{-HC}_2\text{CF}_3)$, the yield of $\text{Ru}(\text{CO})_4(\eta^2\text{-HC}_2\text{CF}_3)$ relative to starting $\text{Ru}(\text{CO})_5$ was 54%.

Synthesis of $\text{Ru}(\text{CO})_4(\text{PMe}_3)_2$

Into a Schlenk tube was transferred $\text{Ru}_3(\text{CO})_{12}$ (105 mg, 0.164 mmol), 75 mL pentane, and a stir bar. The mixture was degassed by two freeze-thaw-evacuation cycles. Under static vacuum, the Schlenk tube was pressurized with ethylene (>1 atm). The mixture was stirred and irradiated with UV light, using a Philips HPK 125 W, high-pressure mercury lamp, filtered through a GWV-glass cutoff filter ($h\nu \geq 370\text{ nm}$), at room temperature. The conversion to $\text{Ru}(\text{CO})_4(\eta^2\text{-C}_2\text{H}_4)$ was complete when all the $\text{Ru}_3(\text{CO})_{12}$ had dissolved and the resulting solution became colourless. The solution was then degassed and 1.1 equivalents of trimethylphosphine were transferred into the Schlenk tube. The solution was stirred for 12 h at 0°C and then allowed to warm to room temperature until all the $\text{Ru}(\text{CO})_4(\eta^2\text{-C}_2\text{H}_4)$ had been consumed (as monitored by IR). The solution was then transferred by cannula into a single-neck flask and the solvent removed *in vacuo* at -50°C . The solid residue was then sublimed, under static vacuum, onto a dry-ice cooled probe, as the flask was warmed to 35°C . Following sublimation, the white, air-stable solid was

scraped from the probe and weighed (119.5 mg, 0.413 mmol). The yield was 83.7%. The spectroscopic data for this compound were in good agreement with the previously reported data. $\text{Ru}(\text{CO})_4(\text{PPh}_3)$ was prepared in an analogous fashion, transferring the phosphine ligand as a 5 mL toluene solution. The yield was 50.4%.

Data for $\text{Ru}(\text{CO})_4(\text{PMe}_3)$

IR(pentane): ν_{CO} 2062 s, 1986 m, 1948 s cm^{-1}

^1H NMR (CD_2Cl_2 , 360 MHz): δ 0.91 (d, $^2J_{\text{HP}} = 10.1$ Hz)

$^{13}\text{C}\{^1\text{H}\}$ NMR (CD_2Cl_2 , 90 MHz, 173 K): δ 205.3 (d, $^2J_{\text{CP}} = 2.3$ Hz)

Data for $\text{Ru}(\text{CO})_4(\text{PPh}_3)$

IR(pentane): ν_{CO} 2061 m, 1988 w, 1955 s cm^{-1}

2.7 References

- (1) (a) Washington, J. Ph. D. Thesis, University of Alberta, 1994. (b) Kiel, G., unpublished results. (c) Burn, M. J.; Kiel, G.; Seils, F.; Takats, J.; Washington, J. *J. Am. Chem. Soc.* **1989**, *111*, 6850. (d) Gagné, M. R.; Takats, J. *Organometallics* **1988**, *7*, 561.
- (2) Cotton, F. A.; Wilkinson, G. *Advanced Inorganic Chemistry*, 5th ed.; John Wiley & Sons: Toronto, 1988.
- (3) Einstein, F. W. B.; Martin, L. R.; Pomeroy, R. K. *Inorg. Chem.* **1985**, *24*, 2777, and references therein.
- (4) *Handbook of Chemistry and Physics*, 54th ed.; Weast, R. C., Ed.; CRC: Cleveland, 1973.
- (5) Klockner, H. W.; Schrotter, H. W. In *Topics in Current Physics*; Weber, A., Ed.; Springer-Verlag: New York, 1979; Vol. 11.
- (6) Berney, C. V.; Cousins, L. R.; Miller, F. A. *Spectrochim. Acta, Part A* **1962**, *19*, 2019.
- (7) Bauman, R. P.; Miller, F. A. *J. Chem. Phys.* **1954**, *22*, 1544.
- (8) Powell, P. *Principles in Organometallic Chemistry*, 2nd ed.; Chapman and Hall: New York, 1988.
- (9) Maslowsky, Jr., E. *Vibrational Spectra of Organometallic Compounds*; Wiley-Interscience: New York, 1977; pp 248-263.
- (10) Bassler, G. C.; Morrill, T. C.; Silverstein, R. M. *Spectroscopic Identification of Organic Compounds*, 4th ed.; John Wiley & Sons: Toronto, 1981.
- (11) Caulton, K. G.; Chardon, C.; Dartiguenave, M.; Eisenstein, O.; Gagné, M. R.; Huffman, J. C.; Jackson, S. A.; Marinelli, G.; Streib, W. E.; Takats, J. *Polyhedron* **1990**, *9*, 1867.

- (12) Friebolin, H. *Basic One- and Two-Dimensional NMR Spectroscopy*; VCH: New York, 1991.
- (13) Fields, R. *Ann. Rep. Nuc. Mag. Res. Spec.* **1977**, *7*, 1.
- (14) Mao, T., personal communication.
- (15) Calderazzo, F.; L'Eplattenier, F. *Inorg. Chem.* **1968**, *7*, 1290.
- (16) Cardaci, G. *J. Organomet. Chem.* **1987**, *323*, C10.
- (17) Johnson, B. F. G.; Lewis, J.; Twigg, M. V. *J. Organomet. Chem.* **1974**, *67*, C75.
- (18) Kiel, G.; Takats, J. *Organometallics* **1989**, *8*, 839.
- (19) Sandercock, P. M. L. M. Sc. Thesis, University of Alberta, 1990.
- (20) Adams, R. D.; Cotton, F. A. In *Stereochemical Nonrigidity in Metal Carbonyl Compounds*; Cotton, F. A.; Jackmann, L. M., Eds.; Dynamic Nuclear Magnetic Resonance Spectroscopy; Academic: New York, 1975.
- (21) Mann, B. E.; Taylor, B. F. In *¹³C NMR Data for Organometallic Compounds*; Maitlis, P. M.; Stone, F. G. A.; West, R., Eds.; Organometallic Chemistry; Academic: Toronto, 1981.
- (22) Shriver, D. F. *The Manipulation of Air-Sensitive Compounds*; McGraw-Hill: Toronto, 1969.
- (23) Perrin, D. D.; Amarego, W. L. F.; Perrin, D. R. *Purification of Laboratory Chemicals*, 2nd ed.; Pergamon: Toronto, 1980.
- (24) Bruce, M. I.; Jensen, C. M.; Jones, N. L. *Inorg. Synth.* **1989**, *26*, 259.
- (25) Dickson, R. S.; Tailby, G. R. *Aust. J. Chem.* **1970**, *23*, 1531.
- (26) Gardner, S. A.; Philips, S. A.; Rausch, M. D. *Inorg. Chem.* **1973**, *12*, 2396.
- (27) Frith, S. A.; Spencer, J. L.; *Inorg. Synth.* **1985**, *23*, 15
- (28) Werner, H.; Klingert, B. J. *J. Organomet. Chem.* **1981**, *218*, 395.
- (29) Ball, R. G.; Graham, W. A. G.; Heinekey, D. M.; Hoyano, J. K.; McMaster, A. D.; Mattson, B. M.; Michel, S. T. *Inorg. Chem.* **1990**, *29*, 2023.

(30) Bor, G.; Koelliker, R. *Inorg. Chem.* **1991**, *30*, 2236.

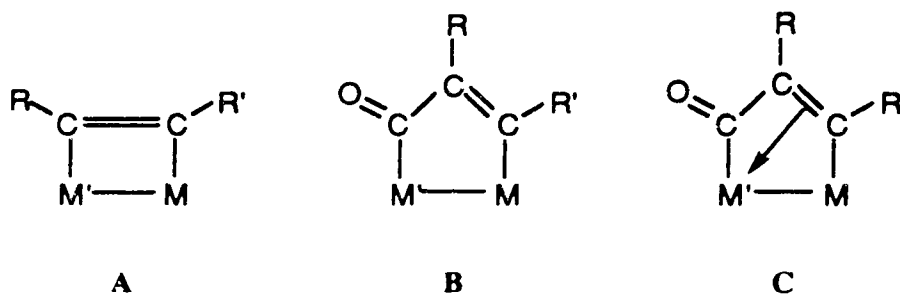
Chapter Three

Synthesis and Characterization of $MM'(CO)_7(L)(\mu-\eta^1,\eta^1-HC_2CF_3)$

Complexes ($M, M' = Ru, Os$; $L = CO, PMe_3$)

3.1 Introduction

Dimetallacycles of the type $MM'(CO)_8(\mu-\eta^1,\eta^1\text{-alkyne})$ ($M, M' = Os, Ru$) have been the subject of ongoing interest in this research group. Complexes employing hexafluorobutene as a bridging ligand were first prepared by Gagné^{1f} *via* the thermal reaction of $M(CO)_4(\eta^2-F_3CC_2CF_3)$ with $M'(CO)_5$. These reactions afforded dimetallacyclobutene products, type A^{1a-q}, for both the same- and mixed-metal complexes. Burn, Kiel, Seils, and Washington^{1d} performed analogous experiments with $Os(CO)_4(\eta^2-HC_2H)$ and $M'(CO)_5$. In the case where $M' = Os$ the observed structure was that of type A, a dimetallacyclobutene. However, when M' was changed to ruthenium the product was of



Scheme 3.1 Three Types of Dimetallacyclic Structure:

A, η^1,η^1 -dimetallacyclobutene; B, η^1,η^1 -dimetallacyclopentenone;

C, η^1,η^3 -dimetallacyclopentenone

type **B**, an η^1, η^1 -dimetallacyclopentenone^{1b,d,o}. Whereas formation of the dimetallacyclobutene products occurred *via* condensation of two 18-electron complexes with the net loss of a carbonyl ligand, formation of the dimetallacyclopentenone product proceeded, remarkably, without net ligand loss. Although structure type **C** is predominant amongst characterized dimetallacyclopentenones^{1d,i,l,2a-d}, no η^1, η^3 structures have been observed by this research group from the condensation of two group 8 metal complexes (M, M' = Os, Ru).

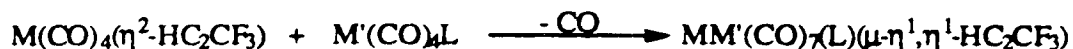
To further probe the chemistry of these group 8 bimetallic complexes, the terminal alkyne trifluoropropyne was employed as a bridging ligand. At question were three issues: would trifluoropropyne function well as a bridging ligand given only one prior literature example of its use³, would the products exhibit exclusively one structural type or many, and, due to the asymmetric nature of the bridging alkyne, would the products exist as single regioisomers or mixtures of several?

In addition to the precursors $M'(CO)_5$, $Ru(CO)_4(PMe_3)$ was also employed in preparing bimetallic complexes. The advantage of the phosphine complex lies partly in its solid nature; $Ru(CO)_5$ and $Os(CO)_5$ are both liquids at working temperature⁴. Furthermore, the presence of the phosphine ligand provides a convenient NMR probe (³¹P is the sole naturally occurring isotope of phosphorus), useful in structure determination.

3.2 Synthesis and Characterization of $MM'(CO)_7(L)(\mu-\eta^1, \eta^1-HC_2CF_3)$

The title compounds were prepared by reacting a cooled hydrocarbon solution of either $Ru(CO)_4(\eta^2-HC_2CF_3)$, **1a**, or $Os(CO)_4(\eta^2-HC_2CF_3)$, **1b**, with one equivalent of $M'(CO)_4L$, followed by warming to room temperature over 2 h. The reactions were monitored by infrared spectroscopy and were judged to be complete when the carbonyl

stretching bands of the reactants had disappeared. Subsequently, the crude residues were extracted and precipitated at reduced temperature (scheme 3.2 and table 3.1).



Scheme 3.2 Preparation of $\text{MM}'(\text{CO})_7\text{L}(\mu\text{-}\eta^1,\eta^1\text{-HC}_2\text{CF}_3)$ Complexes

	M, M'	L	T(°C)	colour	yield(%)
3	Ru, Ru	CO	-35	pale yellow	82
4	Os, Ru	CO	0	pale yellow	87
5	Os, Os	CO	+25	yellow	41
6	Ru, Ru	PMe ₃	-35	white	80
7	Os, Ru	PMe ₃	0	white	79

Table 3.1 Reaction Conditions and Product Yields

Mass spectral data for compounds 3-7 show the appropriate parent ions, followed by the sequential loss of all carbonyl ligands. Product formulations were corroborated by elemental analysis data.

The infrared spectra of the products (L = CO) consist of sharp bands, numbering between five and seven, in the region between 2136 and 2008 cm⁻¹, indicating the presence

of terminal carbonyls only. The positions and relative intensities of these bands are consistent with those observed for the $MM'(CO)_8(\mu-\eta^1,\eta^1-F_3CC_2CF_3)^{1f}$ series and $Os_2(CO)_8(\mu-\eta^1,\eta^1-HC_2H)^{1d}$.

When $L = PMe_3$ the infrared spectra exhibited sharp bands, although the positions of the bands had shifted *ca.* 20 cm^{-1} to lower energy, consistent with a lower carbon-oxygen bond order due to the greater Lewis basicity of PMe_3 versus CO^5 . The carbonyl bands number between five and seven and occur in the region between 2111 and 1984 cm^{-1} , indicating the presence of terminal carbonyls only. Characteristic infrared spectra of both the parent and PMe_3 substituted complexes are provided in figure 3.1. The carbon-carbon stretching band of the coordinated alkyne ligand was not observed for either the $L = CO$ or PMe_3 series of compounds.

For compounds **3**, **4**, **6**, and **7**, the condensation reactions proceeded to completion giving a single tractable product in high yield (79-87%). However, the yield of the osmium complex, **5**, was low (41%) and the reaction was plagued by substantial quantities of $Os(CO)_5$, both from starting material and, presumably, from decomposition of $Os(CO)_4(\eta^2-HC_2CF_3)$, **1b**.

3.3 NMR Spectra and Product Regiochemistry

Although elemental analysis, mass spectral, and infrared data were consistent with formulation of the condensation products as dimetallacyclobutenes, it was not possible to ascertain the orientation of the trifluoropropyne ligand relative to the bimetallic framework on the basis of these data. When $M = M'$ and $L = CO$, determination of the orientation is not an issue; however, introducing two different metals, as for $OsRu(CO)_8(\mu-\eta^1,\eta^1-HC_2CF_3)$, **4**, allows for the possibility of two isomeric condensation products (scheme 3.3). Furthermore, introduction of $L = PMe_3$ adds the possibility of ruthenium or osmium

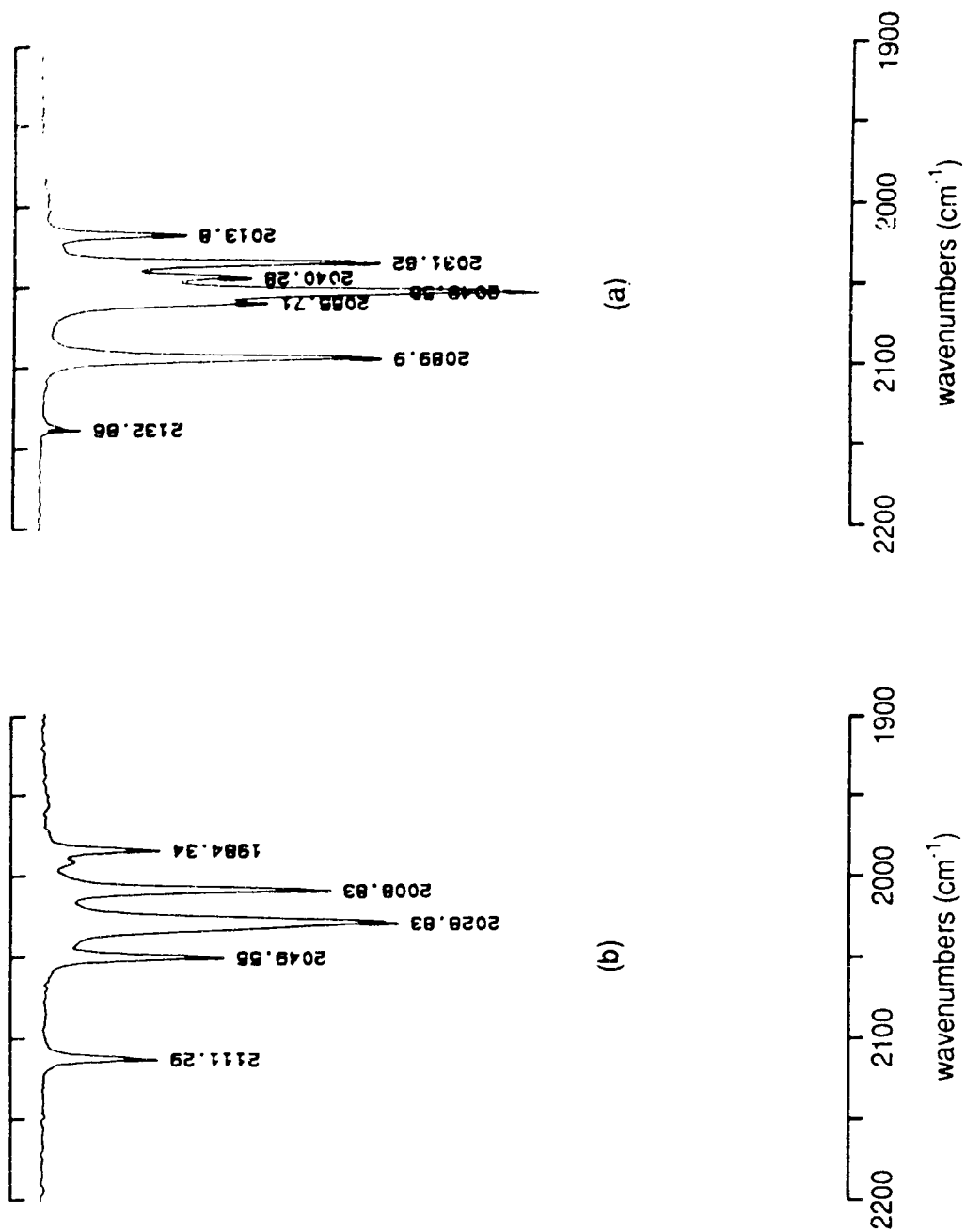
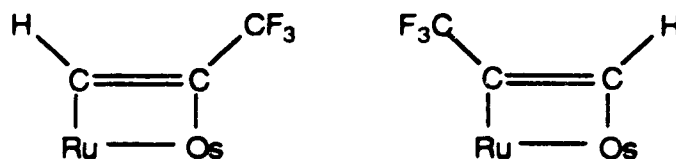


Figure 3.1 Solution IR Spectra of (a) $\text{OsRu}(\text{CO})_8(\mu\text{-}\eta^1, \eta^1\text{-HC}_2\text{CF}_3)$, **4**, and (b) $\text{OsRu}(\text{CO})_7(\text{PMe}_3)(\mu\text{-}\eta^1, \eta^1\text{-HC}_2\text{CF}_3)$, **7**

coordination. As will be borne out in the following section, the simplicity of the NMR spectra revealed that the condensation reactions give single products and proceed in a completely regioselective fashion.



**Scheme 3.3 The Two Possible Regioisomers of
OsRu(CO)₈(μ-η¹,η¹-HC₂CF₃), 4**

For the compounds in which L = CO, **3** (M = M' = Ru), **4** (M = Os, M' = Ru), and **5**, (M = M' = Os), the room temperature ¹H NMR spectra are very similar, all exhibiting single quartet resonances at δ 7.25, 7.34, and 7.49, respectively. The appearance of the quartet resonance is due to four-bond coupling of the proton to the three equivalent fluorines of the perfluoromethyl group (⁴J_{HF} = 2 Hz). These couplings were confirmed by the appearance of doublet resonances in the ¹H-coupled, ¹⁹F NMR spectra. For compounds **6** (M = M' = Ru) and **7** (M = Os, M' = Ru), where L = PMe₃, the room temperature ¹H NMR spectra consist of doublet of quartet resonances at δ 6.81 and 7.01, there being coupling to phosphorus of 16 and 14 Hz⁵, respectively, in addition to the four-bond coupling to fluorine of 2 Hz.

From these data two trends are apparent: the proton shift appears to be both metal and ligand (L = CO or PMe₃) dependent. When the ruthenium center is replaced by osmium, a low-field shift in the ¹H NMR signal results (**3**, δ 7.25; **5**, δ 7.49). When L = CO is replaced by L = PMe₃, the proton chemical shift moves to higher field (**3**, δ 7.25; **6**, δ 6.81). Based upon simple electronic considerations, incorporation of a strongly Lewis

basic ligand into the coordination framework of the complexes should result in greater sp^2 -character of the proton-bearing carbon, commensurate with greater basicity of the metals. Diamagnetic anisotropy would dictate that the proton resonance should shift to lower field⁶. However, the observed shift is contrary to what would be intuitively expected, and perhaps may be due to shielding by the phosphine methyl groups.

It is noteworthy that there is a relatively small difference between the ^1H NMR resonances of the condensation products and the precursor alkyne complexes; the protons of **1a** and **1b** resonate at δ 6.73 and 6.91⁷, respectively. However, in comparison to the proton chemical shift of free trifluoropropyne at δ 3.10⁷, consistent with sp -hybridization of the attached carbon, it is clear that the shifts of the condensation products are most consistent with sp^2 -hybridization of the bridging carbon atoms. As it was concluded in Chapter 2 that the complexes $\text{M}(\text{CO})_4(\eta^2\text{-RC}_2\text{R}')$ (R and R' are electron withdrawing groups) may be regarded as metallacyclopropenes, the condensation products **3-7** may be analogously considered as dimetallacyclobutenes.

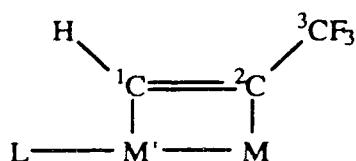
The ^{19}F NMR spectra are essentially indistinguishable for the entire series of compounds consisting of a doublet occurring roughly between δ -65 and -67⁸. These chemical shifts are consistent with those observed for the hexafluorobutyne complexes prepared by Gagné^{1f}. Two points are of note from these data: there is no coupling between fluorine and phosphorus, and there is no phosphine dependence exhibited by the fluorine resonances. Moreover, these two points are consistent with the conclusion that the phosphine is not in close proximity to the perfluoromethyl group.

For the compounds **6** and **7**, the $^{31}\text{P}\{^1\text{H}\}$ NMR spectra consist of singlet resonances at δ -5.68 and -7.16, respectively. Tertiary phosphine complexes of ruthenium exhibit resonances anywhere from δ -19.75 to 23.50⁵, depending upon various known and unknown parameters, such that very little structural information can be gained from the $^{31}\text{P}\{^1\text{H}\}$ NMR data other than that the phosphine is coordinated.

Thus, it is clear from the simplicity of spectroscopic data presented to this point that the condensation reactions are regioselective, generating a single regioisomer in each condensation reaction. However, the regiochemistry of the complexes remains to be elucidated.

The ^{13}C NMR resonances of the alkyne carbons have proven to be sensitive both to metal and ligand environment, and as a result the determination of regiochemistry based on chemical shifts and coupling to fluorine and phosphorus can be made for the product complexes.

The $^{13}\text{C}\{^1\text{H}\}$ NMR spectra of the complexes reveal that the C-F coupling exhibits a marked dependence on the distance between the trifluoropropyne carbon atoms and the three equivalent fluorines. Coupling constants on the order 270, 35, and 7 Hz are observed and it follows that the three carbon atoms can be identified on the basis of $^1J_{\text{CF}} > ^2J_{\text{CF}} > ^3J_{\text{CF}}$. These couplings proved instrumental in determining the relative positions of the carbon atoms within the alkyne ligand and, ultimately, to which metals the alkyne *sp*-carbons were attached. Scheme 3.4 presents the labelling scheme for the alkyne carbons and table 3.2 presents a summary of the ^{13}C data.



Scheme 3.4 Alkyne-carbon Labelling System

C_1 is denoted as the alkyne-carbon having a proton attached to it. As a result of broadband ^1H decoupling of the ^{13}C NMR resonances and the accompanying Nuclear Overhauser Effect (NOE)⁹, C_1 shows a substantial increase in intensity over C_2 and C_3 . It

follows that C₁ can be identified *via* the observed NOE and a coupling to fluorine of *ca.* 7 Hz. Furthermore, C₁ is characterized by its metal-dependence, exhibiting a low-field resonance of δ 120.10, in the case of complex **3**, and a high-field resonance of δ 105.66, in the case of complex **5**.

				<u>δ in ppm</u>		
	<u>L</u>	<u>M'</u>	<u>M</u>	<u>C₁</u>	<u>C₂</u>	<u>C₃</u>
3	CO	Ru	Ru	120.10	115.29	122.60
4	CO	Ru	Os	122.10	100.62	123.67
5	CO	Os	Os	105.66	101.19	122.79
6	PMe ₃	Ru	Ru	130.12	117.56	123.45
7	PMe ₃	Ru	Os	129.04	102.16	121.74

Table 3.2 Summary of Alkyne ¹³C{¹H} NMR Data

The alkyne-carbon that exhibits the largest coupling to fluorine (*ca.* 270 Hz) also shows the least variation in chemical shift (*ca.* 2 ppm) and is clearly not metal-bound; therefore, this signal is assigned as C₃.

It remains that the carbon exhibiting coupling to fluorine of *ca.* 35 Hz is C₂. As would be expected, the chemical shift of this carbon shows metal dependence, exhibiting a low-field resonance at δ 115.29, in the case of the diruthenium complex **3**, and high-field resonances of δ 100.62 and 101.19, in the case of the osmium-ruthenium complex **4** and the diosmium complex **5**, respectively.

Comparing the data for **6** and **7** with that of their L = CO congeners, **3** and **4**, the C₁ resonances exhibit a PMe₃ induced, low-field shift of 7-10 ppm, whereas C₂ is relatively insensitive to the ligand environment: the low-field shift on changing L from CO to PMe₃ is *ca.* 2 ppm.

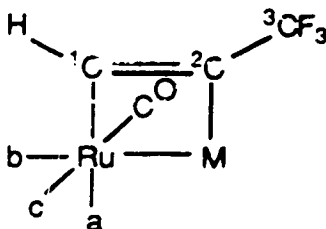
Based on the ¹³C data for the homometallic examples it is apparent that an alkyne-carbon in these complexes will resonate between δ 115-130 if attached to ruthenium or between δ 100-106 if attached to osmium. It is clear from table 3.2 that in complex **4** C₁ (δ 122.10) is bonded to ruthenium and C₂ (δ 100.62) is bonded to osmium, and thereby the regiochemistry of this complex is deduced.

The location of the phosphine relative to the bridging-trifluoropropyne in both complexes **6** and **7** can be further corroborated by the presence or absence of phosphorus coupling to the alkyne carbons. In complexes **6** and **7** C₁ exhibits the only phosphorus-carbon coupling (2.2 Hz and 7.6 Hz, respectively). In complex **7** C₃ exhibits a smaller coupling of 1.3 Hz while in complex **6** no such coupling is observed; therefore, for both complexes C₁ is judged to be in closest proximity to the phosphine ligand.

It follows from the data presented that complexes **6** and **7** have the same regiochemistry; trimethylphosphine remains bonded to ruthenium, and no net ligand migration between the two monometallic starting materials has occurred. However, one piece of the regiochemical puzzle remains to be solved, that being the relative positions of the ancillary ligands about the two metal centers. It is clear that the phosphine is bonded to ruthenium, but not whether it is *trans* to C₁, to the other metal, M, or to a carbonyl (scheme 3.5, carbonyls on M have been omitted for clarity).

The carbonyl regions of the complexes are described in detail in Section 3.5 and only the spectra of **6** and **7** will be briefly described here. For both **6** and **7** the lowest field resonances represent two equivalent carbonyls and show coupling to phosphorus of 11-12 Hz, consistent with two *trans* carbonyls, *cis* to the phosphine. Two possibilities remain, the phosphine is either *trans* to C₁ or to M. The first possibility can be ruled out due to the

relatively small $^2J_{CP}$ coupling of 2-8 Hz observed for both **6** and **7**. Therefore, it can be confidently concluded that the phosphine is *trans* to M and not *trans* to C₁.



Scheme 3.5 Possible Sites of PMe₃ Coordination:
trans to C₁ (a), M (b), or CO (c)

Thus, even in the absence of a solid-state structure, the regiochemistry of the complexes **3-7** can be conclusively assigned by NMR methods alone. Nonetheless, a crystallographic structure determination of compound **7** was undertaken to further corroborate the assigned regiochemistry and verify the *trans* nature of the phosphine and M.

3.4 Solid-State Structure of OsRu(CO)₇(PMe₃)(μ-η¹,η¹-HC₂CF₃), **7**

Repeated attempts at growing a single crystal of **4** for structural analysis were fraught with unsatisfactory crystal morphology. Complex **4** had been chosen in that having both ruthenium and osmium metals allowed for the greatest corroboration and correlation of spectroscopic data with the solid-state structure. Thus, part of the impetus in preparing the

PMe₃ substituted compound, **7**, was to impart better solubility characteristics to the OsRu-TFP framework and promote the growth of single crystals suitable for structural analysis.

The analysis confirms the dimetallacyclobutene structure of the complex, analogous to that of OsRu(CO)₈(μ-η¹,η¹-F₃CC₂CF₃)^{1f} and Os₂(CO)₈(μ-η¹,η¹-HC₂H)^{1d} and confirms the position of the phosphine relative to the metals and the alkyne, bonded to ruthenium in the axial position, *trans* to osmium (see Tables 3.3-3.5 for relevant data). The regiochemistry of **7** is of note: the perfluoromethyl-bearing end of the alkyne remains connected to the osmium center, while the phosphine ligand maintains its original connection to ruthenium (fig. 3.2).

As each metal center has 17 valence electrons based on the ancillary ligands alone, a metal-metal bond is invoked to satisfy the 18-electron rule. Concomitant with such a formulation is a metal-metal separation consistent with bonding distances. Very few examples of structurally characterized osmium-ruthenium carbonyl complexes exist, yet some useful comparisons can still be made.

The osmium-ruthenium bond length in OsRu(CO)₈(μ-η¹,η¹-F₃CC₂CF₃) was determined to be 2.881(1) Å¹⁰. This distance contrasts markedly with the osmium-ruthenium bond lengths of 2.798(2) and 2.722(2) Å determined for the clusters H₂RuOs₃(CO)₁₃¹¹ and (η⁶-C₆H₆)Ru(MeC₂Me)Os₃(CO)₉¹². A further comparison can be made by taking the average bond length of Ru₃(CO)₁₂¹³ and Os₃(CO)₁₂¹³, 2.864 Å. Gladfelter^{1e} has reported that the Ru-Ru bond length in Ru₂(μ-dmpm)₂(CO)₄(μ-η¹,η¹-PhC₂Ph) is 2.938(1) Å. The bond length observed for **7** is 2.9069(6) Å, and falls within reasonable limits of a single Os-Ru bond.

The C₈-C₉ distance of 1.31(1) Å is comparable to those in similar complexes and organic molecules. The C-C separation of ethylene is 1.34 Å¹⁴, that of acetylene is 1.20 Å¹⁴, and the C-C (bridging) separation in OsRu(CO)₈(μ-η¹,η¹-F₃CC₂CF₃) is 1.322(18) Å¹⁰. As the C-C separation in **7** most closely resembles that of ethylene and OsRu(CO)₈(μ-η¹,η¹-F₃CC₂CF₃), these data further supports the dimetallacyclobutene nature of the complexes.

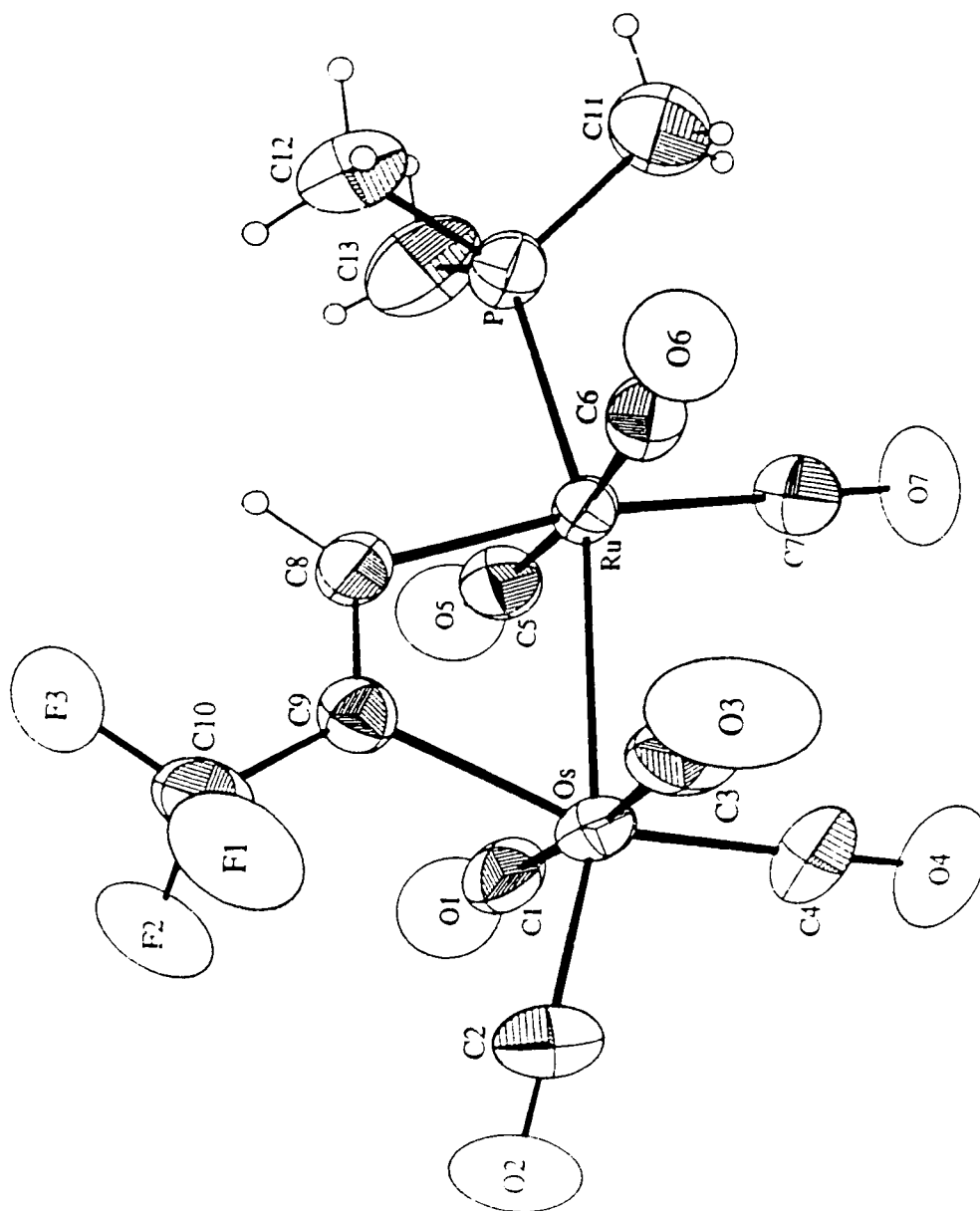


Figure 3.2 Solid-State Structure of $\text{OsRu}(\text{CO})_7(\text{PMe}_3)(\mu\text{-}\eta^1, \eta^1\text{-HC}_2\text{CF}_3)$, 7

3.5 Fluxional Behaviour

The variable temperature $^{13}\text{C}\{^1\text{H}\}$ NMR spectra of **3-7** were determined using the ^{13}CO enriched materials, prepared in an analogous fashion to the non-enriched material. Two points are of note: no acyl carbons were observed, and the complexes fall into two categories, those that exhibit carbonyl exchange at ambient temperature, **3** and **4**, and those that do not exhibit such behaviour, **5-7**.

The high-temperature limiting $^{13}\text{C}\{^1\text{H}\}$ NMR spectrum of **3** conveniently occurs at 25°C and consists of three carbonyl resonances in a 6:1:1 ratio (fig. 3.3). As the temperature is lowered to decoalescence, at approximately -60°C , the largest peak disappears, while the two smaller peaks remain unchanged (fig. 3.3). Below the decoalescence temperature, four signals, two at lower field and two at higher field, begin to appear. At -100°C the low-temperature limiting spectrum is reached, consisting of six resonances in a ratio of 2:2:1:1:1:1 (fig. 3.3) and are assigned as e':e':u':u':a':a, in an analogous fashion to that made for $\text{Ru}_2(\text{CO})_8(\mu\text{-}\eta^1, \eta^1\text{-F}_3\text{CC}_2\text{CF}_3)^{1f}$. This observed fluxionality can be explained by a "merry-go-round" exchange process¹⁵, involving the two axial and four equatorial carbonyls, causing the observed equivalence of e, e', a, and a', while the unique carbonyls *trans* to the alkyne, u and u', remain unchanged (scheme 3.6).

Apart from the expected high-field shift of the osmium carbonyls, relative to those of ruthenium¹⁶, the fluxional behaviour of **4** is similar to that of **3**. The low-temperature limiting spectrum of **4** was achieved at -40°C , and, akin to **3**, the carbonyl resonances appear in a 2:1:1:2:1:1 ratio and are assigned as e':u':a':e':u':a (fig. 3.4). As the sample is warmed, two signals remain unchanged, those corresponding to the unique carbonyls, *trans* to the bridging alkyne ligand. Coalescence of the e, e', a, and a' signals occurs at 42°C , and the only two signals that remain are those of the unique carbonyls. Above 42°C no signal attributable to the six carbonyls in the equatorial plane appears, unlike the case of **3**. As a result of the large chemical shift difference between the exchanging ruthenium and

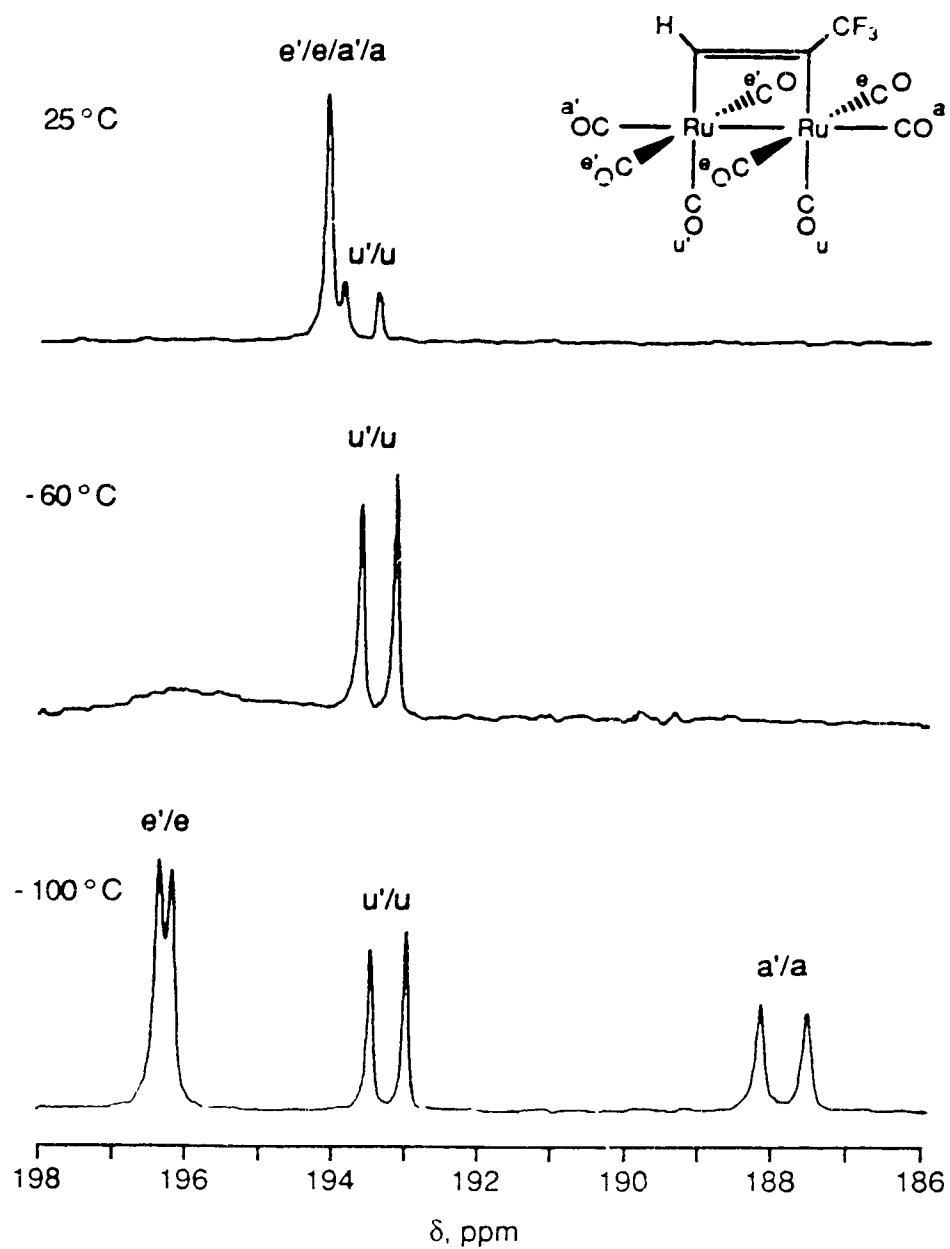
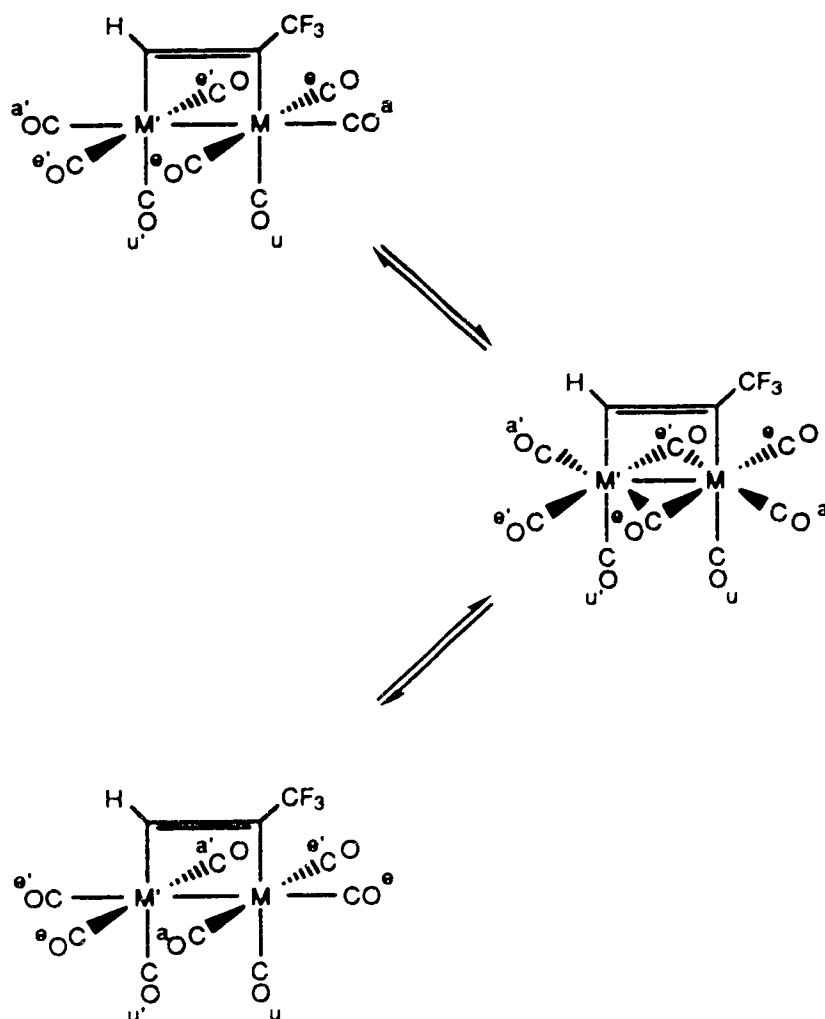


Figure 3.3 Variable Temperature $^{13}\text{C}\{^1\text{H}\}$ NMR Spectra of $\text{Ru}_2(\text{CO})_8(\mu\text{-}\eta^1,\eta^1\text{-HC}_2\text{CF}_3)$, 3

osmium carbonyls, on the order of 30 ppm, higher temperatures are required to achieve the limiting spectrum. Despite warming the sample to 80°C, the high-temperature limiting spectrum of **4** could not be reached; nevertheless, there is sufficient evidence to invoke a "merry-go-round" exchange process¹⁵ for **4**.



Scheme 3.6 "Merry-go-round" Exchange Mechanism of $MM'(CO)_8(\mu-\eta^1, \eta^1-HC_2CF_3)$

A line shape analysis program¹⁷ was applied to the observed variable-temperature carbonyl spectra of **3** and **4**, and energies of activation (ΔG^\ddagger_{298}) of 10.0 ± 0.3 and 14.2 ± 0.3 kcal/mol, respectively, were calculated and compare to those found for the hexafluorobutyne analogues of 11.0 and 14.4 kcal/mol^{1f}.

As mentioned, the diosmium analogue to **3** and **4** is static at room temperature, and its spectrum is compared to the low-temperature limiting spectra of **3** and **4** (fig. 3.4).

Carbonyl exchange was not observed at ambient temperature for the PMe_3 substituted complexes, **6** and **7**. The carbonyl region of **6** exhibits five carbonyl resonances in ratio of 2:2:1:1:1, corresponding to e':e':u':u':a.

The lowest field carbonyl resonance exhibits a two bond coupling to phosphorus of 12 Hz, consistent with its being *cis* to the phosphine (fig. 3.5). The carbonyl region for **7** is essentially identical to that of **6**, exhibiting five carbonyl resonances in a ratio of 2:1:2:1:1, corresponding to e':u':e':u':a. The two lowest field carbonyl resonances exhibit *cis*-coupling to phosphorus of 11 and 5 Hz, respectively (fig. 3.5). For both **6** and **7**, only the low-field carbonyls, the ruthenium carbonyls, exhibit coupling to phosphorus. Based upon the observed ^{13}C - ^{31}P coupling, and the non-fluxionality of the carbonyls, the PMe_3 ligand occupies an axial coordination site, *cis* to the low-field ruthenium-carbonyls, and *trans* to the Ru-M axis.

The low-temperature, limiting spectra of complexes **3-7** are consistent with all the data and structural assignments of the condensation products: all of the complexes adopt a dimetallacyclobutene structure.

3.6 Conclusion

As is the case with the $\text{MM}'(\text{CO})_8(\mu\text{-}\eta^1, \eta^1\text{-F}_3\text{CC}_2\text{CF}_3)^{1f}$ (M, M' = Ru, Os) and $\text{Os}_2(\text{CO})_8(\mu\text{-}\eta^1, \eta^1\text{-HC}_2\text{H})^{1d}$, all the complexes prepared adopt the structure type **A**, that of

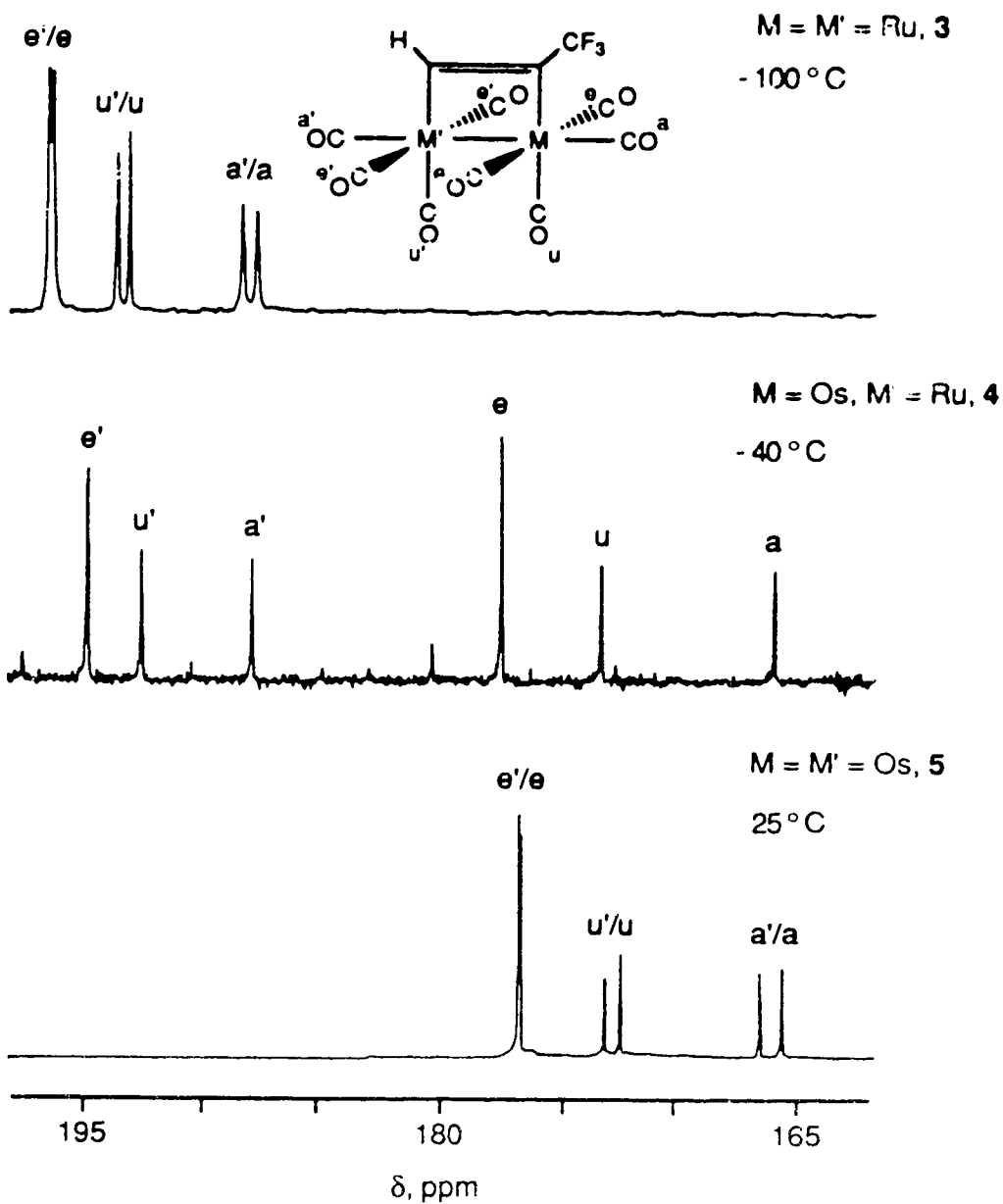


Figure 3.4 Low-temperature Limiting $^{13}\text{C}\{^1\text{H}\}$ NMR Spectra of Carbonyl Region for $\text{MM}'(\text{CO})_8(\mu\text{-}\eta^1, \eta^1\text{-HC}_2\text{CF}_3)$

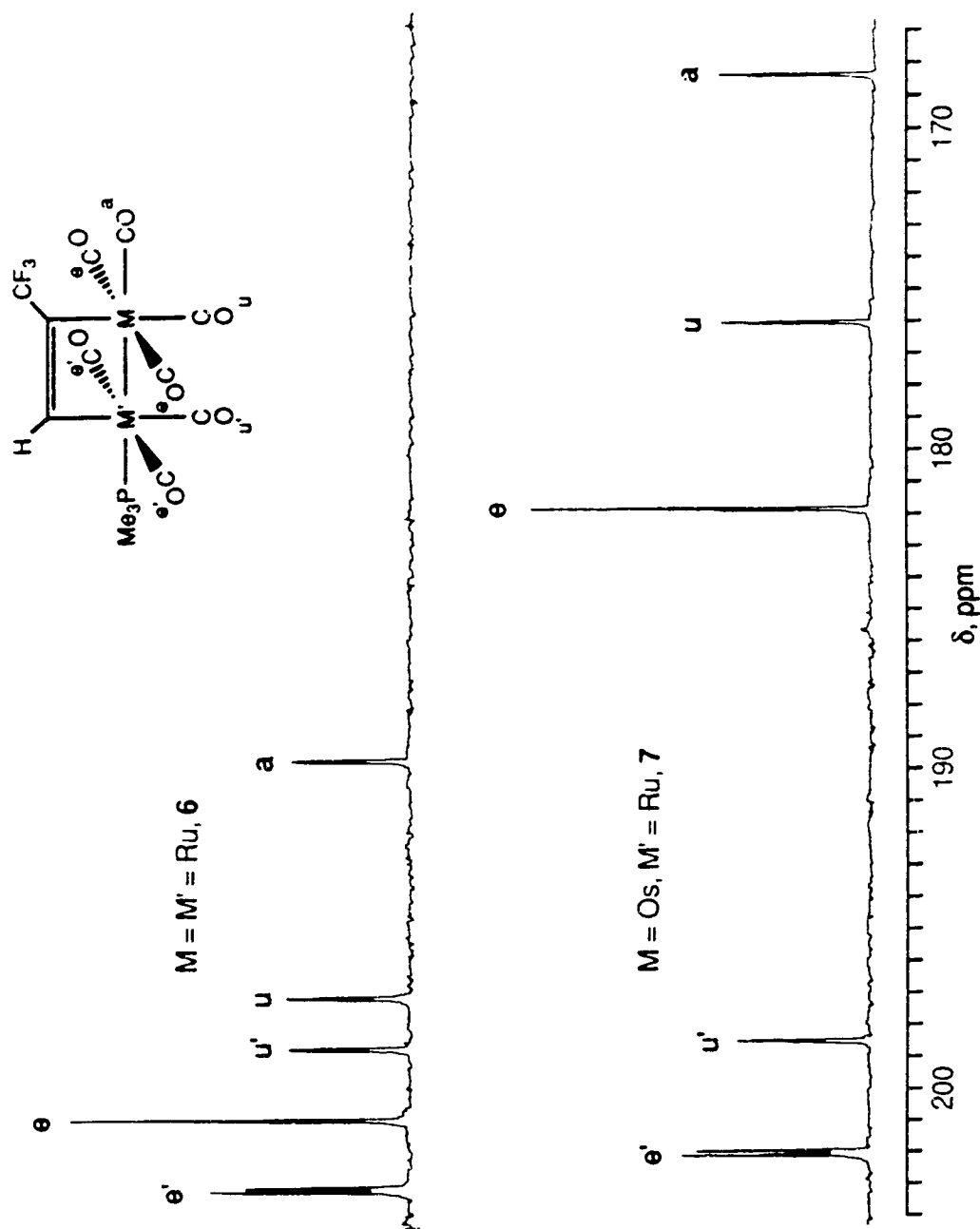


Figure 3.5 $^{13}\text{C}\{^1\text{H}\}$ NMR Spectra of Carbonyl Region for $\text{MM}'(\text{CO})_7(\text{PMe}_3)(\mu\text{-}\eta^1,\eta^1\text{-HC}_2\text{CF}_3)$

a dimetallacyclobutene, with the net loss of one carbonyl ligand upon condensation. Notably, a single regioisomer is observed for each of 3-7 and no net phosphine migration is observed in the preparation of 6 or 7. It should be noted that $\text{Ru}(\text{CO})_4(\eta^2\text{-HC}_2\text{CF}_3)$ decomposes before it can react with either $\text{Os}(\text{CO})_5$ or $\text{Ru}(\text{CO})_4(\text{PPh}_3)$.

The observed regiochemistry of the condensation reactions is typified by the metal M maintaining its connection with C_2 (C-CF₃), while C_1 (C-H) migrates from M to the metal M' (the observed regioisomers are summarized in table 3.2). Furthermore, when L = PMe_3 no net migration of the phosphine from M' is observed. Both of these points suggest a single, regioselective pathway to product formation; however, whether electronic or steric factors dictate this pathway remains to be established.

The reaction of ^{13}C enriched $\text{Os}(\text{CO})_4(\eta^2\text{-HC}_2\text{CF}_3)$ with $\text{Ru}(\text{CO})_4(\text{PMe}_3)$ was conducted at 5°C and monitored by $^{13}\text{C}\{^1\text{H}\}$ NMR spectroscopy. It was found from this study that prior to any discernable product formation the carbonyl signal for $\text{Ru}(\text{CO})_4(\text{PMe}_3)$, at *ca.* δ 205, reached a substantial level of enrichment. Only after enrichment had reached a steady state was any product formation observed. It should be noted that while stirred under a ^{13}C atmosphere at room temperature and in the dark, a solution of $\text{Ru}(\text{CO})_4(\text{PMe}_3)$ undergoes enrichment very slowly, requiring more than three days to achieve *ca.* 10% ^{13}C (as judged by infrared spectroscopy). These findings suggest that some transition state exists on the pathway to the formation of the bimetallic complexes that has a lifetime sufficiently long to allow for carbonyl scrambling, but not long enough to allow for product formation, *i.e.* the transition state may require specific orientation of the precursors, which is manifest in the product regiochemistry.

3.7 Experimental

Synthesis of $\text{Ru}_2(\text{CO})_8(\mu\text{-}\eta^1, \eta^1\text{-HC}_2\text{CF}_3)$, **3**

A solution of $\text{Ru}(\text{CO})_5$ (0.995 mmol) in 70 mL of hexane, cooled to -35°C , was cannulated into a 50 mL hexane solution of $\text{Ru}(\text{CO})_4(\eta^2\text{-HC}_2\text{CF}_3)$, **1a**, (0.65 mmol), also cooled to -35°C . The resulting solution was stirred and allowed to warm to room temperature over 2 h. The solvent was removed *in vacuo* at room temperature and the product extracted from the remaining solid residue with 6x5 mL of hexane. The solution was concentrated to effect precipitation and the solid recrystallized at -30°C to yield 321 mg (0.617 mmol) of the pale yellow product (82% yield).

FW: 520.26

Elemental Analysis: $\text{C}_{11}\text{H}_0\text{F}_3\text{Ru}_2$ calc: C 25.40; H 0.19, found: C 25.27; H 0.18

IR (pentane): ν_{CO} 2129 vw, 2087 s, 2059 m, 2049 s,sh, 2036 s, 2021 vw cm^{-1}

^1H NMR (CD_2Cl_2 , 360 MHz): δ 7.25 (q, HCCCF_3 , $^4J_{\text{HF}} = 2$ Hz)

^{19}F NMR (CD_2Cl_2 , 188 MHz): δ -65.35 (d, HCCCF_3)

$^{13}\text{C}\{^1\text{H}\}$ NMR (CD_2Cl_2 , 90 MHz, 193 K): δ 187.58, 188.20 (1CO_a , $1\text{CO}_a'$), 193.01,

193.49 (1CO_u , $1\text{CO}_u'$), 196.17, 196.34 (2CO_e , $2\text{CO}_e'$) (298 K): δ 193.16 (1CO_u), 193.63 ($1\text{CO}_u'$), 193.85 (6CO_e)

$^{13}\text{C}\{^1\text{H}\}$ NMR (CDCl_3 , 75 MHz, 298 K): δ 115.29 (q, HCCCF_3 , $^2J_{\text{CF}} = 36$ Hz), 120.10

(q, HCCCF_3 , $^3J_{\text{CF}} = 8.2$ Hz), 122.60 (q, HCCCF_3 , $^1J_{\text{CF}} = 270$ Hz)

MS (16 eV, 180°C): $\text{M}^+ = 521$ (4.5%); M-nCO ($n = 1\text{-}8$)

Synthesis of OsRu(CO)₈(μ-η¹,η¹-HC₂CF₃), 4

A solution of Ru(CO)₅ (0.327 mmol) in 70 mL of pentane, cooled to 0°C, was cannulated into a stirred solution of Os(CO)₄(η²-HC₂CF₃), **1b**, (0.33 mmol) in 25 ml of pentane, also cooled to 0°C. The solution was stirred for 2 h at 0°C, and then allowed to warm to room temperature over the next 2 h. The solvent was removed *in vacuo* at room temperature and the solid residue extracted with 6x1 mL of hexane, followed by 1x0.5 mL of CH₂Cl₂. The solution was concentrated to effect precipitation and the product recrystallized at -70°C to yield 173 mg of the pale yellow product (87% yield).

FW: 609.39

Elemental Analysis: C₁₁H₁O₈F₃OsRu calc: C 21.68; H 0.17, found: C 21.86; H 0.16

IR (pentane): ν_{CO} 2132 vw, 2090 s, 2050 m, 2050 s, 2040 m, 2032 s, 2014 w cm⁻¹

¹H NMR (CDCl₃, 360 MHz): δ 7.34 (q, HCCCF₃, ⁴J_{HF} = 2 Hz)

¹⁹F NMR (CD₂Cl₂, 188 MHz): δ -67.21 (d, HCCCF₃)

¹³C{¹H} NMR (CDCl₃, 90 MHz, 233 K): δ 166.07 (1CO_a), 173.31 (1CO_u), 177.47 (2CO_e), 187.77 (1CO_a'), 192.44 (1CO_u'), 194.66 (2CO_e')

¹³C{¹H} NMR (CD₂Cl₂, 75 MHz, 298 K): δ 100.62 (q, HCCCF₃, ³J_{CF} = 8.3 Hz), 122.10 (q, HCCCF₃, ²J_{CF} = 35 Hz), 123.67 (q, HCCCF₃, ¹J_{CF} = 272 Hz)

MS (16 eV, 180°C) M⁺ = 612 (7.0%); M-nCO (n = 1-8)

Synthesis of Os₂(CO)₈(μ-η¹,η¹-HC₂CF₃), 5

To a solution of Os(CO)₄(η²-HC₂CF₃), **1b**, (0.12 mmol in 17 mL of hexane), stirred at room temperature, was added a 7 ml of a hexane solution of Os(CO)₅ (0.12 mmol). The solution was stirred at room temperature for 36 h, during which time a yellow precipitate

formed. The solvent was removed *in vacuo* at room temperature and the product was extracted with 2 mL of CH₂Cl₂. The solution was diluted with 2.5 mL of pentane and cooled to -78°C to effect precipitation of 35.6 mg of the bright yellow product (41% yield).

FW: 698.52

Elemental Analysis: C₁₁H₀F₃O₈Os₂ calc: C 18.91; H 0.14, found: C 19.16; H 0.13

IR (pentane): ν_{CO} 2136 w, 2093 m, 2050 s, sh, 2037 m, 2025 m, 2008 w cm⁻¹

¹H NMR (CD₂Cl₂, 360 MHz): δ 7.49 (q, HCCCCF₃, ⁴J_{HF} = 2 Hz)

¹⁹F NMR (CD₂Cl₂, 188 MHz): δ -67.09 (d, HCCCCF₃)

¹³C{¹H} NMR (CD₂Cl₂, 90 MHz, 213 K): δ 165.73 (1CO_a), 166.67 (1CO_a), 172.46 (1CO_u), 173.13 (1CO_u), 176.64 (2CO_e), 176.68 (2CO_e)

¹³C{¹H} NMR (CD₂Cl₂, 75 MHz, 298 K): δ 101.19 (q, HCCCCF₃, ²J_{CF} = 38 Hz), 105.66 (q, HCCCCF₃, ³J_{CF} = 8.3 Hz), 122.79 (q, HCCCCF₃, ¹J_{CF} = 272 Hz)

MS (16 eV, 200°C): M⁺ = 700 (74.9%); M-nCO (n = 1-8)

Synthesis of Ru₂(CO)₇(PMe₃)(μ-η¹,η¹-HC₂CF₃), **6**

To a solution of Ru(CO)₄(η²-HC₂CF₃), **1a**, (0.19 mmol in 15 mL of hexane) cooled to -35°C was added 56.0 mg Ru(CO)₄(PMe₃) (0.194 mmol). The solution was stirred and allowed to warm to room temperature over 4 h. The solvent was removed *in vacuo* at room temperature and the product dissolved in 8 mL of 5:3 hexane/CH₂Cl₂. The solution was concentrated to effect precipitation and the product recrystallized at -30°C to yield 84.5 mg of the white product (80% yield).

FW: 568.33

Elemental Analysis: C₁₃H₁₀O₇F₃PRu₂ calc: C 27.47; H 1.77, found: 27.54; H 2.11

IR (pentane): ν_{CO} 2108 m, 2050 s, 2038 m, 2029 s, 2019 s, 1993 m, 1984 m cm^{-1}
 ^1H NMR (CDCl_3 , 360 MHz): δ 1.75 (d, $\text{P}(\text{CH}_3)_3$, $^2J_{\text{HP}} = 9.8$ Hz), 6.81 (dq, HCCCF_3 ,
 $^4J_{\text{HF}} = 2$ Hz, $^3J_{\text{HP}} = 16$ Hz)
 ^{19}F NMR (CDCl_3 , 188 MHz): δ -65.44 (d, HCCCF_3)
 ^{31}P NMR (CDCl_3 , 162 MHz): δ -5.68 ($\text{P}(\text{CH}_3)_3$)
 $^{13}\text{C}\{^1\text{H}\}$ NMR ($\text{C}_6\text{D}_5\text{CD}_3$, 90 MHz, 298 K): δ 18.38 (d, $\text{P}(\text{CH}_3)_3$, $^1J_{\text{CP}} = 32$ Hz),
189.63 (1CO_a), 196.93 (1CO_u), 198.48 (1CO_u), 200.65 (2CO_e), 202.77 (d, 2CO_e , $^2J_{\text{CP}}$
= 12 Hz)
 $^{13}\text{C}\{^1\text{H}\}$ NMR (CD_2Cl_2 , 75 MHz, 298 K): δ 117.56 (q, HCCCF_3 , $^2J_{\text{CF}} = 35$ Hz),
123.45 (q, HCCCF_3 , $^1J_{\text{CF}} = 270$ Hz), 130.12 (dq, HCCCF_3 , $^3J_{\text{CF}} = 7.2$ Hz, $^2J_{\text{CP}} = 2.2$
Hz)
MS (16 eV, 200°C): $\text{M}^+ = 568$ (1.0%); $\text{M}-n\text{CO}$ ($n = 1-7$)

Synthesis of $\text{OsRu}(\text{CO})_7(\text{PMe}_3)(\mu\text{-}\eta^1, \eta^1\text{-HC}_2\text{CF}_3)$, **7**

To a solution of $\text{Os}(\text{CO})_4(\eta^2\text{-HC}_2\text{CF}_3)$, **1b**, (0.073 mmol in 8 mL of pentane) cooled to 0°C was added 21.1 mg $\text{Ru}(\text{CO})_4(\text{PMe}_3)$ (0.073 mmol). The solution was stirred and allowed to warm to room temperature over 4 h, resulting in the precipitation of a white solid. The solvent was removed *in vacuo* at room temperature and the product dissolved in 7 ml of 5:2 hexane/ CH_2Cl_2 . The solution was concentrated and the product precipitated at -78°C to yield 38.1 mg of the white product (79% yield).

FW: 657.46

Elemental Analysis: $\text{C}_{13}\text{H}_{10}\text{O}_7\text{F}_3\text{POsRu}$ calc: C 23.75; H 1.53, found: C 23.88; H 1.45

IR (pentane): ν_{CO} 2111 w, 2050 m, 2029 s (br), 2009 s, 1984 w cm^{-1}

^1H NMR (CDCl_3 , 360 MHz): δ 1.82 (d, $\text{P}(\text{CH}_3)_3$, $^2\text{J}_{\text{HP}} = 9.7$ Hz), 7.01 (dq, HCCCF_3 ,

$^4\text{J}_{\text{HF}} = 2$ Hz, $^3\text{J}_{\text{HP}} = 14$ Hz)

^{19}F NMR (CDCl_3 , 188 MHz): δ -66.47 (d, HCCCF_3)

^{31}P NMR (CDCl_3 , 162 MHz): δ -7.16 ($\text{P}(\text{CH}_3)_3$)

$^{13}\text{C}\{^1\text{H}\}$ NMR ($\text{C}_6\text{D}_5\text{CD}_3$, 90 MHz, 298 K): δ 18.18 (d, $\text{P}(\text{CH}_3)_3$, $^1\text{J}_{\text{CP}} = 32$ Hz),

168.48 (1CO_a), 176.13 (1CO_u), 181.84 (2CO_e), 197.17 (d, $1\text{CO}_u'$, $^2\text{J}_{\text{CP}} = 5$ Hz), 201.58
(d, $2\text{CO}_e'$, $^2\text{J}_{\text{CP}} = 11$ Hz)

$^{13}\text{C}\{^1\text{H}\}$ NMR (CDCl_3 , 75 MHz, 298 K): δ 102.16 (q, HCCCF_3 , $^2\text{J}_{\text{CF}} = 35$ Hz), 121.74

(q of d, HCCCF_3 , $^1\text{J}_{\text{CF}} = 272$ Hz, $^4\text{J}_{\text{CP}} = 1.3$ Hz), 129.04 (dq, HCCCF_3 , $^3\text{J}_{\text{CF}} = 8.0$
Hz, $^2\text{J}_{\text{CP}} = 7.6$ Hz)

MS (16 eV, 200°C): $\text{M}^+ = 658$ (14.1%); $\text{M}-n\text{CO}$ ($n = 1-7$)

X-Ray Structure of **7**

X-ray quality, single crystals of **7** were obtained by cooling a saturated pentane solution at 5°C for 4 h. The X-ray structure determination was performed by the staff of Dr. Robin D. Rogers at the University of Northern Illinois, DeKalb, Illinois.

The data were collected on an Enraf-Nonius CAD-4 diffractometer and the reflections were corrected for absorption. The structure was solved using the SHELXS¹⁸ program. Following refinement of the nonhydrogen atoms with anisotropic thermal parameters, refinement of $R = 0.032$ and $R_w = 0.038$ was achieved. The acetylenic hydrogen atom was fixed at a calculated distance of 0.95 Å from C₈ and allowed to ride on that atom with $B = 5.5 \text{ \AA}^2$. The methyl hydrogens were also fixed at 0.95 Å from the bonded carbon atoms, with $B = 5.5 \text{ \AA}^2$.

Table 3.3 provides relevant collection and refinement data. Relevant bond distances and angles are provided in tables 3.4 and 3.5.

**Table 3.3 Crystallographic Data for
OsRu(CO)₇(PMe₃)(μ-η¹,η¹-HC₂CF₃), 7**

formula	OsRuPF ₃ O ₇ C ₁₃ H ₁₀
formula weight	657.46
crystal dimensions, mm	0.15 x 0.25 x 0.25
space group	P $\bar{1}$ (No. 2)
temperature, °C	21
radiation	graphite-monochromated MoK α (λ = 0.71073 Å)
cell parameters	
a, Å	7.318(5)
b, Å	10.259(5)
c, Å	13.706(6)
α , deg	72.33(4)
β , deg	79.62(5)
γ , deg	78.40(6)
volume, Å ³	952.6
Z	2
ρ_{calcd} , g cm ⁻³	2.29
μ_{calcd} , cm ⁻¹	79.8
2 θ range, deg	2 \leq 2 θ \leq 50
scan type	ω -2 θ
scan width, deg	0.80 + 0.35tan θ
reflections measured	3342 (h, \pm k, \pm l)
reflections observed	2750
parameters refined	244
R	0.032 (R = $\Sigma F_o - F_c / \Sigma F_o $)
R _w	0.038 (R _w = $[\Sigma w(F_o - F_c)^2 / \Sigma w F_o^2]^{1/2}$)

**Table 3.4 Bond Distances (Å) for
OsRu(CO)₇(PMe₃)(μ-η¹,η¹-HC₂CF₃), 7**

<u>Metal - Metal</u>		<u>C - C bridging</u>	
Ru - Os	2.9069(6)	C(8) - C(9)	1.31(1)
<u>Metal - C (bridging)</u>			
Ru - C(8)	2.121(7)	Os - C(9)	2.161(7)
<u>Metal - P</u>			
Ru - P	2.329(2)		
<u>Metal - C (carbonyl)</u>			
Ru - C(5)	1.931(9)	Os - C(1)	1.929(9)
Ru - C(6)	1.937(9)	Os - C(2)	1.898(9)
Ru - C(7)	1.939(8)	Os - C(3)	1.95(1)
		Os - C(4)	1.912(8)
<u>C - O</u>			
C(5) - O(5)	1.13(1)	C(1) - O(1)	1.16(1)
C(6) - O(6)	1.137(9)	C(2) - O(2)	1.15(1)
C(7) - O(7)	1.132(9)	C(3) - O(3)	1.14(1)
		C(4) - O(4)	1.16(1)

Numbers in parentheses are estimated standard deviations in the last digit

**Table 3.5 Bond Angles (deg) for
OsRu(CO)₇(PMe₃)(μ-η¹,η¹-HC₂CF₃), 7**

<u>at Ru</u>		<u>at Os</u>	
Os - P - C(8)	69.4(2)	Ru - Os - C(9)	66.9(2)
Os - Ru - C(5)	89.6(3)	Ru - Os - C(1)	88.3(3)
Os - Ru - C(6)	92.0(2)	Ru - Os - C(3)	87.6(2)
Os - Ru - C(7)	99.3(3)	Ru - Os - C(4)	93.6(3)
Os - Ru - P	164.08(6)	Ru - Os - C(2)	166.2(3)
P - Ru - C(5)	89.6(3)	C(2) - Os - C(1)	90.0(4)
P - Ru - C(6)	86.5(2)	C(2) - Os - C(3)	92.8(4)
P - Ru - C(7)	96.6(3)	C(2) - Os - C(4)	100.2(4)
P - Ru - C(8)	94.6(2)	C(2) - Os - C(9)	99.4(4)
C(5) - Ru - C(6)	171.1(3)	C(1) - Os - C(3)	173.6(3)
C(5) - Ru - C(7)	95.1(3)	C(1) - Os - C(4)	93.5(4)
C(5) - Ru - C(8)	86.9(3)	C(1) - Os - C(9)	86.4(3)
C(6) - Ru - C(7)	93.3(3)	C(3) - Os - C(4)	91.6(4)
C(6) - Ru - C(8)	85.5(3)	C(3) - Os - C(9)	87.5(3)
C(7) - Ru - C(8)	168.6(3)	C(4) - Os - C(9)	160.5(4)
 <u>at C (carbonyl)</u>			
Ru - C(5) - O(5)	175.3(8)	Os - C(1) - O(1)	176.1(9)
Ru - C(6) - O(6)	175.2(7)	Os - C(3) - O(3)	175.9(9)
Ru - C(7) - O(7)	178.6(8)	Os - C(4) - O(4)	178.6(9)
		Os - C(2) - O(2)	178.5(9)
 <u>at C (bridging)</u>			
Ru - C(8) - C(9)	110.6(5)	Os - C(9) - C(8)	113.0(5)

atP

Ru - P - C(11) 115.2(4)

Ru - P - C(12) 114.7(3)

Ru - P - C(13) 116.5(4)

Numbers in parentheses are estimated standard deviations in the last digit

3.8 References

- (1) (a) Jenkins, J. A.; Cowie, M. *Organometallics* **1992**, *11*, 2767. (b) Johnson, K. A.; Gladfelter, W. L. *Organometallics* **1992**, *11*, 2534. (c) Mague, J. T. *Polyhedron* **1990**, *9*, 2635. (d) Burn, M. J.; Kiel, G.-Y.; Seils, F.; Takats, J.; Washington, J. *J. Am. Chem. Soc.* **1989**, *111*, 6850. (e) Johnson, K. A.; Gladfelter, W. L. *Organometallics* **1989**, *8*, 2866. (f) Gagné, M. R.; Takats, J. *Organometallics* **1988**, *7*, 561. (g) Burke, M. R.; Takats, J. *J. Organomet. Chem.* **1986**, *302*, C25. (h) Mague, J. T. *Organometallics* **1986**, *5*, 918. (i) Gracey, B. P.; Knox, S. A. R.; Macpherson, K. A.; Orpen, A. G.; Stobart, S. R. *J. Chem. Soc., Dalton Trans.* **1985**, 1935. (j) Cowie, M.; Dickson, R. S.; Hames, B. W. *Organometallics* **1984**, *3*, 1879. (k) Cowie, M.; Sutherland, B. R. *Organometallics* **1984**, *3*, 1869. (l) Dyke, A. F.; Knox, S. A. R.; Naish, P. J.; Taylor, G. E. *J. Chem. Soc., Dalton Trans.* **1982**, 1297. (m) Hoffman, D. M.; Hoffmann, R.; Fisel, C. R.; *J. Am. Chem. Soc.* **1982**, *104*, 3858, and references therein. (n) Cowie, M.; Southern, T. G. *Inorg. Chem.* **1982**, *21*, 246. (o) Dickson, R. S.; Gatehouse, B. M.; Nesbit, M. C.; Pain, G. N. *J. Organomet. Chem.* **1981**, *215*, 97. (p) Cowie, M.; Dickson, R. S. *Inorg. Chem.* **1981**, *20*, 2682. (q) Koie, Y.; Sinoda, S.; Saito, Y.; Fitzgerald, B. J.; Pierpont, C. G. *Inorg. Chem.* **1980**, *19*, 770.
- (2) (a) Kiel, G.-Y.; Takats, J. *Organometallics* **1989**, *8*, 839. (b) Fontaine, X. L. R.; Jacobsen, G. B.; Shaw, B. L.; Thornton-Pett, M. *J. Chem. Soc., Dalton Trans.* **1988**, 741. (c) Hogarth, G.; Kayser, F.; Knox, S. A. R.; Morton, D. A. V.; Orpen, A. G.; Turner, M. L. *J. Chem. Soc., Chem. Commun.* **1988**, 358. (d) Dyke, A. F.; Knox, S. A. R.; Naish, P. J.; Taylor, G. E. *J. Chem. Soc., Chem. Commun.* **1980**, 409.

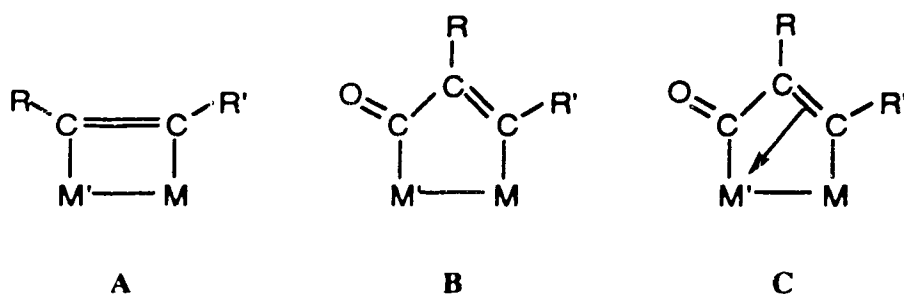
- (3) Puddephatt, R. J.; Thomson, M. A. *Inorg. Chem.* **1982**, *21*, 725.
- (4) Cotton, F. A.; Wilkinson, G. *Advanced Inorganic Chemistry*, 5th ed.; John Wiley & Sons: Toronto, 1988.
- (5) *Phosphorus-31 NMR Spectroscopy in Stereochemical Analysis: Organic Compounds and Metal Complexes*; Quin, L. D.; Verkade, J. G., Eds.; Methods in Stereochemical Analysis; VCH: Deerfield Beach, FL, 1987.
- (6) Bassler, G. C.; Morrill, T. C.; Silverstein, R. M. *Spectroscopic Identification of Organic Compounds*, 4th ed.; John Wiley & Sons: Toronto, 1981.
- (7) Kiel, G.-Y., personal communication.
- (8) Fields, R. *Ann. Rep. Nuc. Mag. Res. Spec.* **1977**, *7*, 1.
- (9) Friebolin, H. *Basic One- and Two-Dimensional NMR Spectroscopy*, VCH: New York, 1991.
- (10) Day, V. W., Gagné, M. R.; Takats, J., unpublished results.
- (11) Budge, J. R., Gates, B. C., Rheingold, A. L., Scott, J. P. *J. Organomet. Chem.* **1987**, *331*, 81.
- (12) Booker, A. T.; Jackson, P. A.; Johnson, B. F. G.; Lewis, J.; Raithby, P. R. *J. Chem. Soc., Dalton Trans.* **1991**, 707.
- (13) Lukehart, C. M. *Fundamental Transition Metal Organometallic Chemistry*; Brooks/Cole: Monterey, CA, 1985.
- (14) March, J. *Advanced Organic Chemistry: Reactions, Mechanisms, and Structure*, 3rd ed.; John Wiley & Sons: Toronto, 1985.
- (15) Bond, E.; Muetterties, E. L. *Chem. Rev.* **1978**, *78*, 639.
- (16) (a) Todd, L. J.; Wilkinson, J. R. *J. Organomet. Chem.* **1974**, *77*, 1. (b) Mann, B. E.; Taylor, B. F. *¹³C NMR Data for Organometallic Compounds*; Academic: Toronto, 1981.
- (17) McClung, R. E. D. *EYRING*: (computer program), University of Alberta.
- (18) Sheldrick, G.M. *Acta Cryst.*, **1990**, *A46*, 467.

Chapter Four

Reactivity of $\text{MRu}(\text{CO})_3(\mu\text{-}\eta^1,\eta^1\text{-HC}_2\text{CF}_3)$

4.1 Introduction

As was first introduced in Chapter 3, two structural types have been observed in this research group from the condensation reactions of $\text{M}(\text{CO})_4(\eta^2\text{-RC}_2\text{R}')$ with $\text{M}'(\text{CO})_5$ ($\text{M}, \text{M}' = \text{Ru}, \text{Os}$; $\text{R}, \text{R}' = \text{H}, \text{CF}_3$)^{1d,f}, **A**^{1a-q,2} and **B**^{1b,d,o,2} (scheme 4.1). From the condensation reactions involving $\text{Os}(\text{CO})_4(\eta^2\text{-HC}_2\text{H})$ with $\text{CpCo}(\text{CO})_2$ or $\text{CpRh}(\text{CO})_2$ structure type **C** is observed^{1d}, while the condensation reactions of $\text{Os}(\text{CO})_4(\eta^2\text{-HC}_2\text{H})$ with $\text{CpIr}(\text{CO})_2$ or $\text{Ru}(\text{CO})_5$ yield structure type **B**^{1d}. When $\text{R} = \text{CF}_3$, $\text{R}' = \text{H}$ ², or $\text{R} = \text{R}' = \text{CF}_3$ ^{1f}, the isolated complexes are exclusively of structure **A**. Thus it would appear that a more strongly π -acidic alkyne ligand disfavours incorporation of a carbonyl into the dimetallacycle.



Scheme 4.1 Three Types of Dimetallacyclic Structure:

A, η^1,η^1 -dimetallacyclobutene; B, η^1,η^1 -dimetallacyclopentenone;

C, η^1,η^3 -dimetallacyclopentenone

One of the goals in reactivity studies of the $\text{MRu}(\text{CO})_8(\mu\text{-}\eta^1, \eta^1\text{-HC}_2\text{CF}_3)$ complexes was to determine whether the dimetallacycles would undergo ligand substitution or whether an incoming nucleophilic ligand would induce carbonyl insertion to yield a dimetallacyclopentenone product. With the use of an asymmetric alkyne, of further interest was the regiochemistry of either the ligand substitution or carbonyl insertion products.

4.2 Reaction of $\text{MRu}(\text{CO})_8(\mu\text{-}\eta^1, \eta^1\text{-HC}_2\text{CF}_3)$ with PMe_3

The first attempt at ligand substitution was undertaken using trimethylphosphine, a ligand well established in its ability to displace carbonyls and promote carbonyl insertion⁴. Typically, the $\text{MRu}(\text{CO})_8(\mu\text{-}\eta^1, \eta^1\text{-HC}_2\text{CF}_3)$ complex was dissolved in dichloromethane at room temperature. Addition of 1.1 equivalents of trimethylphosphine *via* a syringe resulted in immediate reaction, as noted from the solution changing colour from colourless to bright yellow. Subsequently, the crude residues were extracted and precipitated at reduced temperature (scheme 4.2).

Mass spectral data show the loss of eight carbonyls, as well as the parent ions at *m/e* 568 ($\text{M}' = \text{Ru}$) and 688 ($\text{M}' = \text{Os}$). Both the elemental analyses and mass spectra are consistent



8 $\text{M} = \text{Ru}$; 81.0 % yield

9 $\text{M} = \text{Os}$; 73.3 % yield

Scheme 4.2 Preparation of $\text{MRu}(\text{CO})_7(\text{PMe}_3)(\mu\text{-}\eta^1, \eta^1\text{-C}\{\text{O}\}\text{HC}_2\text{CF}_3)$ Complexes

with the incorporation of trimethylphosphine into the starting complexes $\text{MRu}(\text{CO})_8(\mu\text{-}\eta^1, \eta^1\text{-HC}_2\text{CF}_3)$ without the loss of a carbonyl ligand. The products are formulated as $\text{MRu}(\text{CO})_8(\text{PMe}_3)(\text{HC}_2\text{CF}_3)$.

The infrared spectra of the products consist of six ($\text{M} = \text{Ru}$) and seven ($\text{M} = \text{Os}$) sharp carbonyl stretching bands in the region between 2116 and 1993 cm^{-1} (fig. 4.1). The spectra are remarkably similar to those observed for the trimethylphosphine-substituted dimetallacyclobutene products **6** and **7**. Very weak bands occurring at *ca.* 1600 cm^{-1} were observed for both complexes; however, these bands could be equally well assigned as acyl or alkyne stretching frequencies. The strong, higher energy bands suggest only terminal carbonyls, while the lower energy bands, when taken in concert with the established empirical formula, are consistent with acyl carbonyls. Thus, it would appear that the reaction proceeds with carbonyl insertion as shown in scheme 4.2.

4.3 NMR Spectra

Although elemental analysis, mass spectral, and infrared data were all consistent with the formulation of the complexes as carbonyl insertion products, NMR spectroscopy was needed to verify the dimetallacyclopentenone nature of the products. As will be revealed in this section, the trimethylphosphine substitution reactions not only led to carbonyl insertion products, but also proved to be regioselective.

The ^1H NMR data for the products are typical for bimetallic products and very similar to the dimetallacyclobutene products of Chapter 3. The spectrum of **8** ($\text{M} = \text{M}' = \text{Ru}$) exhibits chemical shifts at δ 1.75 and 6.83, identical to $\text{Ru}_2(\text{CO})_7(\text{PMe}_3)(\mu\text{-}\eta^1, \eta^1\text{-HC}_2\text{CF}_3)$, **6**. Whereas the alkyne signal of **6** was a doublet of quartets, the signal of **8** is only a quartet, there being coupling only to fluorine of 1.6 Hz. The spectrum of **9** is essentially identical to **8**, having a doublet resonance at δ 1.75, characteristic of

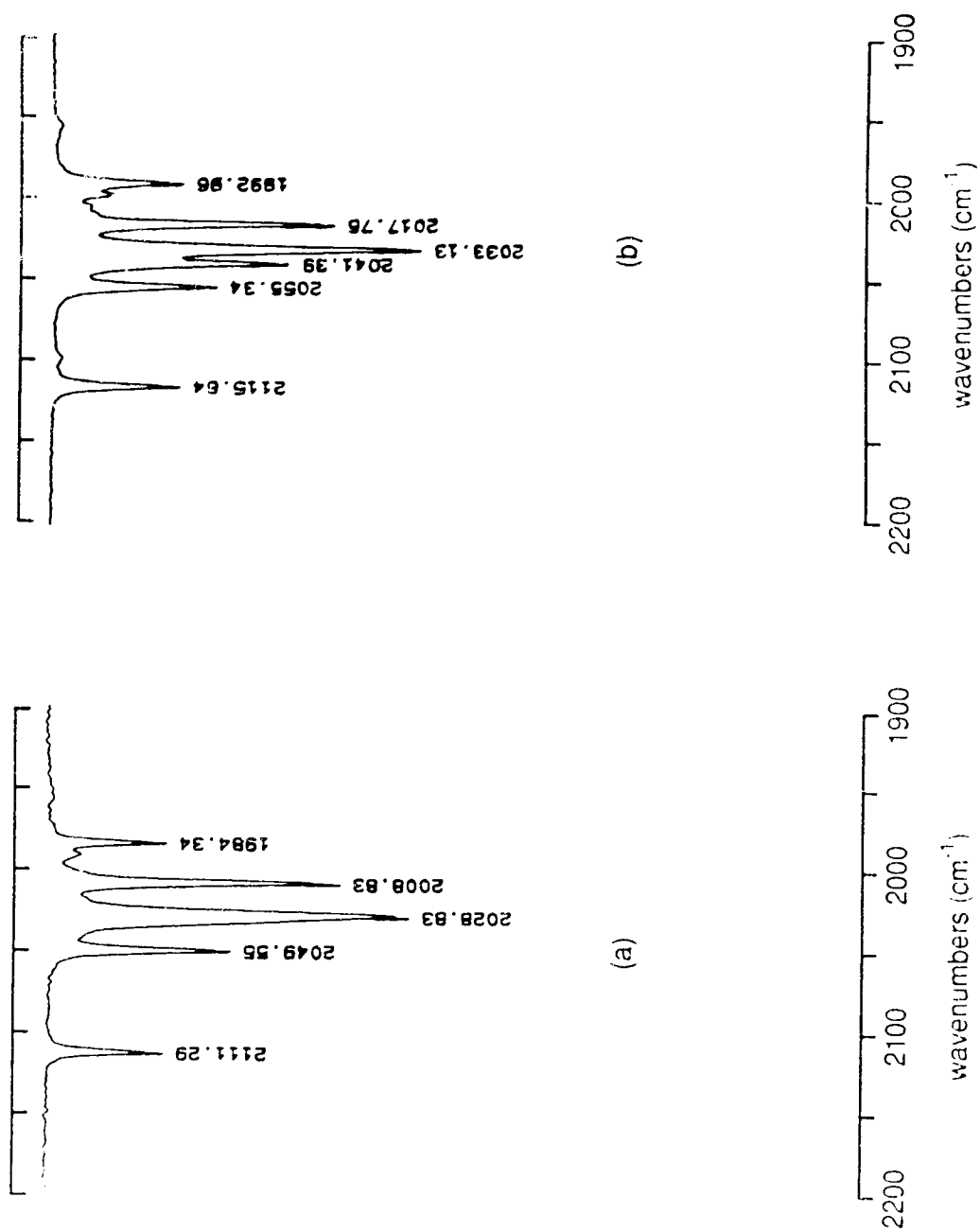


Figure 4.1 Solution IR Spectra of (a) $\text{OsRu}(\text{CO})_7(\text{PMe}_3)(\mu\text{-}\eta^1, \eta^1\text{-HC}_2\text{CF}_3)$, **7**, and (b) $\text{OsRu}(\text{CO})_7(\text{PMe}_3)(\mu\text{-}\eta^1, \eta^1\text{-C(O)HC}_2\text{CF}_3)$, **9**

trimethylphosphine methyl protons⁵, and a quartet resonance at δ 7.29, exhibiting coupling to fluorine of 1.6 Hz. These data suggest that the alkyne proton is further removed from the trimethylphosphine ligand than in complexes **6** and **7**.

The ¹H-coupled, ¹⁹F NMR spectra of **8** and **9** each consist of single fluorine resonances at δ -63.22 and -63.70, respectively. The resonances are similar to those of the dimetallacyclobutene complexes, being shifted to slightly lower field by *ca.* 4 ppm. Most notably, there is no coupling to phosphorus, as might be expected if the phosphine were in closer proximity to the perfluoromethyl end of the alkyne.

The ³¹P{¹H} NMR resonances for **8** and **9** were located at δ -5.50 and -6.60, typical for phosphorus bonded to ruthenium⁵ and comparable to those values determined for the corresponding condensation products **6** and **7**.

Like complexes **6** and **7**, the room-temperature ¹³C{¹H} NMR spectra reveal that both **8** and **9** are non-fluxional, suggesting that the trimethylphosphine ligand has been incorporated into a position that mitigates against carbonyl exchange, either axial or equatorial. The spectrum of **8** is remarkably similar to that of **6**, both exhibiting five carbonyl resonances in a ratio of 2:2:1:1:1 that are assignable as e':e':u':u':a, respectively (fig. 4.2). However, the spectrum of **8** differs in the presence of a low-field resonance at δ 247.15, due to one carbonyl, with coupling to phosphorus of 5.8 Hz. Such a low-field resonance is consistent with a transition metal-acyl moiety. In comparison, the ruthenium-acyl carbons in OsRu(CO)₈(μ - η^1, η^1 -C(O)HC₂H), Ru₂(dmpm)₂(CO)₄(μ - η^1, η^1 -C(O)C₂(CO₂Me)), and Cp₂Ru₂(CO)₂(μ - η^1, η^1 -C(O)PhC₂Ph) resonate at δ 236.3^{1d}, 262.6^{1b}, and 217.8^{1l}, respectively.

The pattern observed in the room-temperature ¹³C{¹H} NMR spectrum of **9** is analogous to that observed for **7**, with the exception of the additional low-field resonance present for **9**. The carbonyl region, between δ 205 and 165, consists of five resonances in a ratio of 2:1:2:1:1 which are assigned as e':u':e':u':a (fig. 4.2). The high-field shift of the e, u, and a carbonyls by *ca.* 20 ppm in **9**, relative to **8**, is consistent with the

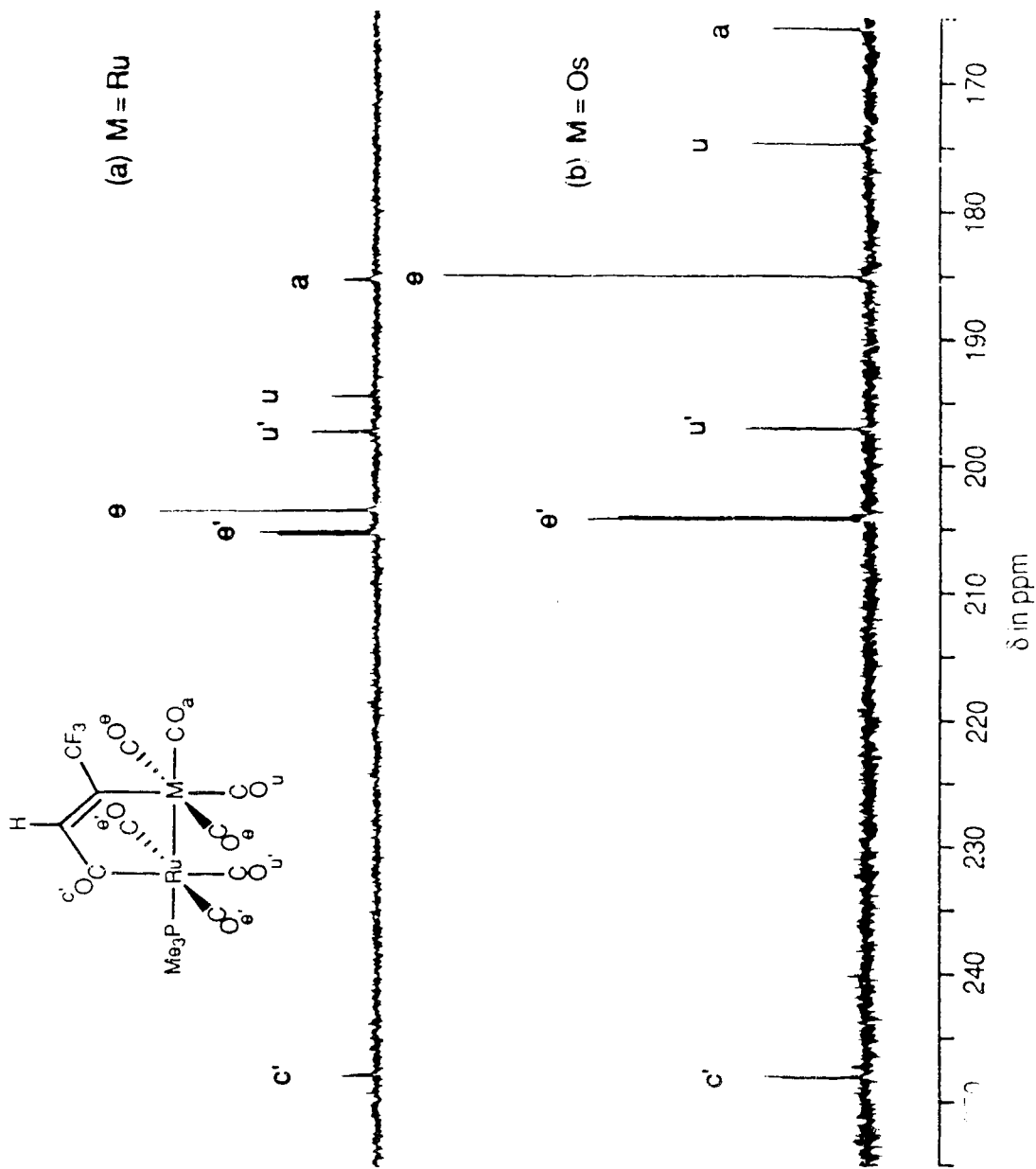
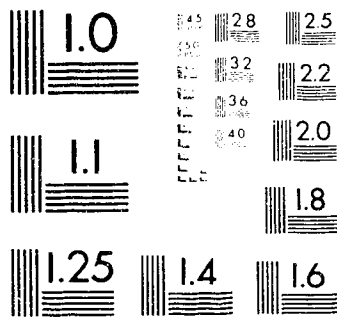


Figure 4.2 $^{13}\text{C}\{^1\text{H}\}$ NMR Spectra of (a) $\text{Ru}_2(\text{CO})_7(\text{PMe}_3)(\mu\text{-}\eta^1, \eta^1\text{-C(O)HC}_2\text{CF}_3)$, **8**, and (b) $\text{OsRu}(\text{CO})_7(\text{PMe}_3)(\mu\text{-}\eta^1, \eta^1\text{-C(O)HC}_2\text{CF}_3)$, **9**

2 of/de 2

PM-1 3½"x4" PHOTOGRAPHIC MICROCOPY TARGET
NBS 1010a ANSI/ISO #2 EQUIVALENT



PRECISIONSM RESOLUTION TARGETS

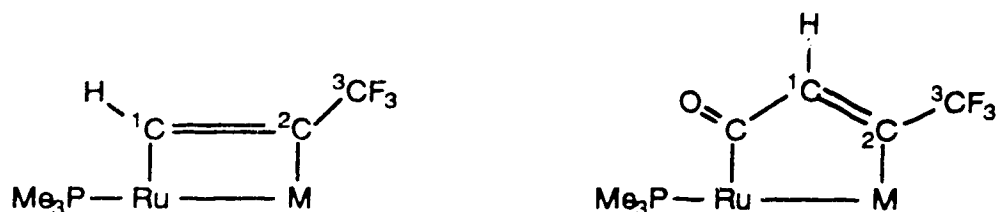
well known resonance shift of second versus third row transition-metal carbonyls⁶. Again, the low-field resonance at δ 247.44 exhibits coupling to phosphorus and is attributable to a ruthenium-acyl, *c'*. The highest field carbonyl at δ 166.78 exhibits coupling to phosphorus of *ca.* 2 Hz. As the phosphine is bonded to the acyl-bearing ruthenium, the coupling of the osmium carbonyl to the phosphorus occurs through the ruthenium-osmium bond *trans* to the trimethylphosphine ligand.

From the simplicity of the NMR data presented for **8** and **9** it is clear that the ligand substitution reactions give rise to dimetallacyclopentenone products with the trimethylphosphine ligand occupying a coordination site *trans* to the metal-metal bond, with the acyl carbon bonded to ruthenium, *cis* to the phosphine. Furthermore, it is clear that only one regioisomer is observed for each of **8** and **9**. What remains to be determined is the orientation of the trifluoropropyne ligand relative to the dimetal framework.

As was the case with the dimetallacyclobutene complexes, the carbon-fluorine coupling data determine the labelling of the alkyne carbons relative to one another. C₃ is assigned on the basis of exhibiting the largest carbon-fluorine coupling, C₂ the next largest, and C₁ the smallest coupling. Whereas phosphorus-carbon coupling was observed for the dimetallacyclobutene examples, no coupling was observed for the dimetallacyclopentenones.

There are three alkyne carbon resonances observed for complex **8**, the highest field carbon being a quartet resonance at δ 129.20, exhibiting coupling to fluorine of 271 Hz, and corresponding to C₃. The lowest field carbon is a quartet resonance at δ 163.40, exhibiting coupling to fluorine of 8.2 Hz, and displaying a much greater intensity relative to the other carbons, a result of the NOE effect⁷. Therefore, the low-field carbon is assigned as C₁ and it remains that the quartet resonance at δ 148.64 is C₂. The spectrum of **9** reveals resonances at δ 164.63, 131.27, and 129.64, corresponding to C₁, C₂, and C₃, respectively. Comparing this data with that of **8**, it is apparent that only C₂ displays metal dependence, exhibiting the characteristic 15-20 ppm high-field shift when bonded to osmium, in contrast to ruthenium^{6,8} (table 4.1). Clearly, the cyclopentenone ring is

oriented such that the alkyne hydrogen is in the α -position, relative to the acyl-group, and the perfluoromethyl group is in the β -position. Furthermore, the dimetallacyclopentenone is arranged in both **8** and **9** such that the acyl-carbon is bonded to ruthenium (scheme 4.3).



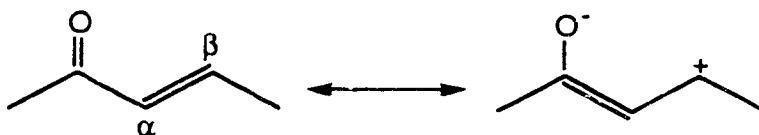
Scheme 4.3 Dimetallacycle Regiochemistry and Carbon Atom Numbering Scheme

	<u>δ in ppm</u>			<u>δ in ppm</u>	
	<u>C₁</u>	<u>C₂</u>		<u>C₁</u>	<u>C₂</u>
6 , M = Ru	130.12	117.56	8 , M = Ru	163.40	148.64
7 , M = Os	129.04	102.16	9 , M = Os	164.23	131.27

Table 4.1 Summary of Dimetallacycle Ring-carbon ¹³C{¹H} NMR Resonances

The dimetallacyclopentenone ring carbons exhibit a low-field shift of *ca.* 30 ppm relative to the dimetallacyclobutene examples in Chapter Three. This observation can be rationalized on the basis of electron density arguments proposed for α,β -unsaturated ketones⁸. Whereas the sp^2 -carbons in cyclopentene resonate at δ 130.8, the α -carbon resonance of the α,β -unsaturated ketone 2,3-cyclopentenone, at δ 133.8, is essentially

unchanged, while the β -carbon is shifted to lower field at δ 165.1. The observed shift is conventionally attributed to the enolate canonical form rendering the β -carbon electron deficient *via* resonance in the π -electron system⁹ (scheme 4.4). Such a rationale can explain the low-field shift of C_2 , relative to the non-acyl derivatives, but it cannot justify the low field shift of C_1 . Such low-field resonances appear to be typical for the α -carbon



Scheme 4.4 The Two Resonance Forms of an α,β -Unsaturated Ketone

of a dimetallacyclopentenone. Recent studies of the dimetallacyclopentenone complexes $\text{CpMOs}(\text{CO})_5(\mu\text{-}\eta^1,\eta^1\text{-C}(\text{O})\text{HC}_2\text{CH}_3)$ ($M = \text{Rh}, \text{Ir}$)² have revealed that the α -carbon, or C_1 , resonates at δ 158.94 and 162.28, respectively. Perhaps, the downfield shift of the C_1 resonance is a result of it no longer being bonded to a metal.

3.4 Solid-State Structure of $\text{OsRu}(\text{CO})_7(\text{PMe}_3)(\mu\text{-}\eta^1,\eta^1\text{-C}(\text{O})\text{HC}_2\text{CF}_3)$, **9**

A single crystal structure analysis of complex **9** was undertaken, confirming both the dimetallacyclopentenone structure **B** and the regiochemistry of the carbonyl insertion (fig. 4.3). As was concluded from the $^{13}\text{C}\{^1\text{H}\}$ NMR data, the phosphine is bonded to

ruthenium, *trans* to the metal-metal bond, and nearest to the acyl-carbon. Furthermore, the trifluoropropyne moiety is confirmed to be oriented with the hydrogen-bound end bonded to the acyl carbon and the perfluoromethyl-bound end bonded to osmium.

As was the case with complex **7**, a metal-metal bonding interaction is invoked for **9** to satisfy the 18-electron rule at each metal center. The ruthenium-osmium separation of 2.9133(8) Å is in close agreement with that observed for **7** of 2.9069(6) Å and consistent with an Os-Ru single bond (see Tables 4.2-4.4 for relevant data). In comparison, the Ru-Ru bonding distance in $\text{Ru}_2(\text{dmpm})_2\text{CO}_4(\mu\text{-}\eta^1,\eta^1\text{-C(O)C}_2\text{(CO}_2\text{Me)})^{1b}$ was determined to be 2.936(1) Å. The solid-state structure of **8** was also determined, but for reasons of brevity and its isostructural nature this structure was not included in the present work. Notably, a ruthenium-ruthenium bond distance of 2.903(1) Å was observed. Taking into account the nearly identical covalent radii of ruthenium and osmium¹⁰, these observed bond lengths appear to be characteristic for such dimetallacyclic complexes.

A striking feature of the structure is the skewing of the two $\text{M}(\text{CO})_4$ fragments, relative to one another (fig. 4.4). The skewing about the metal-metal bond is observed for both **8** and **9**, and is on the order of 20°. Crystal packing reveals no unfavourable contacts to which the skewing could be traced. It should be noted that the solid state structures of $\text{OsRu}(\text{CO})_8(\mu\text{-}\eta^1,\eta^1\text{-C(O)HC}_2\text{H})^{11}$, $\text{CpIrOs}(\text{CO})_5(\mu\text{-}\eta^1,\eta^1\text{-C(O)HC}_2\text{H})^2$, $\text{Ru}_2(\text{dmpm})_2(\text{CO})_4(\mu\text{-}\eta^1,\eta^1\text{-C(O)C}_2\text{(CO}_2\text{Me)})^{1b}$, and $\text{Cp}_2\text{Rh}_2(\text{CO})_2(\mu\text{-}\eta^1,\eta^1\text{-C(O)F}_3\text{CC}_2\text{CF}_3)^{10}$ all exhibit similar skewing and distortion of the α,β -unsaturated ketone fragment. In the latter two instances the observed deviations from planarity have been attributed to relief of steric crowding between the ancillary ligands. This rationale would also seem to be the most plausible explanation for **8** and **9**, in that the skewing best accommodates the steric needs of the molecule, minimizing interactions between the phosphine methyls, the perfluoromethyl, and the carbonyls by staggering these groups with respect to one another as much as possible.

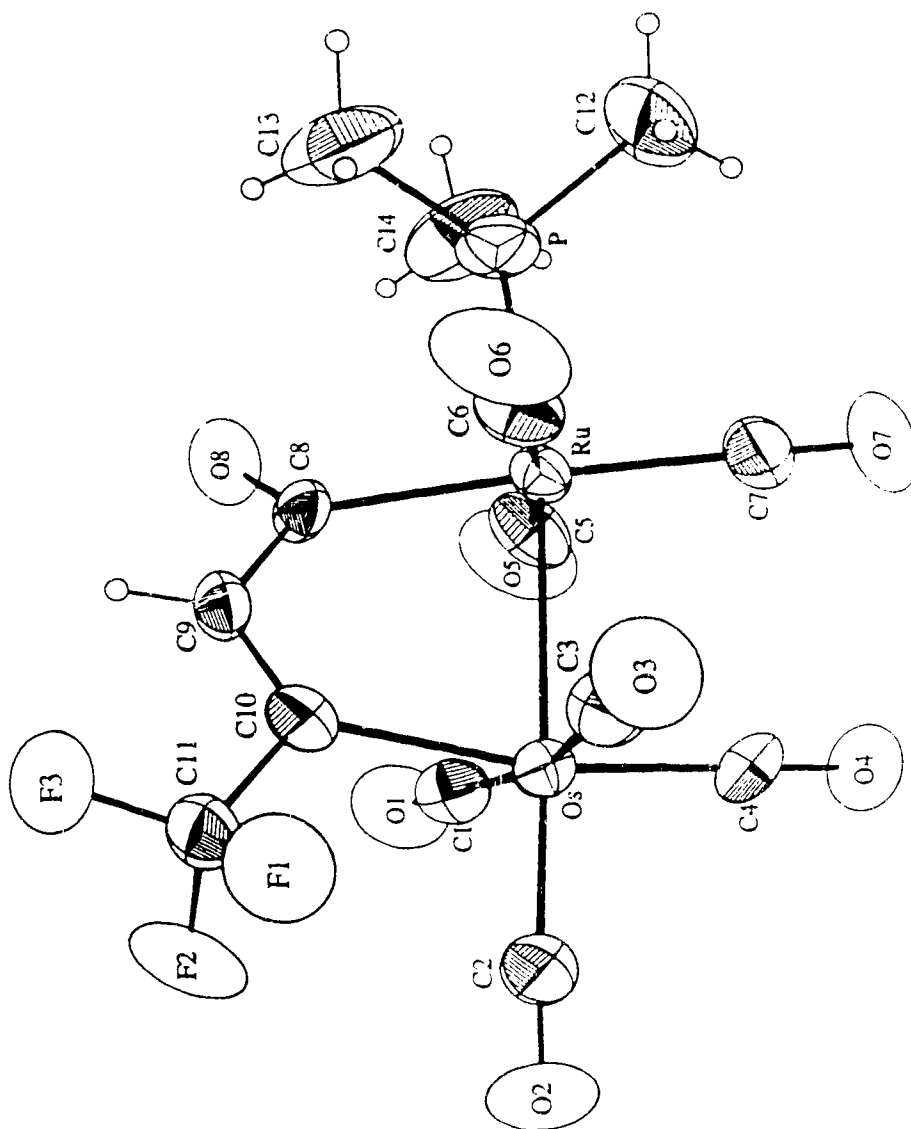


Figure 4.3 Solid-State Structure of $\text{OsRu}(\text{CO})_7(\text{PMe}_3)$
 $(\mu\text{-}\eta^1,\eta^1\text{-C}(\text{O})\text{HC}_2\text{CF}_3)$, 9

The C₈-C₉, C₉-C₁₀, and C₈-O₈ bond lengths observed for **8** of 1.49(1), 1.33(1), and 1.21(1) Å reflect the very localized nature of the trifluoropropenone fragment: the first is consistent with an *sp*²-*sp*², carbon-carbon single-bond distance of 1.48 Å¹², the second reflects the carbon-carbon double-bond distance observed for ethylene of 1.34 Å¹², and the last is consistent with an *sp*²-*sp*², carbon-oxygen double-bond distance of 1.20 Å¹². The distances observed for the diruthenium analogue are 1.48(1), 1.36(1), and 1.26(1) Å, and are in reasonable agreement. Similar localization is observed for both Ru₂(dmpm)₂(CO)₄(μ-η¹,η¹-C(O)C₂(CO₂Me))^{1b} and Cp₂Rh₂(CO)₂(μ-η¹,η¹-C(O)F₃CC₂CF₃)¹⁰, where bond distances of 1.496(4), 1.340(4), and 1.23(3) Å are observed for the former and 1.499(8), 1.336(5), and 1.213(8) Å for the latter.

The carbon-carbon bonding distances suggest that the bonding in the trifluoropropenone fragment is in fact localized and any delocalization of the π-electron system throughout the α,β-unsaturated ketone fragment is negated by the twisting or puckering of the dimetallacyclopentenone framework. Again, this puckering of the trifluoropropenone moiety is attributed to the steric demands of the ligand environment.

4.5 Further Attempts at Ligand Substitution

Several attempts were made at effecting carbonyl insertion into the bridging trifluoropropyne ligand using other ligands, most notably triphenylphosphine, *tert*-butylisocyanide, and carbon monoxide.

The reaction of one equivalent of triphenylphosphine with Ru₂(CO)₈(μ-η¹,η¹-HC₂CF₃), **3**, resulted in a change of the solution colour from colourless to yellow and a small shift in the IR bands of *ca.* 5 cm⁻¹, observations analogous to those for the trimethylphosphine reaction.

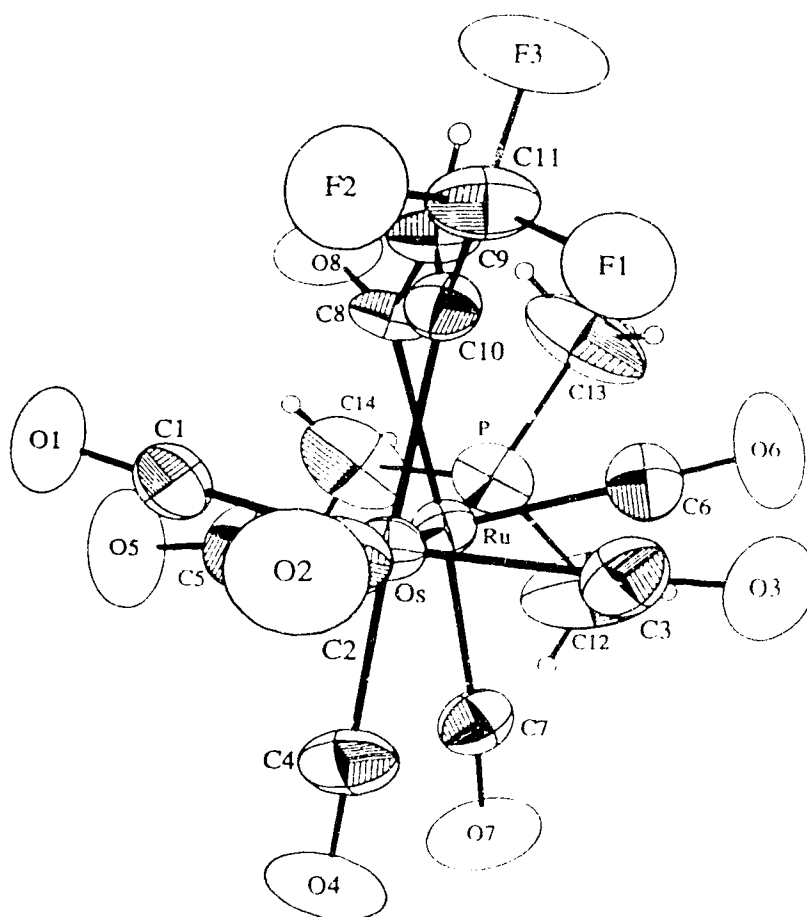


Figure 4.4 View Along The Os-Ru bond: $\text{OsRu}(\text{CO})_7(\text{PMe}_3)(\mu\text{-}\eta^1, \eta^1\text{-C}(\text{O})\text{HC}_2\text{CF}_3)$, 9

Similarly, the reaction of an excess of *tert*-butylisocyanide with **3** resulted in immediate reaction. ^1H NMR and $^{13}\text{C}\{^1\text{H}\}$ NMR data revealed that in fact a carbonyl insertion had occurred, but regrettably also revealed that the reaction was accompanied by minor, yet significant, side-products. In all likelihood the side-products were due to multiple substitution products. The reaction was repeated using 1.1 equivalents of *tert*-butylisocyanide resulting in isolation of a product in very low yield. No further pursuit of the triphenylphosphine or the *tert*-butylisocyanide reactions was made.

Four separate attempts were made at carbon monoxide addition to $\text{Ru}_2(\text{CO})_8(\mu\text{-}\eta^1, \eta^1\text{-HC}_2\text{CF}_3)$, **3**, none of which was successful. The first attempt was made by stirring a solution of **3** under carbon monoxide at room temperature for 24 hours, during which period no reaction was observed. The second attempt was made employing AlCl_3 in a Lewis Acid-assisted carbonyl insertion¹³, resulting in the decomposition of **3**. The third attempt was made using a Carius tube pressurized with 40 psi of carbon monoxide and heated to 83°C for three days. IR data revealed a slight degree of reaction, likely less than 5%. The final attempt involved heating **3** to 87°C in an autoclave under 1000 psi of carbon monoxide for 3 days. These conditions resulted in complete decomposition of the complex to $\text{Ru}(\text{CO})_5$ and $\text{Ru}_3(\text{CO})_{12}$. In all likelihood carbonyl insertion may have been on the pathway to decomposition, as once an additional carbonyl is incorporated into the coordination framework the complex can conveniently decompose to give two eighteen electron fragments.

The preceding reactions were not attempted with the mixed metal complexes **4** ($\text{M} = \text{Os}$, $\text{M}' = \text{Ru}$, $\text{L} = \text{CO}$) and **7** ($\text{M} = \text{Os}$, $\text{M}' = \text{Ru}$, $\text{L} = \text{PMe}_3$), nor were they attempted using the same metal complexes **5** ($\text{M} = \text{M}' = \text{Os}$) and **6** ($\text{M} = \text{M}' = \text{Ru}$, $\text{L} = \text{PMe}_3$).

4.6 Conclusion

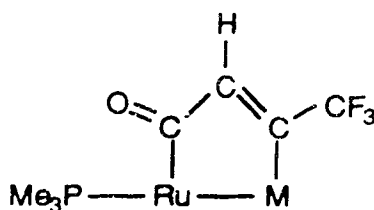
Although dimetallacyclopentenone structures are not observed as products from the condensation reactions outlined in Chapter 3, such structures can be obtained *via* carbonyl insertion into the dimetallacyclobutene complexes. Trimethylphosphine was the most successful in inducing carbonyl insertion, although *tert*-butylisocyanide and triphenylphosphine would also induce insertion, albeit to a limited extent. It appears that there is a qualitative dependence on the nature of the initiating ligand; it may well be that triphenylphosphine is too large and carbon monoxide is too poor a donor to lead to product formation.

Complexes **8** and **9** represent the first documented examples of carbonyl insertion into a metal-carbon bond of a dimetallacyclobutene. Previously reported η^1, η^1 - and η^1, η^3 -dimetallacyclopentenones have been prepared either by 1,2-addition of an alkyne to a bridging carbonyl-metal bond^{1b,i,l,3a-d}, by metathesis¹⁰, or by condensation^{1d}. Such a transformation is interesting from a mechanistic standpoint, insofar as it may model catalytic steps leading to the preparation of hydroquinone, an important industrial reducing agent, from $\text{Ru}_3(\text{CO})_{12}$, acetylene, CO, and water¹⁴.

As was observed with the condensation reactions of Chapter 3, there is a definite regioselectivity to the insertion reaction; the phosphine occupies an axial coordination site, *trans* to the metal-metal bond and *cis* to the acyl-carbon, while the trifluoropropyne moiety is oriented with its proton in closest proximity to the acyl-carbon (scheme 4.5).

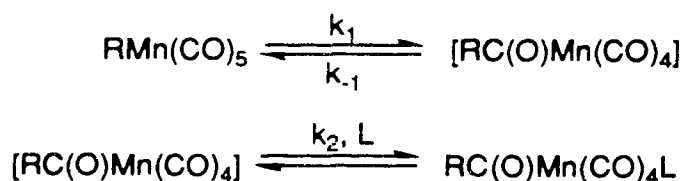
From studies conducted on the group five metal carbonyl dimers, $\text{MM}'(\text{CO})_{10}$ ($\text{M}, \text{M}' = \text{Mn}, \text{Tc}, \text{or Re}$) it has been established that phosphine substitution occurs in an axial position, *trans* to the metal-metal bond, most likely involving dissociation of an equatorial carbonyl, followed by rearrangement¹⁵. This observation is noteworthy in that the $\text{MM}'(\text{CO})_8(\mu\text{-}\eta^1, \eta^1\text{-HC}_2\text{CF}_3)$ complexes are and isoelectronic with the $\text{MM}'(\text{CO})_{10}$ complexes.

Although "carbonyl insertions" outwardly appear to be formal insertion reactions, the majority of "carbonyl insertions" in name are, in fact, alkyl migrations¹⁵. A typical mechanism for the alkyl migration observed for $\text{RMn}(\text{CO})_5$ is outlined in scheme 4.6.



Scheme 4.5 Dimetallacyclopentenone Regiochemistry; M = Ru or Os

Mechanistically, these reactions can be best rationalized in terms of a rapid pre-equilibrium in which the "R" substituent migrates to a carbonyl, forming an acyl-group, followed by a rate determining second step in which the incoming ligand coordinates to the metal center.



Scheme 4.6 Carbonyl Insertion Mechanism for $\text{RMn}(\text{CO})_5$

As was mentioned in Chapter Two, the introduction of an electron-withdrawing substituent onto a π -bound alkene or alkyne results in a greater degree of back-donation of electron density from the metal d_{π} -orbitals to the ligand π^* -orbitals. In this fashion a

synergistic effect is generated between the two participants which, to a point, strengthens the bonding interaction of one with the other.

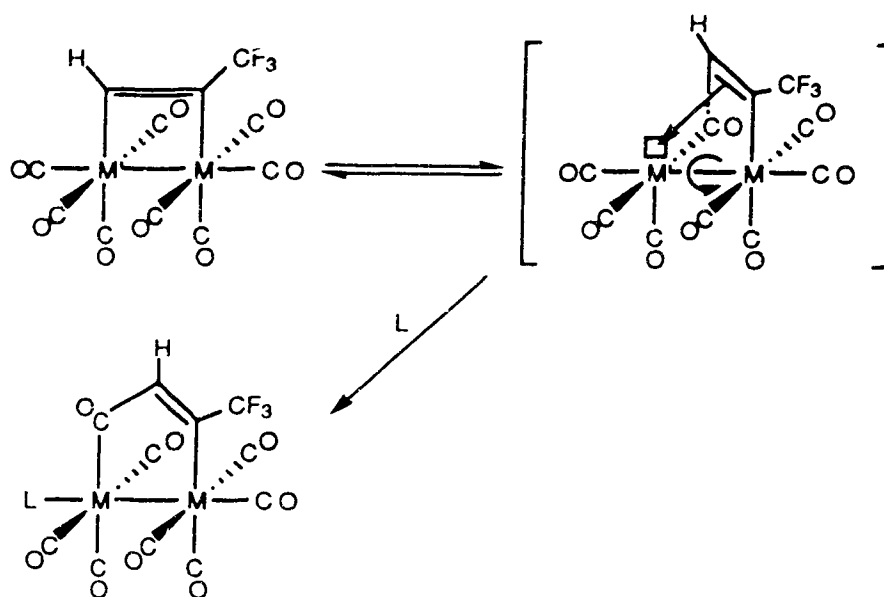
Considering the $MM'(CO)_8(\mu-\eta^1, \eta^1-HC_2CF_3)$ complexes, due to the asymmetry of the trifluoropropyne ligand the perfluoromethyl-bearing end should be bound more strongly to its metal center than the hydrogen-bearing end. Indeed, it is well established that the rates of alkyl migration are greater for more electron donating alkyls than electron withdrawing (*cf.* $-CH_3$ versus $-CF_3$)¹⁶. In the case where $M \neq M'$, where the perfluoromethyl-bearing end of the alkyne is bonded to osmium, the insertion selectivity should be more pronounced due to the increased strength of third-row transition metal-carbon bonds over second-row¹⁷.

In contrast to the $MM'(CO)_{10}$ systems, the $MM'(CO)_8(\mu-\eta^1, \eta^1-HC_2CF_3)$ system has the inherent capability to render one of its two metals coordinatively unsaturated by means of migration of one end of the trifluoropropyne ligand (scheme 4.7). To avoid overly straining the newly formed dimetallacyclopentenone ring the two octahedral metal fragments would rotate relative to one another to either an eclipsed or a slightly staggered conformation. It should be further noted that metal-metal bond rotation in dimetal systems can be quite facile; variable temperature ¹H NMR studies conducted down to $-100^\circ C$ could not halt the *cis-trans* isomerization of $Cp_2Ru_2(CO)_4$ ¹⁸. Presumably, the first step of the dimetallacyclobutene insertion reaction would be rapid.

Once a coordination site has been vacated it may be filled by the π -system of the alkyne, a bonding mode observed for the complexes $CpMOs(CO)_4(\mu-\eta^1, \eta^3-C(O)HC_2H)$ ($M = Co$ or Rh)². Based upon this model, it would seem most likely that the incoming phosphine ligand would coordinate in an equatorial position in the rate determining step, *trans* to a carbonyl; however, this is not observed and clearly some sort of low-energy rearrangement must occur.

Computer modelling of the starting dimetallacyclobutene complex reveals pertinent steric considerations, in the regard that the steric demands of the phosphine would mitigate

against its occupation of any coordination site but the axial site, in closest proximity to the alkyne proton. The perfluoromethyl group is sterically demanding and approach of the phosphine into the remaining axial site would result in severe crowding of the phosphine



**Scheme 4.7 A Proposed Mechanism for Carbonyl
Insertion into Dimetallacycles**

methyl hydrogens and the pendant fluorines. Similarly, the proximity of the two unique coordination sites, or either adjacent pair of equatorial coordination sites, would result in crowding of the adjacent carbonyl by the incoming phosphine.

The steric restrictions of the observed axial coordination site present the most favourable interactions, and this would appear to be the best rationale for the observed product

regiospecificity. Such considerations should also hold true for the $MM'(CO)_{10}$ complexes, as electronic considerations alone, *vis à vis* the *trans* effect¹⁹, would suggest that the incoming phosphine should occupy an equatorial site

As outlined in scheme 4.7, the observed insertion reactions do in fact proceed *via* migration of the hydrogen-bearing end of the alkyne, with complexation of the trimethylphosphine occurring in the sterically most favourable axial position. Each reaction results in the exclusive formation of one regioisomer.

Based on the conclusions made in this section, the complexes $MM'(CO)_8(\mu-\eta^1, \eta^1-F_3CC_2CF_3)$ might be expected to undergo phosphine substitution to give dimetallacyclopentenone complexes, although much more slowly than the trifluoropropyne complexes. Owing not only to the steric bulk of an additional perfluoromethyl group on the alkyne, but also to the increased strength of the metal-carbon(alkyne) bonds, either of the two activation parameters on the pathway to insertion may be too large.

4.7 Experimental

Synthesis of of $\text{Ru}_2(\text{CO})_7(\text{PMe}_3)(\mu\text{-}\eta^1, \eta^1\text{-C}\{\text{O}\}\text{HC}_2\text{CF}_3)$, **8**

To a solution of 58.2 mg $\text{Ru}_2(\text{CO})_8(\mu\text{-}\eta^1, \eta^1\text{-HC}_2\text{CF}_3)$ (0.112 mmol) in 20 mL of CH_2Cl_2 , stirred at room temperature, was added 12 μL (0.12 mmol) of trimethylphosphine. Reaction occurred instantly, as noted by IR and a colour change from pale-yellow to bright-yellow, and all the starting complex had been consumed. The resulting solution was stirred at room temperature for 2 h. The solvent volume was reduced to *ca.* 2 mL and 5 mL of hexane were added. Further reduction of the volume to *ca.* 5 mL and cooling the solution to -78°C resulted in precipitation of 54.1 mg (0.0952 mmol) of the bright-yellow product (81.0% yield).

FW: 596.34

Elemental Analysis: $\text{C}_{14}\text{H}_{10}\text{O}_8\text{F}_3\text{PRu}_2$ calc: C 28.20; H 1.68, found: C 28.33; H 1.59

IR (pentane): ν_{CO} 2111 m, 2056 s, 2046 m, 2034 s, 2027 s, 2000 m, 1993 m cm^{-1} ; ν_{acyl} 1602 vw cm^{-1}

^1H NMR (CD_2Cl_2 , 360 MHz): δ 1.75 (d, $\text{P}(\text{CH}_3)_3$ $^2J_{\text{HP}} = 10.3$ Hz), 6.83 (q, HCCCF_3 , $^4J_{\text{HF}} = 1.6$ Hz)

^{19}F NMR (CD_2Cl_2 , 376 MHz): δ -63.22 (d, HCCCF_3)

$^{31}\text{P}\{^1\text{H}\}$ NMR (CD_2Cl_2 , 81 MHz): δ -5.50 ($\text{P}(\text{CH}_3)_3$)

$^{13}\text{C}\{^1\text{H}\}$ NMR (CD_2Cl_2 , 75 MHz, 298K): δ 19.36 (d, $\text{P}(\text{CH}_3)_3$, $^1J_{\text{CP}} = 33.0$ Hz), 129.20 (q, HCCCF_3 , $^1J_{\text{CF}} = 271$ Hz), 148.64 (q, HCCCF_3 , $^2J_{\text{CF}} = 33.8$ Hz), 163.40 (q, HCCCF_3 , $^3J_{\text{CF}} = 8.2$ Hz), 186.09 (1CO_a , d, $^3J_{\text{CP}} = 4.5$ Hz), 194.93 (1CO_u), 197.66 (1CO_u , d, $^2J_{\text{CP}} = 5.2$ Hz), 203.75 (2CO_e), 205.46 (2CO_e , d, $^2J_{\text{CP}} = 11.2$ Hz), 247.15 (1CO_{acyl} , d, $^2J_{\text{CP}} = 5.8$ Hz)

MS (16 eV, 220 °C): $M^+ = 568$ (7.5%); $M-nCO$ ($n = 1-8$)

Synthesis of $OsRu(CO)_7(PMe_3)(\mu-\eta^1, \eta^1-C\{O\}HC_2CF_3)$, **9**

To a solution of 60.0 mg $OsRu(CO)_8(\mu-\eta^1, \eta^1-HC_2CF_3)$ (0.0985 mmol) in 20 mL CH_2Cl_2 , stirred at room temperature, was syringed 11 μ L (0.11 mmol) of trimethylphosphine. Reaction occurred instantly, as noted by IR and a colour change from pale-yellow to bright-yellow, and all the starting complex was consumed. The resulting solution was stirred at room temperature for 2 h. The solvent was removed *in vacuo* at room temperature and the product extracted from the remaining solid residue with 5x1 mL of hexane, followed by 2x1 mL of CH_2Cl_2 . The product was crystallized at $-78^\circ C$ overnight to yield 49.5 mg (0.0722 mmol) of the bright-yellow product (73.3% yield).

FW: 685.47

Elemental Analysis: $C_{14}H_{10}O_8F_3PRuOs$ calc: C 24.53; H 1.62, found: C 24.62; H 1.40

IR (pentane): ν_{CO} 2116 m, 2055 s, 2041 m, 2033 s, 2018 m, 1993 m, ν_{acyl} 1602 $vw\ cm^{-1}$

1H NMR (CD_2Cl_2 , 360 MHz): δ 1.75 (d, $P(CH_3)_3$ $^2J_{HP} = 10.3$ Hz), 7.29 (q, $HCCCF_3$, $^4J_{HF} = 1.6$ Hz)

^{19}F NMR (CD_2Cl_2 , 376 MHz): δ -63.70 (d, $HCCCF_3$)

$^{31}P\{^1H\}$ NMR (CD_2Cl_2 , 81 MHz): δ -6.60 ($P(CH_3)_3$)

$^{13}C\{^1H\}$ NMR (CD_2Cl_2 , 75 MHz, 298K): δ 19.35 (d, $P(CH_3)_3$, $^1J_{CP} = 33.0$ Hz), 129.64 (q, $HCCCF_3$, $^1J_{CF} = 273$ Hz), 131.27 (q, $HCCCF_3$, $^2J_{CF} = 32.4$ Hz), 164.63 (q, $HCCCF_3$, $^3J_{CF} = 7.0$ Hz), 166.78 ($1CO_a$, m), 175.53 ($1CO_u$), 185.78 ($2CO_e$), 197.46 ($1CO_u'$, d, $^2J_{CP} = 6.0$ Hz), 204.38 ($2CO_e'$, d, $^2J_{CP} = 11$ Hz), 247.44 ($1CO_{acyl}$, d, $^2J_{CP} = 6.0$ Hz)

MS (16 eV, 200 °C): $M^+ = 688$ (19.2%); $M-nCO$ ($n = 1-8$)

X-Ray Structure of 9

X-ray quality, single crystals of **9** were obtained by cooling a saturated hexane solution at 5°C for 4 h. The X-ray structure determination was performed by the staff of Dr. Robin D. Rogers at the University of Northern Illinois, DeKalb, Illinois.

The data were collected on an Enraf-Nonius CAD-4 diffractometer and the reflections were corrected for absorption. The structure was solved using the SHELXS²⁰ program. Following refinement of the nonhydrogen atoms with anisotropic thermal parameters, refinement of $R = 0.036$ and $R_w = 0.043$ was achieved. The acetylenic hydrogen atom was fixed at a calculated distance of 0.95 Å from C₉ and allowed to ride on that atom with $B = 5.5 \text{ \AA}^2$. The methyl hydrogens were also fixed at 0.95 Å from the bonded carbon atoms, with $B = 5.5 \text{ \AA}^2$.

Table 4.2 provides relevant collection and refinement data. Relevant bond distances and angles are provided in tables 4.3 and 4.4.

**Table 4.2 Crystallographic Data for
OsRu(CO)₇(PMe₃)(μ-η¹,η¹-C{O}HC₂CF₃), 9**

formula	OsRuPF ₃ O ₈ C ₁₄ H ₁₀
formula weight	685.47
crystal dimensions, mm	0.12 x 0.15 x 0.35
space group	P $\bar{1}$ (No. 2)
temperature, °C	19
radiation	graphite-monochromated MoK α ($\lambda = 0.71073 \text{ \AA}$)
cell parameters	
a, \AA	7.216(4)
b, \AA	10.937(3)
c, \AA	13.560(2)
α , deg	69.54(2)
β , deg	87.48(3)
γ , deg	79.60(6)
volume, \AA^3	986.0
Z	2
ρ_{calcd} , g cm ⁻³	2.31
μ_{calcd} , cm ⁻¹	77.2
2 θ range, deg	2 \leq 2 θ \leq 50
scan type	ω -2 θ
scan width, deg	0.80 + 0.35tan θ
reflections measured	3461 (h, \pm k, \pm l)
reflections observed	2560
parameters refined	262
R	0.036 (R = $\Sigma F_o - F_c / \Sigma F_o $)
R _w	0.043 (R _w = $[\Sigma w(F_o - F_c)^2 / \Sigma wF_o^2]^{1/2}$)

**Table 4.3 Bond Distances (Å) for
OsRu(CO)₇(PMe₃)(μ-η¹,η¹-C{O}HC₂CF₃), 9**

<u>Metal - Metal</u>		<u>C - C bridging</u>	
Ru - Os	2.9133(8)	C(8) - C(9)	1.49(1)
		C(10) - C(9)	1.33(1)
<u>Metal - C (bridging)</u>			
Ru - C(8)	2.13(1)	Os - C(10)	2.16(1)
<u>Metal - P</u>			
Ru - P	2.339(3)		
<u>Metal - C (carbonyl)</u>			
Ru - C(5)	1.94(1)	Os - C(1)	1.94(1)
Ru - C(6)	1.91(1)	Os - C(2)	1.89(1)
Ru - C(7)	1.96(1)	Os - C(3)	1.94(1)
		Os - C(4)	1.94(1)
<u>C - O</u>			
C(5) - O(5)	1.12(1)	C(1) - O(1)	1.14(1)
C(6) - O(6)	1.16(1)	C(2) - O(2)	1.16(1)
C(7) - O(7)	1.14(1)	C(3) - O(3)	1.17(1)
C(8) - O(8)	1.21(1)	C(4) - O(4)	1.13(1)

Numbers in parentheses are estimated standard deviations in the last digit

**Table 4.4 Bond Angles (deg) for
OsRu(CO)₇(PMe₃)(μ - η^1, η^1 -C(O)HC₂CF₃), 9**

<u>at Ru</u>		<u>at Os</u>	
Os - Ru - C(8)	81.5(2)	Ru - Os - C(10)	81.8(2)
Os - Ru - C(5)	92.8(3)	Ru - Os - C(1)	83.9(3)
Os - Ru - C(6)	87.4(3)	Ru - Os - C(3)	88.0(2)
Os - Ru - C(7)	96.1(3)	Ru - Os - C(4)	86.0(3)
Os - Ru - P	169.96(9)	Ru - Os - C(2)	177.6(3)
P - Ru - C(5)	91.4(4)	C(2) - Os - C(1)	93.9(5)
P - Ru - C(6)	87.1(3)	C(2) - Os - C(3)	93.9(5)
P - Ru - C(7)	92.8(3)	C(2) - Os - C(4)	95.3(5)
P - Ru - C(8)	89.8(3)	C(2) - Os - C(10)	96.9(4)
C(5) - Ru - C(6)	171.7(5)	C(1) - Os - C(3)	167.1(4)
C(5) - Ru - C(7)	91.5(5)	C(1) - Os - C(4)	95.6(5)
C(5) - Ru - C(8)	84.4(5)	C(1) - Os - C(10)	83.2(4)
C(6) - Ru - C(7)	96.7(5)	C(3) - Os - C(4)	93.8(5)
C(6) - Ru - C(8)	87.4(5)	C(3) - Os - C(10)	85.7(4)
C(7) - Ru - C(8)	175.2(4)	C(4) - Os - C(10)	167.8(4)
<u>at C (carbonyl)</u>			
Ru - C(5) - O(5)	176(1)	Os - C(1) - O(1)	177.5(9)
Ru - C(6) - O(6)	176(1)	Os - C(3) - O(3)	176(1)
Ru - C(7) - O(7)	175(1)	Os - C(4) - O(4)	179.8(4)
		Os - C(2) - O(2)	177(1)

at C (bridging)

Ru - C(8) - C(9)	119.4(7)	Os - C(10) - C(9)	125.0(7)
Ru - C(8) - O(8)	123.2(7)	Os - C(10) - C(11)	118.5(7)
O(8) - C(8) - C(9)	117.3(9)	C(8) - C(9) - C(10)	120.0(9)
C(9) - C(10) - C(11)	116.3(9)		

at P

Ru - P - C(12)	115.2(5)
Ru - P - C(13)	116.6(5)
Ru - P - C(14)	115.3(6)

Torsional Angles

C(1) - Os - Ru - C(5)	22.8
C(3) - Os - Ru - C(6)	21.2
C(4) - Os - Ru - C(7)	18.5
C(11) - C(10) - C(9) - C(8)	4.8
C(10) - C(9) - C(8) - O(8)	30.4

Numbers in parentheses are estimated standard deviations in the last digit.

Due to calculation of torsional angles with a local program, estimated standard deviations could not be determined.

4.8 References

- (1) (a) Jenkins, J. A.; Cowie, M. *Organometallics* **1992**, *11*, 2767. (b) Johnson, K. A.; Gladfelter, W. L. *Organometallics* **1992**, *11*, 2534. (c) Mague, J. T. *Polyhedron* **1990**, *9*, 2635. (d) Burn, M. J.; Kiel, G.-Y.; Seils, F.; Takats, J.; Washington, J. *J. Am. Chem. Soc.* **1989**, *111*, 6850. (e) Johnson, K. A.; Gladfelter, W. L. *Organometallics* **1989**, *8*, 2866. (f) Gagné, M. R.; Takats, J. *Organometallics* **1988**, *7*, 561. (g) Burke, M. R.; Takats, J. *J. Organomet. Chem.* **1986**, *302*, C25. (h) Mague, J. T. *Organometallics* **1986**, *5*, 918. (i) Gracey, B. P.; Knox, S. A. R.; Macpherson, K. A.; Orpen, A. G.; Stobart, S. R. *J. Chem. Soc., Dalton Trans.* **1985**, 1935. (j) Cowie, M.; Dickson, R. S.; Hames, B. W. *Organometallics* **1984**, *3*, 1879. (k) Cowie, M.; Sutherland, B. R. *Organometallics* **1984**, *3*, 1869. (l) Dyke, A. F.; Knox, S. A. R.; Naish, P. J.; Taylor, G. E. *J. Chem. Soc., Dalton Trans.* **1982**, 1297. (m) Hoffman, D. M.; Hoffmann, R.; Fisel, C. R.; *J. Am. Chem. Soc.* **1982**, *104*, 3858, and references therein. (n) Cowie, M.; Southern, T. G. *Inorg. Chem.* **1982**, *21*, 246. (o) Dickson, R. S.; Gatehouse, B. M.; Nesbit, M. C.; Pain, G. N. *J. Organomet. Chem.* **1981**, *215*, 97. (p) Cowie, M.; Dickson, R. S. *Inorg. Chem.* **1981**, *20*, 2682. (q) Koie, Y.; Sinoda, S.; Saito, Y.; Fitzgerald, B. J.; Pierpont, C. G. *Inorg. Chem.* **1980**, *19*, 770.
- (2) Washington, J. S. Ph. D. Thesis, University of Alberta, 1994.
- (3) (a) Kiel, G.-Y.; Takats, J. *Organometallics* **1989**, *8*, 839. (b) Fontaine, X. L. R.; Jacobsen, G. B.; Shaw, B. L.; Thornton-Pett, M. *J. Chem. Soc., Dalton Trans.* **1988**, 741. (c) Hogarth, G.; Kayser, F.; Knox, S. A. R.; Morton, D. A. V.; Orpen, A. G.; Turner, M. L. *J. Chem. Soc., Chem. Commun.* **1988**, 358. (d)

- Dyke, A. F.; Knox, S. A. R.; Naish, P. J.; Taylor, G. E. *J. Chem. Soc., Chem. Commun.* **1980**, 409.
- (4) Collman, J. P.; Hegedus, L. S.; Norton, J. R.; Finke, R. G. *Principles and Applications of Organotransition Metal Chemistry*, University Science Books: Mill Valley, CA 1981.
- (5) *Phosphorus-31 NMR Spectroscopy in Stereochemical Analysis: Organic Compounds and Metal Complexes*; Quin, L. D.; Verkade, J. G., Eds.; Methods in Stereochemical Analysis; VCH: Deerfield Beach, FL, 1987.
- (6) (a) Todd, L. J.; Wilkinson, J. R. *J. Organomet. Chem.* **1974**, 77, 1. (b) Mann, B. E.; Taylor, B. F. In *¹³C NMR Data for Organometallic Compounds*; Maitlis, P. M.; Stone, F. G. A.; West, R., Eds.; Organometallic Chemistry; Academic: Toronto, 1981.
- (7) Friebolin, H. *Basic One- and Two-Dimensional NMR Spectroscopy*, VCH: New York, 1991.
- (8) Mann, B. E.; Taylor, B. F. *¹³C NMR Data for Organometallic Compounds*; Academic: Toronto, 1981.
- (9) Bassler, G. C.; Morrill, T. C.; Silverstein, R. M. *Spectrometric Identification of Organic Compounds* 4th ed.; John Wiley & Sons: Toronto, 1981.
- (10) Emsley, J. *The Elements* 2nd ed.; Clarendon: Toronto, 1992.
- (11) Day, V. W.; Kiel, G.; Takats, J., unpublished results.
- (12) March, J. *Advanced Organic Chemistry: Reactions, Mechanisms, and Structure*, 3rd ed.; John Wiley & Sons: Toronto, 1985.
- (13) Alcock, N. W.; Butts, S. B.; Holt, E. M.; Shriver, D. F.; Stimson, R. E.; Strauss, S. H. *J. Am. Chem. Soc.* **1980**, 102, 5093.
- (14) Parshall, G. W. *Homogeneous Catalysis: The Applications of Catalysis by Soluble Transition Metal Complexes*; Wiley-Interscience: Toronto, 1980.

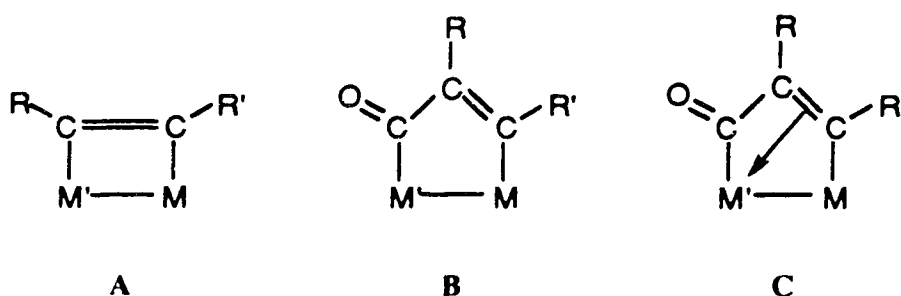
- (15) Atwood, J. D. *Inorganic and Organometallic Reaction Mechanisms*; Brooks/Cole: Monterey, CA, 1985.
- (16) Axe, F. U.; Marynick, D. S. *J. Am. Chem. Soc.* **1988**, *110*, 3728.
- (17) Cotton, F. A.; Wilkinson, G. *Advanced Inorganic Chemistry*, 5th ed.; John Wiley & Sons: Toronto, 1988.
- (18) Adams, R. D.; Cotton, F. A. In *Dynamic Nuclear Magnetic Resonance Spectroscopy*; Cotton, F. A.; Jackman, L. M. Eds.; Academic: New York, 1975.
- (19) Huheey, J. E. *Inorganic Chemistry: Principles of Structure and Reactivity*, 3rd ed.; Harper & Row: New York, 1983.
- (20) Sheldrick, G.M. *Acta Cryst.*, **1990**, *A46*, 467.

Chapter Five

**Synthesis and Characterization of $\text{Cp}'\text{MRu}(\text{CO})_5(\mu\text{-}\eta^1,\eta^1\text{-HC}_2\text{CF}_3)$
Complexes ($\text{M} = \text{Rh, Ir}$; $\text{Cp}' = \text{Cp, Cp}^*$)**

5.1 Introduction

Apart from condensation reactions with $\text{Ru}(\text{CO})_5$ and $\text{Os}(\text{CO})_5$, the $\text{M}(\text{CO})_4(\eta^2\text{-RC}_2\text{R}')$ ($\text{M} = \text{Ru, Os}$; $\text{R, R}' = \text{H, CF}_3$)^{1d,f} complexes also yield dimetallacyclic products from their reactions with $\text{Cp}'\text{M}'(\text{CO})_2$ ($\text{Cp}' = \text{C}_5\text{H}_5, \text{C}_5\text{Me}_5$; $\text{M}' = \text{Co, Rh, Ir}$)^{1d,2}. While exhibiting the typical structures now associated with the Group 8 dimetallacycles, **A**^{1a-q} and **B**^{1b,d,o} (scheme 5.1), these mixed Group 8/9 dimetallacycles introduce an additional structural type, that of the bridging η^1,η^3 -dimetallacyclopentenone, **C**^{2,3a-d}. Condensation reactions involving $\text{Os}(\text{CO})_4(\eta^2\text{-HC}_2\text{H})$ with $\text{CpCo}(\text{CO})_2$ or $\text{CpRh}(\text{CO})_2$ yield products exhibiting structure **C**, while the reaction with $\text{CpIr}(\text{CO})_2$ yields structure **B**^{1d}.



Scheme 5.1 Three Types of Dimetallacyclic Structure:

A, η^1,η^1 -dimetallacyclobutene; B, η^1,η^1 -dimetallacyclopentenone;

C, η^1,η^3 -dimetallacyclopentenone

However, no dimetallacyclopentenone structures are observed when a perfluoromethyl group replaces one or both hydrogens on the alkyne ligand, as the reactions of $\text{Ru}(\text{CO})_4(\eta^2\text{-F}_3\text{CC}_2\text{CF}_3)^{1f}$ and $\text{Os}(\text{CO})_4(\eta^2\text{-HC}_2\text{CF}_3)^2$ with the $\text{Cp}'\text{M}'(\text{CO})_2$ reagents yield exclusively dimetallacyclobutene products, A.

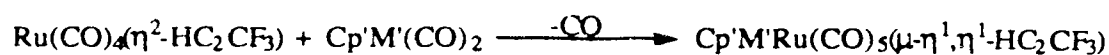
While the $\text{Ru}(\text{CO})_4(\eta^2\text{-F}_3\text{CC}_2\text{CF}_3)$ complex has proved to be quite reactive towards the Group 9 complexes, the same cannot be said for the analogous acetylene precursor. The ruthenium carbonyl acetylene complex decomposes above -40°C , before reaction can occur with any of the aforementioned Group 9 complexes⁴.

The impetus for the present work was to establish whether $\text{Ru}(\text{CO})_4(\eta^2\text{-HC}_2\text{CF}_3)$ was sufficiently stable to react with the Group 9 complexes to yield dimetallacyclic products. Given this, of further interest was the structure of any dimetallacycles formed and whether there would be any selectivity in the attachment of the trifluoropropyne ligand to the dimetal framework.

5.2 Synthesis and Characterization of $\text{Cp}'\text{M}'\text{Ru}(\text{CO})_5(\mu\text{-}\eta^1, \eta^1\text{-HC}_2\text{CF}_3)$

The title compounds were prepared by the reaction of a hydrocarbon solution of $\text{Ru}(\text{CO})_4(\eta^2\text{-HC}_2\text{CF}_3)$, cooled to -50°C , with the appropriate $\text{Cp}'\text{M}'(\text{CO})_2$ solution, followed by warming to 0°C . The reactions were monitored by infrared spectroscopy and were judged to be complete when the carbonyl bands of the reactants had disappeared. Subsequently, the crude residues were extracted and precipitated at reduced temperature (scheme 5.2). Due to the thermal instability of the products, mass spectral data were obtained using fast atom bombardment. The spectra exhibited the loss of five carbonyls, as well as parent ions (table 5.1). Both elemental analyses and mass spectral data are consistent with bimetallic products, as formulated in scheme 5.2.

The infrared spectra of the products are essentially identical, consisting of a distinctive pattern of five sharp carbonyl stretching frequencies, occurring in the region typically between 2115 and 1969 cm^{-1} (fig. 5.1), indicating the presence of terminal carbonyls only. The positions and relative intensities of these bands are consistent with those observed for the characterized series of $\text{Cp}'\text{M}'\text{Ru}(\text{CO})_5(\mu\text{-}\eta^1, \eta^1\text{-F}_3\text{CC}_2\text{CF}_3)$ dimetallacyclobutene complexes^{1f}; therefore, the trifluoropropyne analogues are also formulated as dimetallacyclobutenes. Neither acyl-carbonyl stretching frequencies nor coordinated alkyne carbon-carbon stretching frequencies were observed in the spectra.



Scheme 5.2 Preparation of $\text{Cp}'\text{M}'\text{Ru}(\text{CO})_5(\mu\text{-}\eta^1, \eta^1\text{-HC}_2\text{CF}_3)$ Complexes

M'	Cp'	T(°C)	colour	yield(%)	M ⁺ (m/e)
10, Rh	C ₅ H ₅	-50	red-brown	88	504
11, Rh	C ₅ Me ₅	-35	red-brown	26	574
12, Ir	C ₅ Me ₅	-50	orange	79	665

Table 5.1 Reaction and Product Data

Although the $\text{MM}'(\text{CO})_7(\text{L})(\mu\text{-}\eta^1, \eta^1\text{-HC}_2\text{CF}_3)$ and $\text{Cp}'\text{M}'\text{Ru}(\text{CO})_5(\mu\text{-}\eta^1, \eta^1\text{-F}_3\text{CC}_2\text{CF}_3)$ complexes are thermally stable^{1f}, the $\text{Cp}'\text{M}'\text{Ru}(\text{CO})_5(\mu\text{-}\eta^1, \eta^1\text{-HC}_2\text{CF}_3)$ complexes are not. At room temperature 10, 11, and 12 all undergo decomposition as solids, as observed by colour change, IR and NMR spectroscopies. Moreover, warming a

solution of **11** to room temperature results in the formation of a very dark green solution and the appearance of new IR stretching frequencies as well as those attributable to $\text{Cp}^*\text{Rh}(\text{CO})_2$. Only after numerous attempts was the bimetallic complex **11** isolated in analytically pure form. Unfortunately, the reaction mixtures could not be successfully separated by chromatography; however, by employing fractional crystallization methods it was possible to separate **11** from a trinuclear by-product **11a** (*vide infra*).

Attempts to prepare bimetallic complexes from the reactions of $\text{Ru}(\text{CO})_4(\eta^2\text{-HC}_2\text{CF}_3)$ and the $\text{Cp}^*\text{Co}(\text{CO})_2$, $\text{CpCo}(\text{CO})_2$, and $\text{CpIr}(\text{CO})_2$ were unsuccessful. When reaction solutions containing the latter two complexes were allowed to warm to room temperature

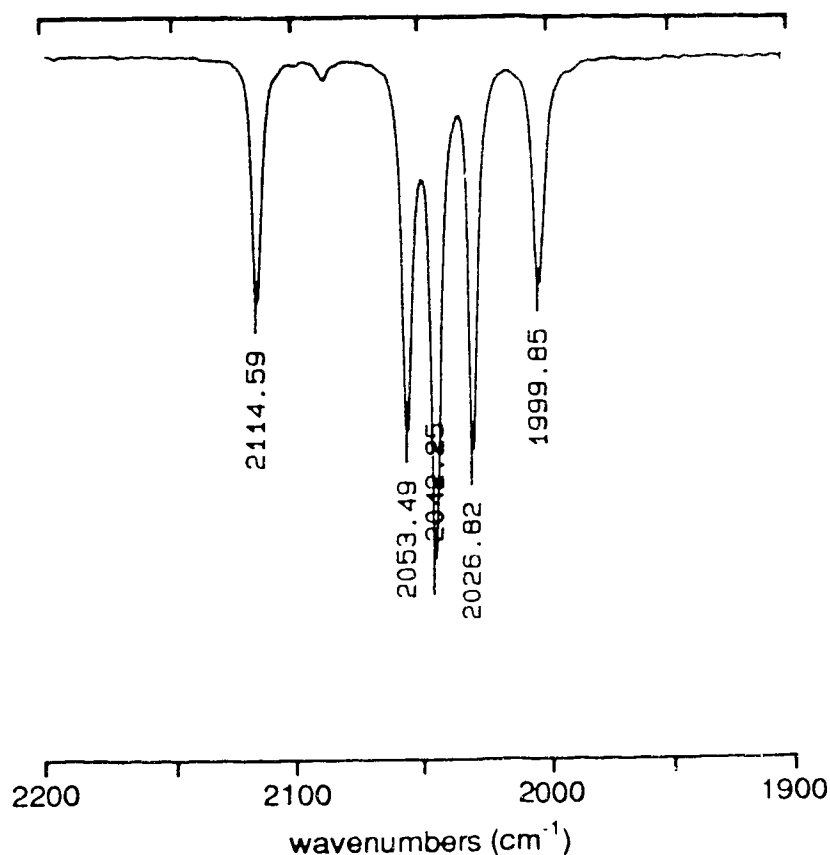


Figure 5.1 Solution IR Spectrum of $\text{CpRhRu}(\text{CO})_5(\mu\text{-}\eta^1, \eta^1\text{-HC}_2\text{CF}_3)$, **10**

Decomposition of the $\text{Ru}(\text{CO})_4(\eta^2\text{-HC}_2\text{CF}_3)$ resulted with no observable bimetallic product formation, as indicated by IR spectroscopy. With $\text{Cp}^*\text{Co}(\text{CO})_2$ a complicated mixture of products was obtained, which could not be separated by chromatographic methods. No further purification attempts were made.

5.3 NMR Spectra and Fluxional Behaviour

The room temperature ^1H NMR spectra of **10** and **11** are similar to those already observed for the $\text{MRu}(\text{CO})_7(\text{PMe}_3)(\mu\text{-}\eta^1, \eta^1\text{-HC}_2\text{CF}_3)$ complexes ($M = \text{Os, Ru}$) and discussed in Chapter 3. Both **10** and **11** exhibit low-field sextet resonances, occurring at δ 8.09 and 7.56, respectively. The apparent 1:3:6:6:3:1 sextets are the result of overlapping quartets, due to the small Rh-H coupling of 4.4 Hz for **10** and 3.0 Hz for **11** and F-H coupling of 2 Hz. These resonances integrated to one proton and are clearly due to the alkyne proton. The remaining ^1H NMR signals for **10** and **11** occur at δ 5.53 and 1.94, respectively, and correspond to the C_5H_5 and $\text{C}_5(\text{CH}_3)_5$ protons.

While the alkyne proton resonances of **10** and **11** are quite sharp, the resonance observed for **12** at δ 8.05 is broad at room temperature and no coupling to fluorine can be observed. Cooling the sample to -80°C results in no appreciable sharpening of the signal and heating achieves no broadening, only decomposition. Furthermore, as the ^{19}F NMR spectrum is also broad, no coupling data could be gathered for **12**. The Cp^* hydrogens resonate at δ 2.06 and the signal is sharp.

The ^{19}F NMR resonances for **10**, **11**, and **12** are very similar occurring at δ -63.18, -63.32, and -63.13, and are comparable to those observed for the $\text{MM}'(\text{CO})_7(\text{L})(\mu\text{-}\eta^1, \eta^1\text{-HC}_2\text{CF}_3)$ complexes in Chapter 3. Due to their remarkable similarity, the fluorine resonances offer little structural information; however, it should be noted that the rhodium-ruthenium bimetallic complexes do not display fluorine-rhodium coupling. Since

the alkyne proton exhibits coupling to rhodium, that end of the alkyne ligand is most likely bonded to rhodium. This assertion is consistent with the regiochemistry of the $MM'(CO)_7(L)(\mu-\eta^1, \eta^1-HC_2CF_3)$ complexes as well as that observed in the solid-state structure of $Cp^*IrOs(CO)_5(\mu-\eta^1, \eta^1-HC_2CF_3)_2$.

The variable temperature $^{13}C\{^1H\}$ NMR spectra of **10** and **12** were determined using the ^{13}CO enriched materials, prepared in an analogous fashion to the unenriched materials. In both cases the complexes were found to be fluxional.

The room temperature $^{13}C\{^1H\}$ NMR spectrum of **10** (fig. 5.2) and the $-40^\circ C$ spectrum of **12** (fig. 5.2) each consist of three carbonyl resonances in a ratio of 1:2:2. The resonances for **10** occur at δ 194.17, 193.65, and 190.62, while those for **12** occur at δ 196.71, 190.10, and 184.69. Of note is the resonance at δ 193.65, which exhibits coupling to rhodium of 39.3 Hz. Decoalescence is achieved upon cooling **10** to 213 K. Decoalescence of the signals observed for **12** occurs at 173 K, at which point the higher field resonances have broadened into the baseline and only the low-field signals at δ 194.17 and 196.71 remain invariant. Neither low- nor high-temperature limiting spectra could be obtained for **10** and **12**; however, both limiting spectra were determined for $Cp^*IrOs(CO)_5(\mu-\eta^1, \eta^1-HC_2CF_3)$. The exchange mechanism and carbonyl labelling scheme is outlined in scheme 5.3². Complexes **10** and **12** appear to mimic this fluxional behaviour.

At room temperature the exchange rate is sufficiently rapid such that the two carbonyls **b** and **b'** appear to simultaneously occupy two sites, one on rhodium and one on ruthenium. The observed chemical shift is the average of the two low-temperature limiting signals, as is the rhodium-carbon coupling (at the low-temperature limit one carbonyl is coupled to rhodium and one is not). Similarly, the equivalent **t** and **t'** carbonyls are an average of the two low-temperature limiting equatorial sites. If the system could be cooled to the low-temperature limit, the time averaged signals would decoalesce and each would reappear as two signals, due to the asymmetric nature of the ground state structure of the molecule.

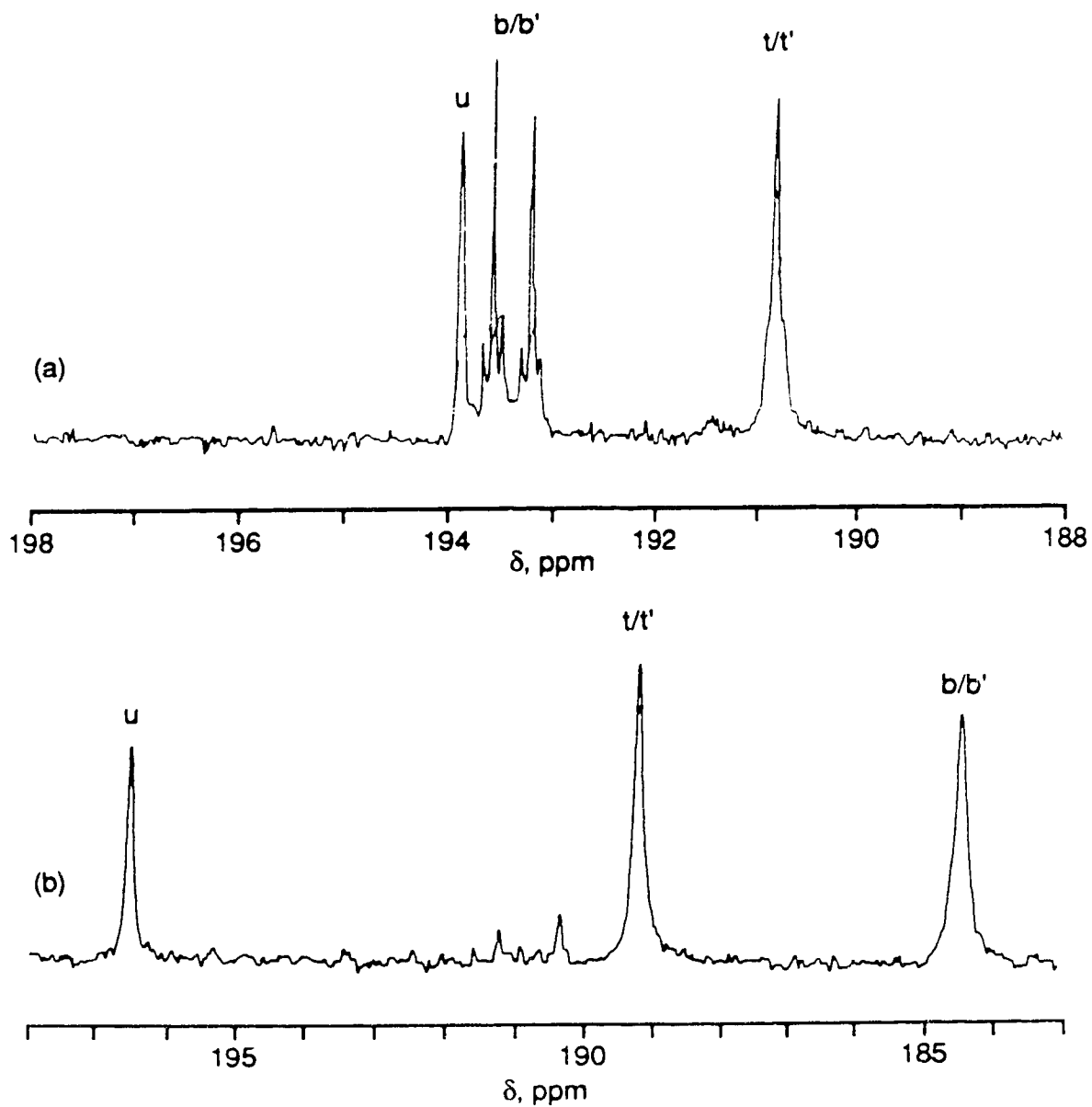
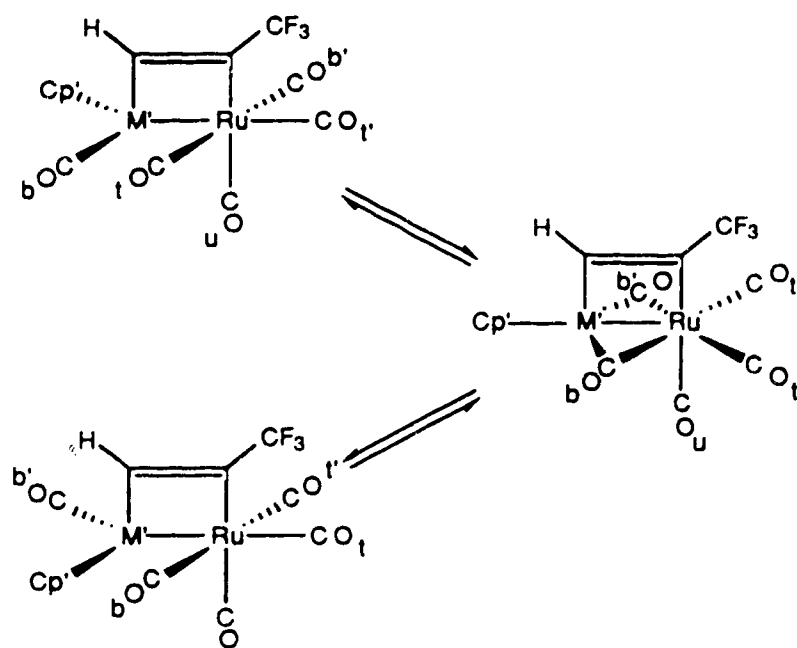


Figure 5.2 (a) Room Temperature $^{13}\text{C}\{^1\text{H}\}$ NMR Spectrum of $\text{CpRhRu}(\text{CO})_5(\mu\text{-}\eta^1, \eta^1\text{-HC}_2\text{CF}_3)$, 10, and (b) -40°C Spectrum of $\text{Cp}^*\text{IrRu}(\text{CO})_5(\mu\text{-}\eta^1, \eta^1\text{-HC}_2\text{CF}_3)$, 12

The fluxional process generates a symmetric transition state which leads to the simplicity of the observed spectra.

The fluxional behaviour, below -40°C , observed for **12** is analogous to that of **10**; an invariant low-field signal at δ 196.40 corresponds to the u carbonyl attached to ruthenium, the next lowest field signal at δ 189.14 corresponds to the equivalent t and t' carbonyls, and the highest field signal at δ 184.47 corresponds to the equivalent b and b' carbonyls.



Scheme 5.3 Proposed Fluxional Exchange Process for $\text{Cp}'\text{M}'\text{Ru}(\text{CO})_5(\mu\text{-}\eta^1, \eta^1\text{-HC}_2\text{CF}_3)$

The assignment of the latter two signals is based upon the expected high-field shift of the b/b' carbonyls, as in the ground state structure one carbonyl is bonded to iridium⁵. Above -40°C the fluxional behaviour of becomes more complicated. In dichloromethane- d_2

solvent, warming the sample to room temperature results in broadening of the δ 189.14 resonance, while the δ 184.47 resonance remains much sharper, but gradually disappearing into the baseline. In toluene-*d*₈ solvent the room temperature spectrum exhibits two sharp resonances at δ 196.96 and 189.06 and a broader resonance at δ 184.58. Furthermore, heating the solution to 333 K results in sharpening of the two higher field signals as the low-field signal at δ 196.96 disappears into the baseline. The process appears to be reversible, but the nature of the high-temperature fluxionality is unclear.

Due to the considerable difficulty in preparing $\text{Cp}^*\text{RhRu}(\text{CO})_5(\mu\text{-}\eta^1, \eta^1\text{-HC}_2\text{CF}_3)$ the ^{13}C enriched material was not synthesized. Furthermore, due to the thermally unstable nature of the $\text{Cp}^*\text{M}^*\text{Ru}(\text{CO})_5(\mu\text{-}\eta^1, \eta^1\text{-HC}_2\text{CF}_3)$ complexes, reliable $^{13}\text{C}\{^1\text{H}\}$ NMR data for the non-carbonyl carbons could not be gathered, with the exception of $\text{Cp}^*\text{IrRu}(\text{CO})_5(\mu\text{-}\eta^1, \eta^1\text{-HC}_2\text{CF}_3)$ for which the pentamethylcyclopentadienyl (δ 9.47, $\text{C}_5(\text{CH}_3)_5$; 97.63, $\text{C}_5(\text{CH}_3)_5$) and perfluoromethyl (δ 124.99, quartet, HCCCF_3 , $^1J_{\text{CF}} = 271$ Hz) carbons were conclusively detected.

5.4 Thermal Disproportionation of $\text{Cp}^*\text{RhRu}(\text{CO})_5(\mu\text{-}\eta^1, \eta^1\text{-HC}_2\text{CF}_3)$, 11

When $\text{Cp}^*\text{Rh}(\text{CO})_2$ was reacted with $\text{Ru}(\text{CO})_4(\eta^2\text{-HC}_2\text{CF}_3)$ the initial product formed below 0°C was the Rh-Ru bimetallic as verified by the solution infrared spectrum. When the solution was gradually warmed to room temperature it became increasingly dark in colour, eventually turning from yellow-orange to a very dark, dichromic green-violet colour. Coincident with the colour change was the slow precipitation of a very dark green solid which, when isolated, proved to be completely insoluble in hydrocarbon solvent and stable at room temperature for periods well beyond those expected for a heterobimetallic product. In diethyl ether solvent the dark green solid gave an infrared spectrum having bands at 2038 s, 1982 m, 1966 w, and 1820 m cm^{-1} (fig.5.3), that clearly differs from the

$\text{Cp}^*\text{RhRu}(\text{CO})_5(\mu\text{-}\eta^1,\eta^1\text{-HC}_2\text{CF}_3)$ IR bands of 2104 m, 2043 s, 2031 s, 2015 s, and 1983 m cm^{-1} . Notably, the infrared profile of the dark green material matched very well the pattern observed for perpendicular alkyne-bridged complex $\text{Cp}^*\text{RhRu}(\text{CO})_3(\mu\text{-CO})(\mu\text{-}\eta^2,\eta^2\text{-F}_3\text{CC}_2\text{CF}_3)$ ⁶. Although by all appearances the dark green complex seemed analogous to the former, perpendicular bridged hexafluorobutene complex, the electron impact mass spectrum of the complex revealed a parent ion of m/e 812, the loss of five carbonyls, and an isotopic pattern consistent with two rhodium metals and one ruthenium. Thus, the mass spectral data suggested the formulation of $\text{Cp}^*_2\text{Rh}_2\text{Ru}(\text{CO})_5(\text{HC}_2\text{CF}_3)$.

The ^1H NMR spectrum of **11a** consists of two $\text{C}_5(\text{CH}_3)_5$ singlets at δ 1.77 and 1.85, respectively, each equivalent to fifteen protons, and a doublet of doublets at δ 5.37, equivalent to one proton and having coupling to rhodium of 1.3 and 3.4 Hz. The latter resonance is consistent with that of the alkyne protons observed for the bimetallic products of preceding chapters in that there is no coupling to fluorine and the resonance is considerably more shielded (*ca.* 2.5 ppm upfield) than would be expected for a dimetallacyclobutene/pentenone product.

It is well established that diamagnetic anisotropy will affect the shielding of protons bound to the carbon atoms⁷. In the case of sp -hybridization, the result of diamagnetic anisotropy is greater shielding of the protons attached to the multiply bonded carbon atom, while sp^2 -hybridization results in reduced shielding. For example, the alkyne proton in uncoordinated trifluoropropyne resonates at δ 3.10, but the same proton resonates at δ 7.25 in the dimetallacyclobutene complex $\text{Ru}_2(\text{CO})_8(\mu\text{-}\eta^1,\eta^1\text{-HC}_2\text{CF}_3)$. The observed resonance, being intermediate to the above limits, suggests that the double bond may be coordinated to another metal in the trinuclear framework.

A particularly remarkable feature in the $^{13}\text{C}\{^1\text{H}\}$ NMR spectrum of **11a** is an intense apparent triplet at δ 70.80 ($J_{\text{RhC}} = \sim 5$ Hz). The triplet resonance is likely due to coupling to two nearly equivalent rhodium atoms. The data for the perpendicular bridging alkyne complex $\text{Cp}^*\text{RhRu}(\text{CO})_3(\mu\text{-CO})(\mu\text{-}\eta^1,\eta^1\text{-F}_3\text{CC}_2\text{CF}_3)$ ⁶ reveal a doublet resonance at δ

56.96 ($J_{\text{RhC}} = 22 \text{ Hz}$), consistent with an sp^3 -carbon⁷ bridging two metal centers. As seen in Chapter 3, the dimetallacyclobutene and -pentenone alkyne carbons resonate anywhere from δ 100 to 165, consistent with sp^2 -hybridization. Clearly, the high-field resonance for the alkyne carbon suggests a significant departure from sp^2 -hybridization, which is corroborated by the more shielded resonance of the alkyne proton. The perfluoromethyl carbon occurs as a quartet at δ 127.84 ($^1J_{\text{CF}} = 276 \text{ Hz}$). A discrete resonance attributable to the perfluoromethyl bearing alkyne carbon could not be assigned.

That there are two independent Cp* ligands is further verified by the two methyl resonances at δ 9.30 and 10.53, and by the quaternary carbon doublet resonances at δ

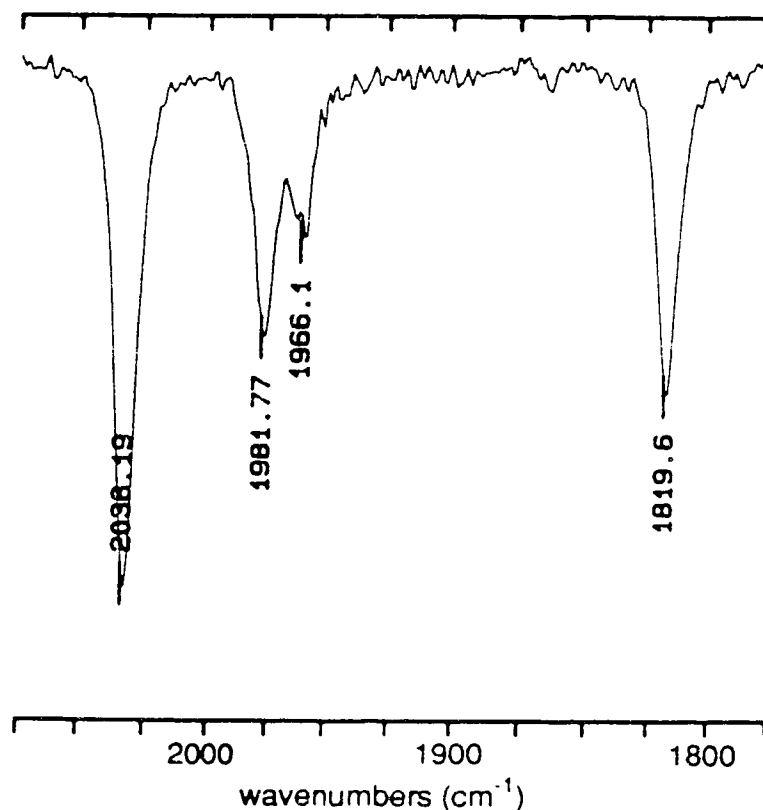
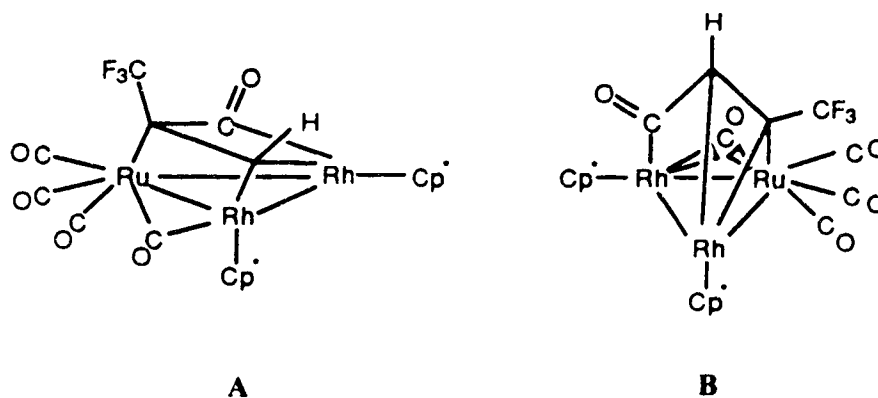


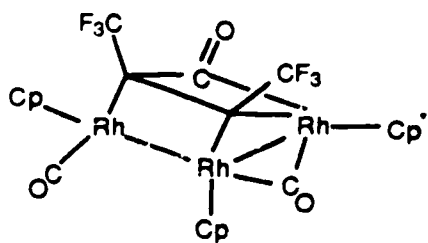
Figure 5.3 IR Spectrum of $\text{Cp}^*_2\text{Rh}_2\text{Ru}(\text{CO})_5(\text{HC}_2\text{CF}_3)$, 11a

104.78 ($^1J_{\text{CRh}} = 4.5$ Hz) and 105.92 ($^1J_{\text{CRh}} = 3.8$ Hz). The carbonyl region contains four discernable resonances in a 1:1:1:1 ratio occurring as singlets at δ 190.41, 193.21, 214.13, and a doublet at 221.41 ($J_{\text{CRh}} = 31.7$). The high-field signals are consistent with carbonyls bonded to ruthenium, while the low-field resonance is consistent with either an acyl group or a bridging carbonyl. A signal attributable to the fifth carbonyl could not be confidently assigned, although poorly resolved resonances were observed at both high- and low-field.

Although a conclusive structure is not suggested by the data presented, literature precedence does suggest two possibilities, structures **A** and **B** (scheme 5.4). Structure **A** is analogous to the structure of $\text{Cp}_2\text{Cp}^*\text{Rh}_3(\text{CO})_3(\mu\text{-F}_3\text{CC}_2\text{CF}_3)$ reported by Dickson⁸ (scheme 5.5), the only significant difference being the formulation of a metal-metal bond between ruthenium and the back rhodium to satisfy the eighteen electron rule. The trirhodium cluster was prepared by the thermal reaction of $\text{Cp}_2\text{Rh}_2(\mu\text{-CO})(\mu\text{-}\eta^2,\eta^2\text{-F}_3\text{CC}_2\text{CF}_3)$ and $\text{Cp}^*\text{Rh}(\text{CO})_2$, an interesting parallel to the conditions leading to **11a**. Structure **B** differs from **A** in that the acyl has been formed by insertion of a carbonyl into



Scheme 5.4 Possible Structures for $\text{Cp}^*_2\text{Rh}_2\text{Ru}(\text{CO})_5(\text{HC}_2\text{CF}_3)$, **11a**



Scheme 5.5 Structure of $\text{Cp}_2\text{Cp}^*\text{Rh}_3(\text{CO})_3(\text{F}_3\text{CC}_2\text{CF}_3)$

the hydrogen-bearing end of the alkyne, consistent with the observations made in the carbonyl insertions of $\text{RuM}(\text{CO})_8(\mu\text{-}\eta^1, \eta^1\text{-HC}_2\text{CF}_3)$ (*vide infra*). Both structures are in reasonable agreement with the data; however, a conclusive assignment could only be made from a solid-state structure determination. Unfortunately, single crystals of **11a** suitable for diffraction could not be obtained.

Attempts at preparing the heterotrinnuclear cluster $\text{Cp}^*\text{RhIrRu}(\text{CO})_5(\mu\text{-HC}_2\text{CF}_3)$ from the thermal reaction of $\text{Cp}^*\text{RhRu}(\text{CO})_5(\mu\text{-HC}_2\text{CF}_3)$ and one equivalent of $\text{Cp}^*\text{Ir}(\text{CO})_2$ were unsuccessful, resulting in the formation $\text{Cp}^*\text{Rh}_2\text{Ru}(\text{CO})_5(\mu\text{-HC}_2\text{CF}_3)$, $\text{Cp}^*\text{IrRu}(\text{CO})_5(\mu\text{-}\eta^1, \eta^1\text{-HC}_2\text{CF}_3)$, and $\text{Cp}^*\text{Ir}(\text{CO})_2$. These observations would suggest that once the Rh-Ru bimetallic complex is formed at low temperature warming it results in fragmentation and generation of either of two reactive sixteen-electron constituents, $\text{Ru}(\text{CO})_3(\eta^2\text{-HC}_2\text{CF}_3)$ or $\text{Cp}^*\text{Rh}(\text{CO})$. Once disproportionation has occurred the alkyne fragment can then react with $\text{Cp}^*\text{Ir}(\text{CO})_2$ to form the Ir-Ru bimetallic, while the $\text{Cp}^*\text{Rh}(\text{CO})$ fragment would react with remaining Rh-Ru bimetallic complex to form the Rh_2Ru cluster. It should be noted that Dickson *et al.* also found $\text{Cp}_2\text{Rh}_2(\mu\text{-CO})(\mu\text{-}\eta^2, \eta^2\text{-F}_3\text{CC}_2\text{CF}_3)$ was unreactive towards $\text{Cp}^*\text{Ir}(\text{CO})_2$, although it would react with $\text{Cp}^*\text{Co}(\text{CO})_2$. No attempts were made to react $\text{Cp}^*\text{RhRu}(\text{CO})_5(\mu\text{-HC}_2\text{CF}_3)$ with $\text{Cp}^*\text{Co}(\text{CO})_2$.

5.5 Conclusion

Although the complexes $MM'(CO)_7(L)(\mu-\eta^1,\eta^1-HC_2CF_3)$ ($M, M' = Ru$ or Os ; $L = CO$ or PMe_3) are rather robust compounds, existing at room temperature in both solution and solid state for extended periods of time, the complexes $Cp'MRu(CO)_5(\mu-HC_2CF_3)$ ($Cp' = C_5H_5, C_5Me_5$; $M = Rh, Ir$) have proven to be unstable under the same conditions. This instability is most pronounced in the case of $Cp^*RhRu(CO)_5(\mu-HC_2CF_3)$, **11**, which can only be prepared in an equilibrium mixture with the trinuclear cluster $Cp^*_2Rh_2Ru(CO)_5(\mu-HC_2CF_3)$, **11a**. Further limitations in the reactivity of $Ru(CO)_4(\eta^2-HC_2CF_3)$ were identified, in that decomposition occurred before reaction could occur with either $CpCo(CO)_2$ or $CpIr(CO)_2$. In Chapter 3 it was found that decomposition occurred before $Ru(CO)_4(\eta^2-HC_2CF_3)$ could react with $Os(CO)_5$ or $Ru(CO)_4(PPh_3)$, and as a result bimetallic complexes containing osmium had to be prepared from $Os(CO)_4(\eta^2-HC_2CF_3)$. In contrast, $Ru(CO)_4(\eta^2-F_3CC_2CF_3)$ reacts readily with the aforementioned metal fragments to form bimetallic products. It would seem that both the insufficient π -acidity of the trifluoropropyne ligand and the well established lability of $4d$ transition metals conspire against the complex $Ru(CO)_4(\eta^2-HC_2CF_3)$ and lead to its thermal instability.

5.6 Experimental

Synthesis of $(\eta^5\text{-C}_5\text{H}_5)\text{RhRu}(\text{CO})_5(\mu\text{-}\eta^1,\eta^1\text{-HC}_2\text{CF}_3)$, **10**

To a stirred solution of $\text{Ru}(\text{CO})_4(\eta^2\text{-HC}_2\text{CF}_3)$ (0.12 mmol in 9.5 mL pentane), cooled to -50°C , was added 25.7 mg $\text{CpRh}(\text{CO})_2$ (0.114 mmol). The solution was allowed to warm to room temperature over 4 h. The solvent was removed *in vacuo* and the product washed with 3x1 mL pentane and the product redissolved in a minimal amount of pentane. The product was precipitated from solution at -78°C over 24 h and dried *in vacuo* at -50°C to yield 51.0 mg of the red-brown product (88% yield).

FW: 503.16

Elemental Analysis: $\text{C}_{13}\text{H}_6\text{O}_5\text{F}_3\text{RhRu}$ calc: C 31.03; H 1.20, found C 31.03; H 1.10

IR (pentane): ν_{CO} 2115 m, 2054 s, 2042 s, 2027 s, 2000 m cm^{-1}

^1H NMR (CD_2Cl_2 , 360 MHz): δ 5.53 (C_5H_5), 8.09 (dq, HCCCF_3 , $^4J_{\text{HF}} = 2$ Hz, $^2J_{\text{HRh}} = 4.4$ Hz)

^{19}F NMR (CD_2Cl_2 , 376.5 MHz): δ -63.18 (d, HCCCF_3)

^{13}C NMR (CD_2Cl_2 , 90 MHz, 298 K): δ 194.17 (1CO_u), 193.65 (d, $2\text{CO}_b/\text{CO}_b'$, $^1J_{\text{CRh}} = 39.3$ Hz), 190.62 ($2\text{CO}_l/\text{CO}_l'$)

MS (FAB, *m*-nitrobenzyl alcohol): $\text{M}^+ = 504$ (14.9%); M-nCO ($n = 1\text{-}5$)

Synthesis of $(\eta^5\text{-C}_5\text{Me}_5)\text{RhRu}(\text{CO})_5(\mu\text{-}\eta^1,\eta^1\text{-HC}_2\text{CF}_3)$, **11**

To a stirred solution of $\text{Ru}(\text{CO})_4(\eta^2\text{-HC}_2\text{CF}_3)$ (0.18 mmol in 12 mL pentane), cooled to -35°C , was added 79.5 mg $\text{Cp}^*\text{Rh}(\text{CO})_2$ (0.270 mmol). The solution was allowed to

warm to room temperature over 4 h. The solvent was removed in vacuo at -50°C. The residue was warmed to room temperature and the product washed first with 5x1 mL pentane to extract all soluble products, and then washed with 2x1 mL CH₂Cl₂ to extract the remaining product. The pentane-soluble product was precipitated from solution at -78°C over 24 h and dried *in vacuo* at -50°C to yield 26.5 mg of the red-brown product (26% yield).

FW: 573.29

Elemental Analysis: C₁₈H₁₆O₅F₃RhRu calc: C 37.71; H 2.81, found: C 38.03; H 2.84

IR (pentane): ν_{CO} 2104 m, 2043 s, 2031 s, 2015 s, 1983 m cm⁻¹

¹H NMR (CD₂Cl₂, 360 MHz, 238 K): δ 1.94 (C₅(CH₃)₅), 7.56 (dq, HCCCF₃, ⁴J_{HF} = 21 Hz, ²J_{HRh} = 3.0 Hz)

¹⁹F NMR (CD₂Cl₂, 376.5 MHz, 238 K): δ -63.32 (d, HCCCF₃)

MS (FAB, *m*-nitrobenzyl alcohol): M⁺ = 574 (23.9%); M-nCO (n = 1-5)

Synthesis of (η⁵-C₅Me₅)₂Rh₂Ru(CO)₅(μ-HC₂CF₃), 11a

Compound 11a was isolated from the CH₂Cl₂ soluble extracts from the preparation of 11. The solution was reduced to dryness and the black residue washed with pentane to remove any remaining soluble impurities and then dried *in vacuo* at room temperature. 18.1 mg of product was isolated (12% yield).

FW: 811.42

IR (Et₂O): ν_{CO} 2038 s, 1982 m, 1966 w, and 1820 m cm⁻¹

¹H NMR (CD₂Cl₂, 360 MHz): δ 1.77, 1.85 (C₅(CH₃)₅), 5.37 (dd, HCCCF₃, ²J_{HRh} = 1.3 and 3.4 Hz)

^{19}F NMR (CD_2Cl_2 , 376.5 MHz): δ -58.30 (HCCCF_3)

^{13}C NMR (CD_2Cl_2 , 75 MHz, 298 K): δ 9.30, 10.53 ($\text{C}_5(\text{CH}_3)_5$), 70.80 (dd, $J_{\text{CRh}} = \sim 5$ Hz), 104.78 (d, $\text{C}_5(\text{CH}_3)_5$, $^1J_{\text{CRh}} = 4.5$ Hz), 105.9 (d, $\text{C}_5(\text{CH}_3)_5$, $^1J_{\text{CRh}} = 3.8$ Hz), 127.84 (quartet, HCCCF_3 , $^1J_{\text{CF}} = 276$ Hz), 190.41 (CO), 193.21 (CO), 214.13 (CO), 221.41 (d, $^1J_{\text{CRh}} = 31.7$ Hz)

MS (16 eV, 200°C): $\text{M}^+ = 812$ (15.6%); M-nCO ($n = 1-5$)

Synthesis of $(\eta^5\text{-C}_5\text{Me}_5)\text{IrRu}(\text{CO})_5(\mu\text{-}\eta^1,\eta^1\text{-HC}_2\text{CF}_3)$, **12**

To a stirred solution of $\text{Ru}(\text{CO})_4(\eta^2\text{-HC}_2\text{CF}_3)$ (0.092 mmol in 12 mL pentane) cooled to -78°C was added 35.1 mg $\text{Cp}^*\text{Ir}(\text{CO})_2$ (0.0915 mmol). The solution was degassed *via* two freeze-thaw cycles and allowed to warm, with stirring, to -20°C . The solution was stirred for 2 h at -20°C and then allowed to warm to 10°C . The solution was concentrated at -78°C for 48 h to precipitate the product and then dried *in vacuo* at -50°C to yield 48.1 mg of the yellow-orange product (79% yield)

FW: 662.61

Elemental Analysis: $\text{C}_{18}\text{H}_{16}\text{O}_5\text{F}_3\text{IrRu}$ calc: C 32.63; H 2.43, found: C 32.90; H 2.24

IR (pentane) ν_{CO} 2106 s, 2045 s, 2030 s, 2014 s, 1969 m cm^{-1}

^1H NMR (CD_2Cl_2 , 360 MHz): δ 2.06 ($\text{C}_5(\text{CH}_3)_5$), 8.05 (broad, HCCCF_3)

^{19}F NMR (CD_2Cl_2 , 376.5 MHz): δ -63.13 (broad, HCCCF_3)

^{13}C NMR (CD_2Cl_2 , 75 MHz, 298 K): δ 9.47 ($\text{C}_5(\text{CH}_3)_5$), 97.63 ($\text{C}_5(\text{CH}_3)_5$), 124.99 (quartet, HCCCF_3 , $^1J_{\text{CF}} = 271$ Hz), 196.40 (1CO_u), 189.14 ($2\text{CO}_b/\text{CO}_b'$), 184.47 ($2\text{CO}_t/\text{CO}_t'$)

MS (FAB, *m*-nitrobenzyl alcohol): $\text{M}^+ = 665$ (50.3%); M-nCO ($n = 1-5$)

5.7 References

- (1) (a) Jenkins, J. A.; Cowie, M. *Organometallics* **1992**, *11*, 2767. (b) Johnson, K. A.; Gladfelter, W. L. *Organometallics* **1992**, *11*, 2534. (c) Mague, J. T. *Polyhedron* **1990**, *9*, 2635. (d) Burn, M. J.; Kiel, G.-Y.; Seils, F.; Takats, J.; Washington, J. *J. Am. Chem. Soc.* **1989**, *111*, 6850. (e) Johnson, K. A.; Gladfelter, W. L. *Organometallics* **1989**, *8*, 2866. (f) Gagné, M. R.; Takats, J. *Organometallics* **1988**, *7*, 561. (g) Burke, M. R.; Takats, J. *J. Organomet. Chem.* **1986**, *302*, C25. (h) Mague, J. T. *Organometallics* **1986**, *5*, 918. (i) Gracey, B. P.; Knox, S. A. R.; Macpherson, K. A.; Orpen, A. G.; Stobart, S. R. *J. Chem. Soc., Dalton Trans.* **1985**, 1935. (j) Cowie, M.; Dickson, R. S.; Hames, B. W. *Organometallics* **1984**, *3*, 1879. (k) Cowie, M.; Sutherland, B. R. *Organometallics* **1984**, *3*, 1869. (l) Dyke, A. F.; Knox, S. A. R.; Naish, P. J.; Taylor, G. E. *J. Chem. Soc., Dalton Trans.* **1982**, 1297. (m) Hoffman, D. M.; Hoffmann, R.; Fisel, C. R.; *J. Am. Chem. Soc.* **1982**, *104*, 3858, and references therein. (n) Cowie, M.; Southern, T. G. *Inorg. Chem.* **1982**, *21*, 246. (o) Dickson, R. S.; Gatehouse, B. M.; Nesbit, M. C.; Pain, G. N. *J. Organomet. Chem.* **1981**, *215*, 97. (p) Cowie, M.; Dickson, R. S. *Inorg. Chem.* **1981**, *20*, 2682. (q) Koie, Y.; Sinoda, S.; Saito, Y.; Fitzgerald, B. J.; Pierpont, C. G. *Inorg. Chem.* **1980**, *19*, 770.
- (2) Washington, J. S. Ph. D. Thesis, University of Alberta, 1994.
- (3) (a) Kiel, G.-Y.; Takats, J. *Organometallics* **1989**, *8*, 839. (b) Fontaine, X. L. R.; Jacobsen, G. B.; Shaw, B. L.; Thornton-Pett, M. *J. Chem. Soc., Dalton Trans.* **1988**, 741. (c) Hogarth, G.; Kayser, F.; Knox, S. A. R.; Morton, D. A. V.; Orpen, A. G.; Turner, M. L. *J. Chem. Soc., Chem. Commun.* **1988**, 358. (d)

- Dyke, A. F.; Knox, S. A. R.; Naish, P. J.; Taylor, G. E. *J. Chem. Soc., Chem. Commun.* **1980**, 409.
- (4) Kiel, G.-Y., personal communication.
- (5) Todd, L. J.; Wilkinson, J. R. *J. Organomet. Chem.* **1974**, *77*, 1.
- (6) Jacke, J.; Takats, J., unpublished results.
- (7) Bassler, G. C., Morrill, T. C.; Silverstein, R. M. *Spectrometric Identification of Organic Compounds* 4th ed.; John Wiley & Sons: Toronto, 1981.
- (8) Dickson, R. S.; Evans, G. S.; Fallon, G. D.; Pain, G. N. *J. Organomet. Chem.* **1985**, *295*, 109.

Chapter Six

Conclusions

6.1

The preparation of $M(\text{CO})_4(\eta^2\text{-alkyne})^{1,2,3}$ ($M = \text{Ru}, \text{Os}$) complexes has been an ongoing pursuit in these labs and past research has established the synthetic methodology leading to and the properties of both acetylene and hexafluoro-2-butyne complexes. As bimetallic complexes can be prepared with $\text{Ru}(\text{CO})_4(\eta^2\text{-F}_3\text{CC}_2\text{CF}_3)^1$, but not with $\text{Ru}(\text{CO})_4(\eta^2\text{-HC}_2\text{H})^4$ owing to its thermal instability, it was of interest to establish the feasibility of $\text{Ru}(\text{CO})_4(\eta^2\text{-HC}_2\text{CF}_3)$ as a precursor in the preparation of alkyne-bridged bimetallic complexes. Given that $\text{Ru}(\text{CO})_4(\eta^2\text{-HC}_2\text{CF}_3)$ would form bimetallic products, of further interest was the structural and regiochemical nature of the products.

Prior work by this research group on the condensation reactions of the $M(\text{CO})_4(\eta^2\text{-alkyne})$ series of complexes had established the general trend that electron-rich alkynes, such as propyne, and 2-butyne, would generate dimetallacyclopentenone structures and electron-poor alkynes such as hexafluoro-2-butyne (HFB) would yield dimetallacyclobutene structures^{1,2,3}. Trifluoropropyne, by nature of its having only one very strongly electron withdrawing substituent would be expected to show a marked preference in coordination to a heterobimetallic framework.

The condensation reactions of $\text{Ru}(\text{CO})_4(\eta^2\text{-HC}_2\text{CF}_3)$ with either an $M(\text{CO})_4\text{L}$ ($M = \text{Os}, \text{Ru}$; $\text{L} = \text{CO}, \text{PR}_3$) complex or $\text{Cp/Cp}^*\text{M}(\text{CO})_2$ ($M = \text{Co}, \text{Rh}, \text{Ir}$) were met with limited success. While the trifluoropropyne complex would react to form dimetallacycles, unlike the acetylene analogue, the complexes with which it would react were limited in comparison to the HFB analogue. As a result, it was necessary to prepare all osmium containing products from $\text{Os}(\text{CO})_4(\eta^2\text{-HC}_2\text{CF}_3)$.

Whereas the dimetallacycles formed with the group 9 metal complexes proved to be unstable, the products formed with the group 8 metal complexes proved to be quite thermally robust.

All the condensation reactions performed proved to be regiospecific. For the mixed metal examples it was found that the perfluoromethyl bearing alkyne carbon maintained its metal-carbon bond while it was the hydrogen bearing carbon that migrated to the incoming metal. This observation reflects the strong electron withdrawing character of perfluoromethyl group. The examples where $L = \text{PMe}_3$ established that the phosphine maintained its original metal attachment and coordinated to the dimetallacyclobutene network *trans* to the metal-metal bond.

Although the chemistry of $\text{Ru}(\text{CO})_4(\eta^2\text{-HC}_2\text{CF}_3)$ proved to be problematic it was not without its rewards. The dimetallacyclobutene products $\text{Ru}_2(\text{CO})_8(\mu\text{-}\eta^1, \eta^1\text{-HC}_2\text{CF}_3)$ and $\text{OsRu}(\text{CO})_8(\mu\text{-}\eta^1, \eta^1\text{-HC}_2\text{CF}_3)$ exhibited the unique habit of carbonyl insertion when treated with a nucleophilic ligand. Although dimetallacyclobutenes and dimetallacyclopentenones are closely related by simple carbonyl insertion the examples presented in this work are the first documented examples to appear. Like the condensation reactions, the insertion reactions are regiospecific, the carbonyl inserting into the Ru-C(H) bond and the phosphine coordinating *trans* to the metal-metal, adjacent to the newly formed acyl.

The complex $\text{Ru}(\text{CO})_4(\eta^2\text{-HC}_2\text{CF}_3)$ has proven to be a rather enigmatic member of the $\text{M}(\text{CO})_4(\eta^2\text{-alkyne})$ series of complexes. The complex sufficiently stable to form only a limited number of dimetallacycles. However, it may prove that it is this very nature that has led to the interesting reactivity observed for the condensation products of $\text{Ru}(\text{CO})_4(\eta^2\text{-HC}_2\text{CF}_3)$.

6.2 References

- (1) Gagné, M. R.; Takats, J. *Organometallics* **1988**, *7*, 561.
- (2) Washington, J. Ph. D. Thesis, University of Alberta, 1994.
- (3) Burn, M. J.; Kiel, G.; Seils, F.; Takats, J.; Washington, J. *J. Am. Chem. Soc.* **1989**, *111*, 6850.
- (4) Kiel, G., unpublished results.